“The Enhancement of Non-Destructive Testing and Evaluation Through the Use of Active Infrared Thermography to Identify Internal Pipe Wall Thinning and Corrosion Under Paint”

By

Muhammad Nazrin Bin Sohaili

Dissertation submitted is partial fulfilment of

the requirements for the

Bachelor of Engineering (Hons.)

(Petroleum Engineering)

MAY 2013

Universiti Teknologi PETRONAS

Bandar Seri Iskandar

31750 Tronoh

Perak Darul Ridzuan

CERTIFICATION OF APPROVAL

“The Enhancement of Non-Destructive Testing and Evaluation Through the Use of Active Infrared Thermography to Identify Internal Pipe Wall Thinning and Corrosion Under Paint”

By:

Muhammad Nazrin Bin Sohaili

A project dissertation submitted to the:

Petroleum Engineering Program

Universiti Teknologi PETRONAS

In partial fulfilment of the requirement for the:

Bachelor of Engineering (Hons.)

PETROLEUM ENGINEERING

Approved by,

____

(Ir. Dr. Mohd Shiraz Bin Md. Aris)

UNIVERSITI TEKNOLOGI PETRONAS

TRONOH, PERAK

MAY 2013

CERTIFICATION OF ORIGINALITY

This is to certify that I am responsible for the work submitted in this project, that the original work is my own except as specified in the references and acknowledgements, and that the original work contained herein have not been undertaken or done by unspecified sources or persons.

____

(Muhammad Nazrin Bin Sohaili)

ABSTRACT

The objective of this research is to study the potential of infrared thermography as early identification method and as complement to Non-Destructive Testing (NDT) to identify piping wall thinning and corrosion under paint. Three (3) steel plates (IRT-S1, IRT-S2, and IRT-S3) are fabricated to simulate mass loss. While one (1) corroded steel plate (IRT-S4) is modified and painted to simulate corrosion hidden under paint. Active infrared thermography is applied to those plates to detect the defects which are not visible via normal visual inspection. The experiments are assisted by heat stimulation device and an infrared camera. The mass loss on the three (3) plates are successfully identified through thermal images captured by infrared camera. The temperature difference between defect and non-defect body are high enough to give an interpretable thermal image profile. Other than that, the hidden corrosion on IRT-S4 plate surface is able to be detected by the same setup. Corroded area hidden under the paint is successfully be detected and captured in thermal images. The positive results gives a verification that there is a potential for infrared thermography to be used to detect pipe thinning and corrosion under paint.

ACKNOWLEDGEMENT

I would like to express the highest gratitude and thanks to people that have contribute in completion of this project. Among those is my FYP Supervisor, Ir. Dr. Mohd. Shiraz Bin Md Aris for his valuable assistance and guidance throughout the project. He has been very helpful in giving me clear directions and paths, his sincere help and encouragement to solve any problem raised.

I also would like to thank Mr. Mohammed Omer, PHD student of Mechanical Engineering for his support while author conducting experiments and handling the equipment. Thank you also for the tips and information that are very useful and helps me in my experiment.

To Mr. Azhar, a Senior Technician who greatly helped in completing the electrical-related equipment used for the experiments.

Not to forget my colleagues from Petroleum Engineering Department whom often give words of advice and opinions related to the project.

Last but not least, to my family and most importantly, to Allah SWT for the strength given by Him for me to complete the project despite the obstacle and challenges faced. Alhamdulillah.

TABLE OF CONTENTS

LIST OF FIGURES

LIST OF TABLES

CHAPTER 1

1. INTRODUCTION

1.1.Background of Study

In industry, equipment is designed to perform certain function with an expectation that it will perform well and trouble-free within designated period of time. However, after a certain time period of service provided by the equipment, defect is generated and formed. If there is no precaution taken to detect the defect in early stage, which is before the equipment fail to operate, it will contribute to the “domino effect” that can lead to process shutdown and production loss.

One of the defects occurs during in-service period is the wall thinning of steel pipe in piping assembly. The failure due to pipe wall thinning is not uncommon. Among common piping failure occurred due to piping wall thinning are piping burst, fracture, and crack. About 400 failures by wall thinning have been reported during the last three decades around the world (USNRC, 1989; Chexal et.al., 1998; Ting and Ma, 1999; Choi and Kang, 2000; Michel et.al, 2001).

Another defects that typically occurs is corrosion. Common corrosion effect to metal is reduction of strength of metal due to surface losses (stains and pits) (Swiderski, 2012). While hidden corrosion often unable to be detected visually, but it is indirectly detectable in form of structural discontinuities such as flaws and void, and reduction in wall thickness (Yolken & Matzanin, 2008). It is important to detect the hidden corrosion (often hidden under paint) to avoid unpredictable repair activities or catastrophic tragedies. There is, therefore, a need to detect the defect before the failure occurs.

The defects can be detected through a technical assessment called Non-Destructive Testing (NDT). NDT is done to the components, equipment, or systems in order to identify their "health condition" without destruction and without affecting its operability.

This project is proposing the usage of one of the emerging NDT methods, Active Infrared Thermography to detect pipe wall thinning in piping systems and corrosion under paint in steel plate surface. Milled steel plates will be used to simulate metal loss due to erosion, and a corroded steel plates will be modified to simulate corrosion hidden under paint. Infrared camera will be used to detect the infrared radiation emitted by the steel plates (in which are stimulated by external heat source) and will be converted to thermal image. Thermal maps from the images then will be analysed in term of temperature difference and specific image characteristics in order to detect presence of pipe thinning and corrosion under paint.

1.2.Problem Statement

The implementation of current point-to-point measurement and inspection to detect piping wall thinning become not feasible when it involves long and substantial length of piping. Current NDT technique such as Ultrasonic Testing (that based on grid system for the inspection of the whole piping system) to gauge pipe wall thickness is both time and cost consuming.

While corrosion under paint is not easily detected through visual inspection, and will keep hidden until a sign of paint swelling and cracks starts to occur. By that time, it is too late but to execute major repair and maintenance activities that often poses higher cost than scheduled maintenance.

1.3.Objectives

The objectives of this project therefore are:

- To qualitatively detect pipe wall thinning or pitting in steel pipe using Active Infrared Thermography method.
- To qualitatively detect corrosion under paint at the surface of steel plate using Active Infrared Thermography method.
- To identify the potential of Active Infrared Thermography as early NDT identification method to detect mass loss and corrosion under paint in steel surface.

1.4.Scope of Study

Generally, it is aimed for this project to study the potential of infrared thermography to detect pipe thinning and corrosion under paint, by means of experimental studies in controlled condition. The potential of infrared thermography will be determined by qualitative results and interpretation based on the experiments held.

There is a need for quantitative analysis for better results and verification, but it is out of the scope of this project. Therefore, the scopes of study of this project are:

- Fabricate steel plates in order to simulate mass loss in piping internal wall thinning phenomena, by manipulating parameters such as area of defects (a) and depth of mass loss (d).
- Conduct Active Infrared Thermography experiment to the steel plates.
- Modify corroded steel sample to simulate corrosion under paint phenomena.
- Conduct Active Infrared Thermography experiment to steel sample.

1.5. The Relevancy of the Project

If the objectives are achieved, Infrared Thermography can be used by factories, manufacturing plants, power generation industry, petrochemical industry or others that owns thousand miles of piping and various process equipment. After the presence of pipe wall thinning and/or corrosion under paint have been estimated, the inspection area can be narrowed down for further intensive inspection before maintenance activities can be carried out. The time consumed for the inspection can be spend efficiently thus increasing the productivity of the plant and the inspection contractor.

1.6. Feasibility of the Project

The time-frame given to complete the project is good and enough. Material acquisition, **Project Activity 1** and part of **Project Activity 2** were done during FYP I, while **Project Activity 3** and **Project Activity 4** will be completed during FYP II. The experiments will be planned wisely in order to avoid any delay for the project.

CHAPTER 2

2. LITERATURE REVIEW AND THEORY

2.1.Piping Wall Thinning

To several industries, local wall thinning of metals is a serious issue (Vageswar, Balasubraniam, Krishnamurthy, Jayakumar, & Raj, 2008). And wall thinning defect is gaining more awareness because the integrity assessment of piping components directly affect the piping system that relates with the operability and safety of an operation (Kim, Park, & Lee, 2009). Piping failure due to wall thinning can cost millions in OPEX for unscheduled piping replacement, production loss due to shutdown, and gives bad image to the company if industrial disaster occurs. To maintain the integrity of the piping system, therefore, it is critical to assess the condition of the pipe that related to local wall thinning (Ahn, 2001).

In power generation industries, steel pipe is susceptible to Flow Accelerated Corrosion (FAC) under conditions of high temperature and high velocity fluid flow (Kim & Park, 2003). Corrosion also can reduce the life of a pipe by causing a deterioration and gradual decay and “eating” the wall thickness (Muniff, 2012). These pipes also are subjected to erosion/corrosion (E/C) that contributes to a wall thickness thinning at the inside piping wall (Ahn, 2001) (**Figure 1).** Among factors that contribute towards pipe wall thinning are; the velocity, temperature and pressure of fluids travel inside the piping system, and the geometry and location of the pipe.

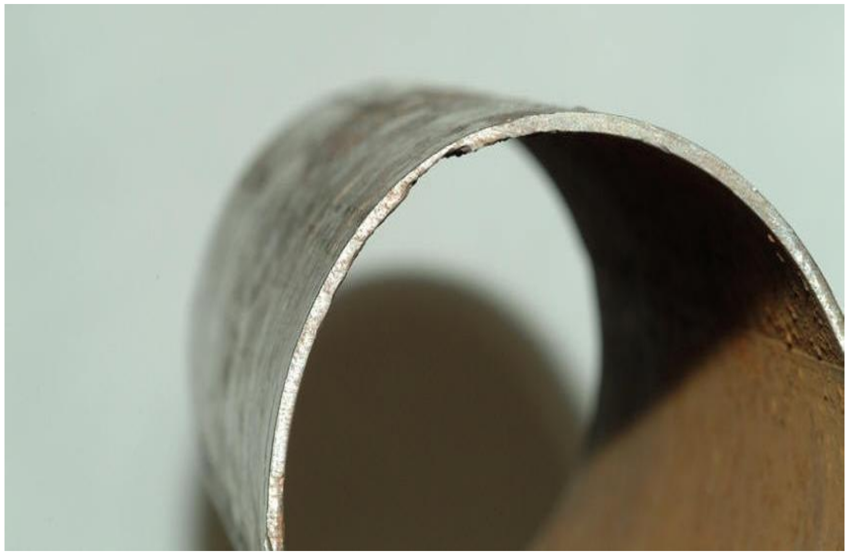

Figure 1: The wall thinning and pitting in piping. (Image courtesy by Stroud Systems Inc.)

The velocity of fluid travels inside the pipe affects the rate of pipe wall thinning. The velocity of four feet per second (4ft/s) is considered as critical velocity that adversely affects the pipe wall thinning in any industries. It involves the removal of dissolved metal ions and is called as erosion corrosion. Typically, it can be identified near with the turbulence points with the formation of grooves, gullies, or waves inside the pipe wall (Muniff, 2012). In nuclear power plant, piping is subjected to high pressure and high temperature of water or steam which can accelerate the rate of piping wall thinning (Kim & Park, 2003); (Miyazaki, Kanno, Ishiwata, Hasegawa, & et.al, 2001); (Takahashi, Kato, Ando, Hisatsune, & et.al., 2006).

Piping wall thinning is also affected by the location of the pipe in the process flow. In power generation plant, the elbow and tee are the most prone to pipe wall thinning **(Ahn, 2001)** because at the location of tee and elbow (**Figure 2**), the direction of the fluid is changing. Other than elbow and tee, deadleg in piping system also can cause the presence of stagnant area in which the the flow rates are slower than the designated requirements. Thus the stagnant areas can cause underdeposit corrosion and eventually “eat” the pipe wall and reducing its thickness **(McConnel, 2010)** (**Figure 3**).

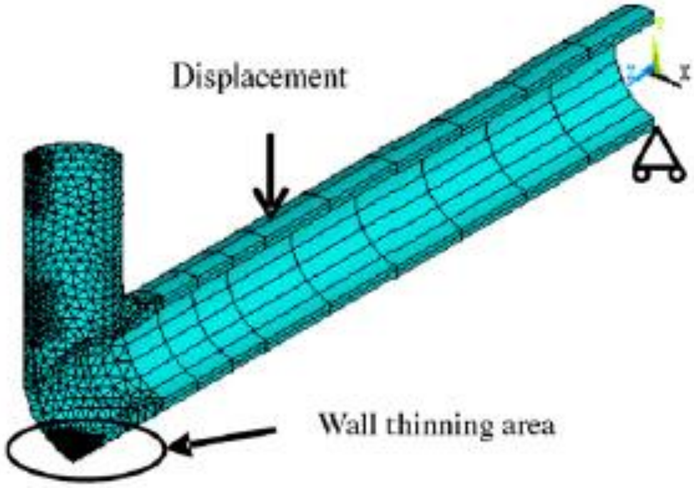

Figure 2: Modeling Image of pipe wall thinning at the elbow of piping assembly (Image source: Fracture and Deformation Behaviours of Tee Pipe with Local Wall Thinning, Takahasi, K. et.al, 2007)

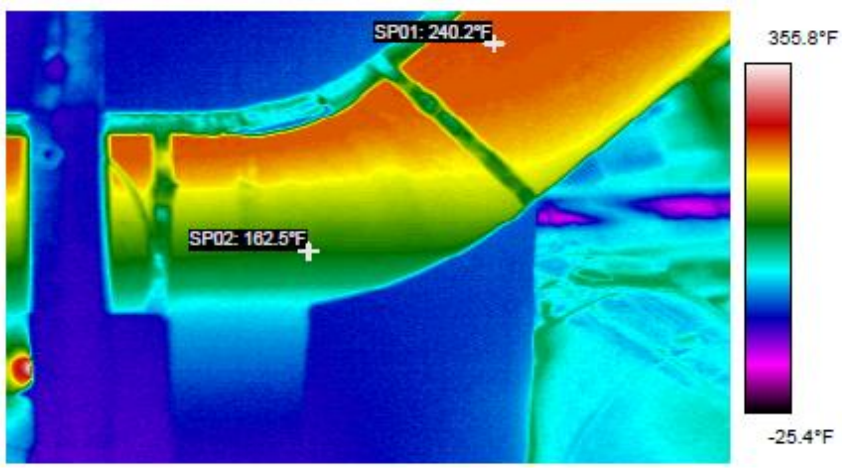

Figure 3: Stagnant area in piping assembly, detected by using infrared camera (Image source: Applications of Thermography in Diagnosing Corrosion and Material Issues in Today's Refinery, Mc. Connel, M.D., 2010)

Since pipe wall thinning can threatening the reliability and safety of carbon steel pipes that typically used in power generation industries and petrochemical plant, therefore scheduled non-destructive testing is a vital action in order to ensure safe operation (Xu, Wu., Li, & Kang, 2012).

2.2. Corrosion under paint

Corrosion is a common phenomenon occur in industries around the world. From manufacturing to military, corrosion poses a serious problem in which it can affect the safety and operability of an equipment and/or a process. It can dissolve and wearing away metal by means of chemical reaction and generally cause thinning, corrosion pits, or cracking. It can even change a smooth surface of steel to an uneven and irregular surface (Madaras & Anastasi, 2005).

Swinderski, W. (2012) mentioned some important factors that can contribute in corrosion process and among them are;

- Properties of metal – surface condition, contaminations, composition of elements
- Surroundings of metal – in contact with corrosion-caused elements
- Work conditions of metal – geometry, joining method and fatigue factors
- Temperature – frequent surrounding temperature change and high temperature exposure favour rapid corrosion process
- Time

According to Swinderski, W. (2012), the category of corrosion can be defined as shown in **Figure 5** and the explanation of each category is tabulated in **Table 1**.

When corrosion occurs under a layer of paint, swelling of the paint and increase in thickness will occur and eventually crack and chip. **Figure 4** shows a surface of paint that is swelling and crack starts to occur.

Figure 4: Swelling and crack occurs due to corrosion under paint (Image source: Mechanic Support; Zinc Vs Galvanized Hardware – Which is better?)

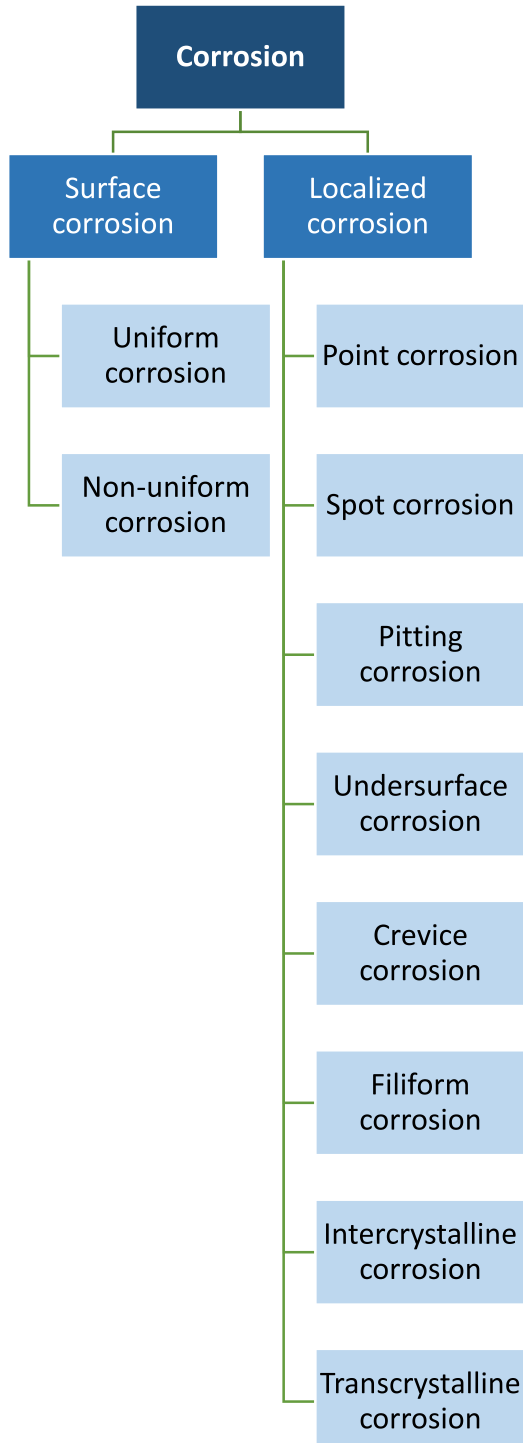

Figure 5: General category of corrosion

Table 1: Explanation for each corrosion category as per illustrated in **Figure 5**

Category	**Explanation**
Surface corrosion	Occur on all metal surface
Localized corrosion	Occur in fixed places of metal
Uniform corrosion	Uniformly covering surface of metal
Non-uniform corrosion	Covering certain places on metal surface
Point corrosion	Corrosion occurs on scattered points in different points of metal surface
Spot corrosion	Spot of corrosion occurs on metal surface
Pitting corrosion	Corrosion occurs in concentrated place and causing deep pits
Undersurface corrosion	Occurs under protective coat surface such as paint
Intercrystalline corrosion	Occurs on borders of crystal grains which is caused by separation of different phases
Transcrystalline corrosion	Corrosion that propagating deep in material by crystal grains of metal

While corrosion on an unpainted surface is easy to be detected through visual inspection, the presence of corrosion under paint is difficult to detect. The corrosion under paint is much more dangerous because it will be left undetected and unchecked until a failure and disaster occur. High-profile disasters such as Guadalajara Sewer Explosion (1992), Boeing 747 Freighter Crash (1992) and Erika Tanker Oil Spill (1999) (Malcolm, 2013) can be avoided if a proper inspection to detect the hidden corrosion is taken.

In aviation industry, painted aircraft structure must be scraped and stripped to detect corrosion occurs underneath the paint (Alexander Steel, AMCOM CPO.NDT, 2013) in which can be very costly. Thus, there is a need to improve NDT method to detect corrosion hidden under paint.

2.3.Non-Destructive Testing (NDT)

According to (Raj, Jayakumar, & Thavasimuthu, 2007)

> “Non-destructive testing (NDT) are the term used to represent the techniques that are based on the application of physical principle employed for the purpose of determining the characteristics of materials or components or systems and for detecting and assessing the inhomogeneitis and harmful defects without impairing the usefulness of such materials or components or systems” (p.1)

And, according to Hellier, (2001)

> “A general definition of NDT is an examination, test, or evaluation performed on any type of test object without changing or altering that object in any way, in order to determine the absence or presence of the conditions or discontinuities that may have an effect on the usefulness or serviceability of that object.”

Both definitions carry a meaning of NDT that performed on components in order to identify its “health condition” without destructing it. NDT can be carried out even during the equipment inspected are in service and need no shutdown. With proper and appropriate usage of NDT, it can saves cost, time, and increase the efficiency of the maintenance scheduled for the equipment. One or more NDT can be applied to increase the confidence about the defect detected and can be used to validate the inspection result. The selection of NDT is based on the following factors (Raj, Jayakumar, & Thavasimuthu, 2007):

- type and origin of discontinuity,
- material manufacturing process,
- accessibility of the component to perform NDT,
- type of equipment available,
- time available,
- cost

Among NDT method available nowadays are Radiography Testing, Ultrasonic Testing, Magnetic Particle, Liquid Penetrant Testing, Magnetic Particle, Visual Testing, Electromagnetic Testing, Acoustic Emission, and Infrared Thermography. The latter three (3) NDTs mentioned fall under nonconventional methods, while others are regard as conventional methods (Basrawi & Keck, 2003). NDT also can be categorized by its ability; to detect surface defects, volumetric defects, or both.

For this project, the scope of study is focusing on the ability of NDT method to detect volumetric defect that directly correlated to mass loss in pipe wall thinning. The ability of the method to detect corrosion under paint also will be evaluated. Thus for the purpose, three (3) NDT that are mainly used to detect internal pipe wall thinning and corrosion, which are Ultrasonic Testing, Radiography Testing, and Infrared Thermography will be focused on.

2.3.1. Ultrasonic Testing (UT)

Ultrasonic Testing is used to detect surface and internal defect and discontinuities (Raj, Jayakumar, & Thavasimuthu, 2007). UT is utilizing ultrasonic waves that can propagate thought various types of medium and detects any discontinuities along the way. By using transducer, ultrasonic waves are generated and introduced to the medium by contact. As the waves propagate through the medium, any discontinuity will reflect some of the waves back to the transducer and other waves will be reflected back once it hit the boundary of the medium. The waves reflected will be converted to images on a screen in waves form. Any defect will make changes in the wave form compared to the normal waves, indicating a different medium passed by the waves at the defect area. Refer **Figure 6**.

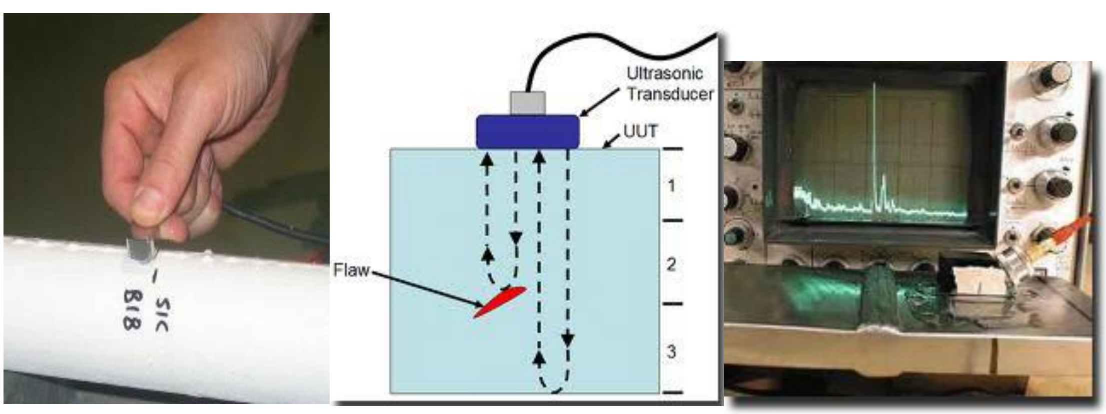

Figure 6: Conventional Ultrasonic Testing for Thickness Measurements (Images courtesy by Stroud Systems Inc. and Worcester NDT)

2.3.2. Radiography Testing (RT)

Radiography testing is utilizing the ability of short wavelength electromagnetic radiations such as X-rays or gamma rays to penetrate object of interest. After the radiation is "released" on the object, some of it will be absorbed by the object. As the radiation passed by the discontinuity (defect) in the object, lesser radiation will be absorbed and more radiation will be released on the other side of the object, compared to the radiation that absorbed by solid (no defect) object (Raj, Jayakumar, & Thavasimuthu, 2007). The variation of radiation released on the other side of the object will be recorded by a recording film (**Figure 8**). Thus, the difference and variations of the amount of radiation recorded on the film is indicating the pattern of the defect inside the object (**Figure 7**). If there is no variation of the radiation recorded, it means that the object has no density change which correlate with the absence of volumetric defects.

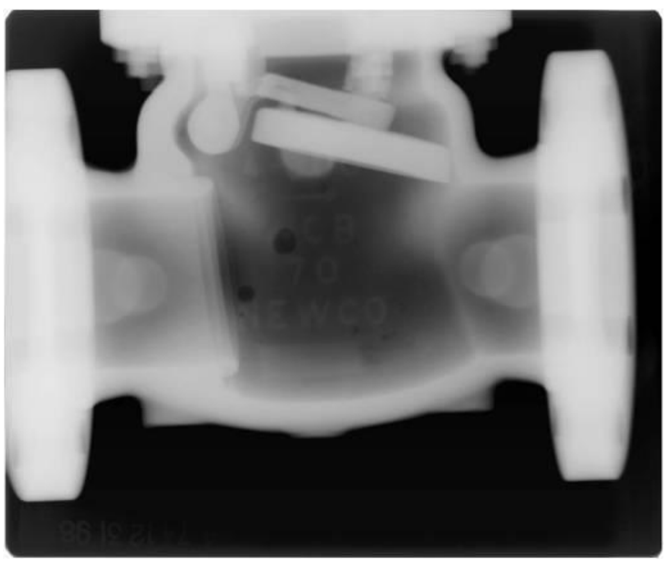

Figure 7: Sample image from Radiography Testing film (Image source: ASNT Region 19 News & Articles, 2012)

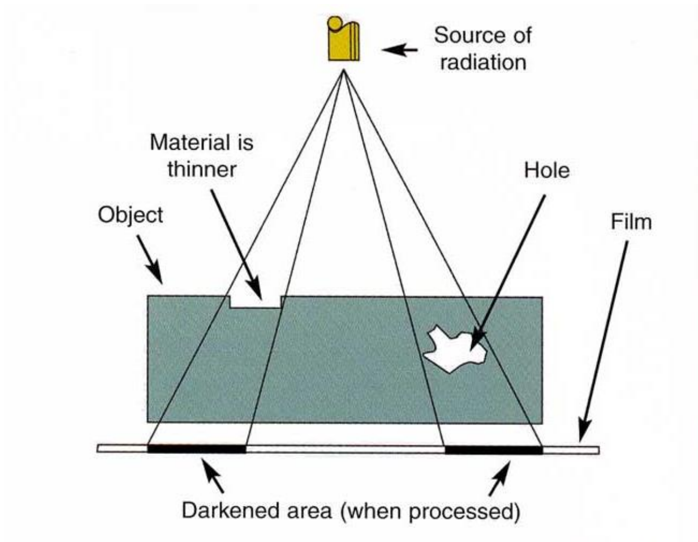

Figure 8: Principle of radiography testing (Image source: NDT Method Summary)

2.3.3. Infrared Thermography

Infrared Thermography is an NDT method that using infrared camera to detect the amount of heat released and the temperature distribution of an object (Maldague, 2001, p. 1). The image produced by the infrared camera is a representative of infrared energy emitted by the object. Theoretically, the higher the amount of heat emitted by the object, the higher the amount of infrared energy released (**Figure 9**). Infrared thermography can be utilize to evaluate and estimate the behaviour beneath the surface by assessing the distribution of infrared radiation and converting the reading to temperature scale (Hung, Chen, Ng., Huang, & et.al, 2009). There are two (2) types of infrared thermograpy, namely Passive Infrared Thermography and Active Infrared Thermography. Passive IR thermography is utilizing the natural amount of IR emitted by a certain object, while Active IR thermography is done by stimulating the object with external heat source in order to enhance the heat distribution and temperature difference on the inspected object (Hung, Chen, Ng., Huang, & et.al, 2009). Thermal stimulation can be divided to two (2) types, which are superficial and volumic. Typically superficial heating is utilizing optical radiation or gas (fluid), while volumic heating can be applied by using microwaves or ultrasonic waves (Swiderski, 2012).

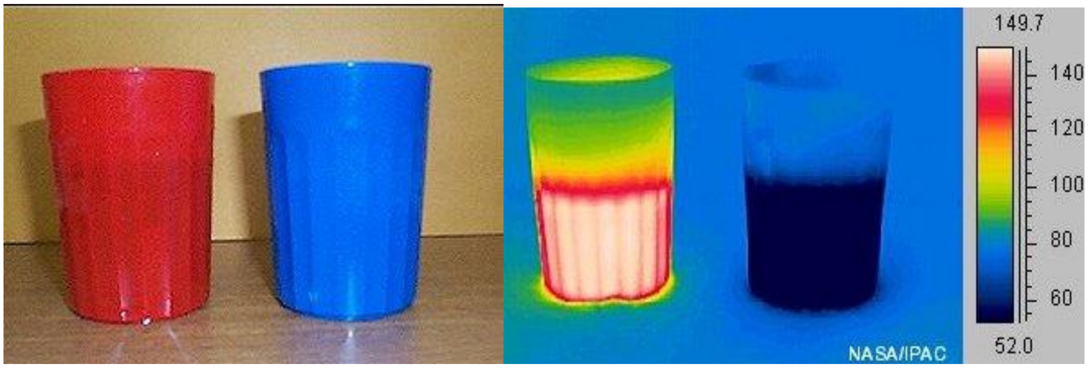

Figure 9: Left images show the visible light picture, while the right image shows the infrared picture. Note the high-temperature water inside the red cup shown by the infrared image (Image source: Teachers Guide to the Infrared, Cool Cosmos and NASA).

2.3.4. Advantages and Disadvantages of NDT

Table 1 below are the advantages and disadvantages of focused NDT; Ultrasonic Testing, Radiography Testing, and Infrared Thermography (Raj, et.al, 2007, p.g. 77 and 110; Bond, L.J., 2001; Shen, G. & Li, T., 2007).

Table 2: Advantages and Disadvantages of NDT

NDT Method	Advantages	Disadvantages
Ultrasonic Testing	• Testing can done in one side of the material • Can gives accurate thickness and distance measurement • Immediate results • Part preparation required is minimum	• Require a clean and low roughness surface • High-skilled operated is needed to operate and analyse the inspection data • Defects that parallel with sound beam can be undetectable • Point-to-point inspection consumed much time for long piping inspection
Radiography Testing	• Able to detect surface and subsurface defects • Multi-layered structure inspection capability • Can inspect wide range of materials	• Safe distance from radiation source is needed during inspection work • High-skilled operator is required • High thickness area takes much time • Radiation beam to non-volumetric defects orientation is important

Infrared Thermography	• Non-contact NDT • Fast and harmless operation • Able to inspect large portion of inspection at shorter time compared to Ultrasonic Testing • Simple and easy equipment setup • Image interpretation is relatively easy to understand • Straightforward post-inspection data processing	• Emissivity of the surface may affect the interpretation • External heat need to be introduced for better heat distribution • Time factor is important for Active Infrared Thermography (transient heat transfer)

2.4. Active Infrared Thermography as NDT method to inspect pipe wall thinning and corrosion under paint

2.4.1. Concept

The concept of Active Infrared Thermography in detecting defects is that the surface thermal radiation of objects can be monitored to “see the unseen”. The disturbance of thermal radiation due to change in volumetric temperature (due to inner defects) can be seen in infrared image. The irregularities are representing a specific obstacle to the heat flux that is diffusing in the inspected material (Swiderski, 2012).

2.4.2. Application

According to Basile, G., Clienti, C., Fargione, G.A., Geraci, A.L., and Risitano, A., (2011), thermography can be used to trigger the points of corrosion phenomena in piping by detecting discontinuity conditions. The surface thermal maps are generated to detect the anomalies underneath. The qualitative thermography can give a quick and fast application in searching thermal pattern difference or profile (ISO 18434-1). Thus active infrared thermography can serve as early identification for pipe thinning and corrosion under paint.

2.4.3. Advantages

Infrared Thermography is an emerging NDT method to estimate and detect pipe wall thinning and corrosion is due to non-contact operation, able to inspect both metal and non-metal (Swiderski, 2012) and simple data representative. Besides, Infrared Thermography able to do more inspection (Hung, Chen, Ng., Huang, & et.al, 2009) compared to other NDTs’ point-to-point-method can cover in the same period of time. It also requires lesser surface pre-inspection work such as pipe outer surface cleaning. Other than that, IR Thermography data post processing is easy compared to Ultrasonic and Radiography testing in order to determine the location of corroded defects. By identifying corrosion before it become visible with visual checking would minimize cost and repairs and eventually avoiding potential structural problems (Madaras & Anastasi, 2005).

2.4.4. Limitations

However, there are some limitations for IR Thermography for pipe wall thinning inspection (Shen & Li, 2007) and for corrosion under paint. In order to enhance the identification of the defects under the surface, more heat is required thus active infrared thermography is more favoured compared to passive infrared thermography. Besides, due to high thermal conductivity of steel, heat distribution will be fast thus it is important for the infrared camera to capture the heat distribution images before the steel reached equilibrium states. Other than that, the temperature difference between the eroded part with the normal part should be 0.5ºC or greater in order for IR Thermography to detect defects. The higher the temperature difference, the better the detection of defects (Ron Newport Academy of Infrared Thermography, 2013). Lastly, as the area of thinned wall pipe decreasing, the percentage of erosion should be increased in order for the defect detectable. All the limitation will be taken into account during the experiment process and field inspection later on.

2.5. Standards

Throughout the project, one of the main reference used is **ISO 18434-1**; Condition Monitoring and Diagnostics of Machines – Thermography. The standard is mainly dealing with general procedures to apply infrared thermography experiments and lab works. The standard also used as a safety guidelines to conduct infrared thermography works in the field as well as during the interpretation of infrared images.

Other standard used is **ISO 12944** to categorize the typical environment of corroded steel plate for the corrosion under paint experiment. The standard also used to set the coating standard for the steel plate.

CHAPTER 3

3. METHODOLOGY

3.1. Research methodology

This project is an experiment-based project, which is consist of two (2) experiments;

For the first experiment, steel plates are fabricated in order to simulate mass loss in piping internal wall thinning, by manipulating parameters such as Area of defect, *a* and Thickness of mass loss, *t*. Then, Active Infrared Thermography experiment will be carried out to qualitatively detect pipe wall thinning or pitting in steel pipe.

For the second experiment, a corroded steel plate is modified to simulate corrosion hidden under paint. Then, Active Infrared Thermography will be applied to the steel plate to qualitatively detect corrosion under paint at the surface of steel pipe using Active Infrared Thermography method. Refer to **Figure 10** for the methodology flow of the project.

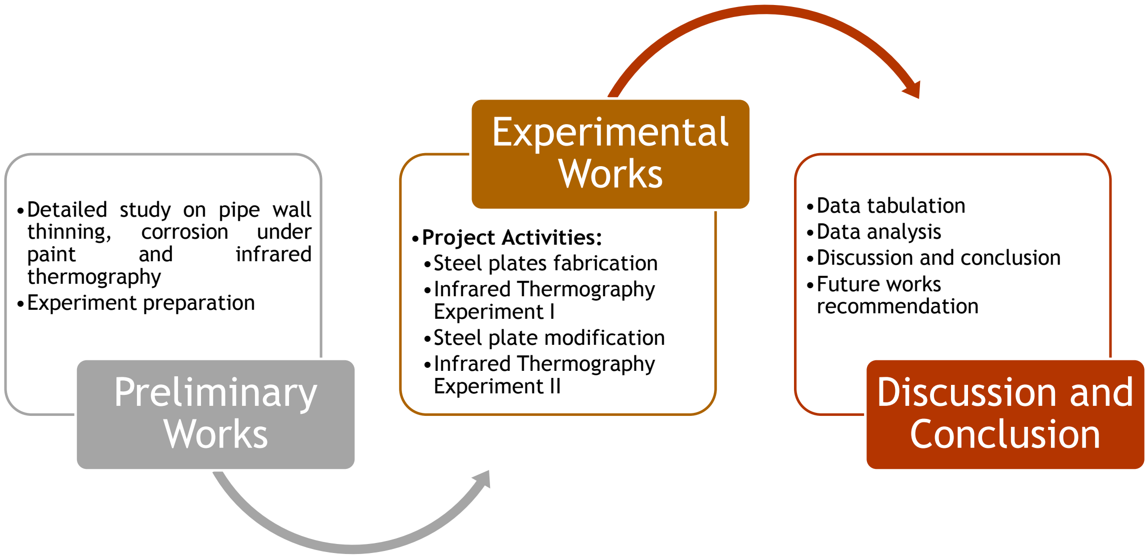

Figure 10: Methodology flow of the project

3.2. Project Activities

3.2.1. Project Activity 1: Steel Plates Fabrication

Mild carbon steel plates will be used in order to simulate mass loss in piping internal wall thinning. In total, three (3) steel plates with each will have different Area of defect, *a*, and Thickness of mass loss, *t*. Computer Numerical Control (CNC) machine will be used to fabricate the defect on each plates in order to obtain uniform shape of defect and precise thickness of mass loss. The shape of the defect will be made is circular shape. **Table 3** shows the sample number and variables set for the plates. **Figure 11, Figure 12,** and **Figure 13** shows the dimension of IRT-S1, IRT-S2, and IRT-S3, respectively.

3.2.1.1 Recommendation from previous research and experiment

Based on previous experiment, the plate is too thick until it results in the appearance of the defects in thermal image are not visible. Therefore, in this experiment, steel plates with thickness of 9.00mm will be used instead of 10.00mm used during last experiment. Other than that, the defects variable will be more compared to previous experiment. Among the parameter manipulated is the radius of the defects (which directly correlate with the area of the defects). In addition, different steel plates will be used to simulate different mass loss with respect to original thickness of the plates

The recommendation also include the effect of rust to the quality of thermal image produced. In order to obtain minimum noisy thermal image, the surface of the defect should be free from rust and sprayed to black colour.

All recommendations are taken into account for this experiment for better data acquisition and interpretation.

Table 3: Steel plates dimensions

Sample No.	Radius of defect, r (mm)	Area of defect, a (mm^2)	Thickness of sample, d (mm)	Thickness of mass loss, t_m (mm)	Percentage of t_m with d (%)
IRT - S1	5.64	100.00	9.00	6.75	75.00
	11.28	400.00	9.00	6.75	75.00
	17.00	900.00	9.00	6.75	75.00
IRT - S2	5.64	100.00	9.00	4.50	50.00
	11.28	400.00	9.00	4.50	50.00
	17.00	900.00	9.00	4.50	50.00
IRT - S3	5.64	100.00	9.00	2.25	25.00
	11.28	400.00	9.00	2.25	25.00
	17.00	900.00	9.00	2.25	25.00

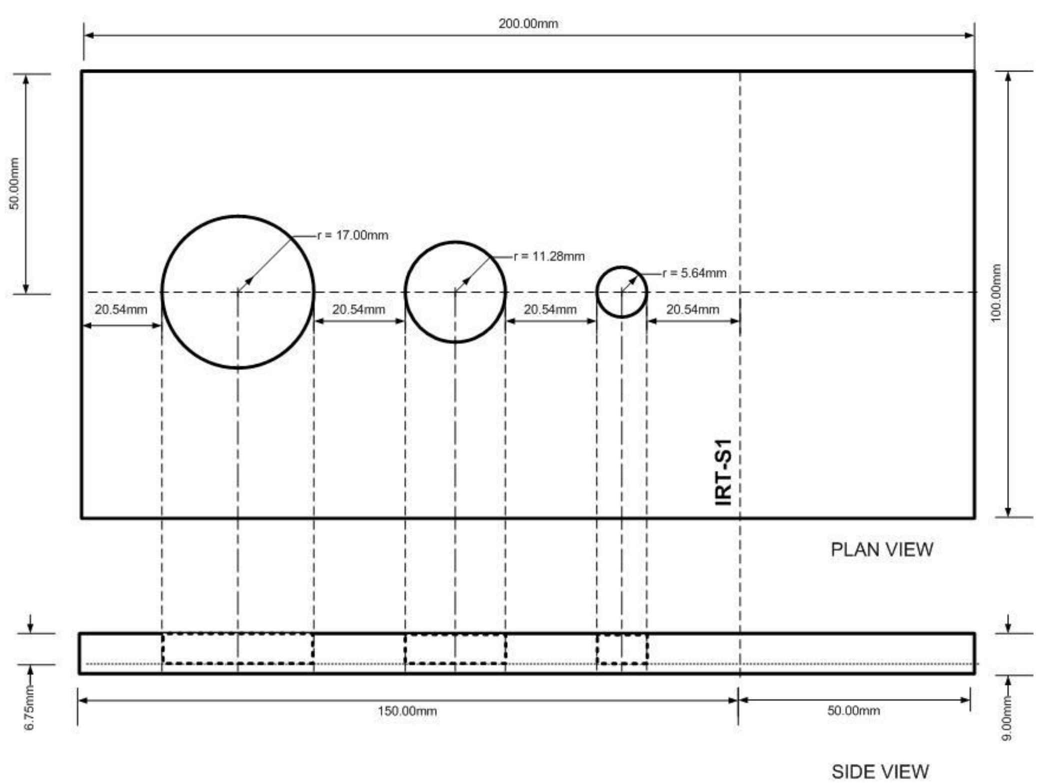

Figure 11: Dimension of the plate, Plan View and Side View of IRT-S1

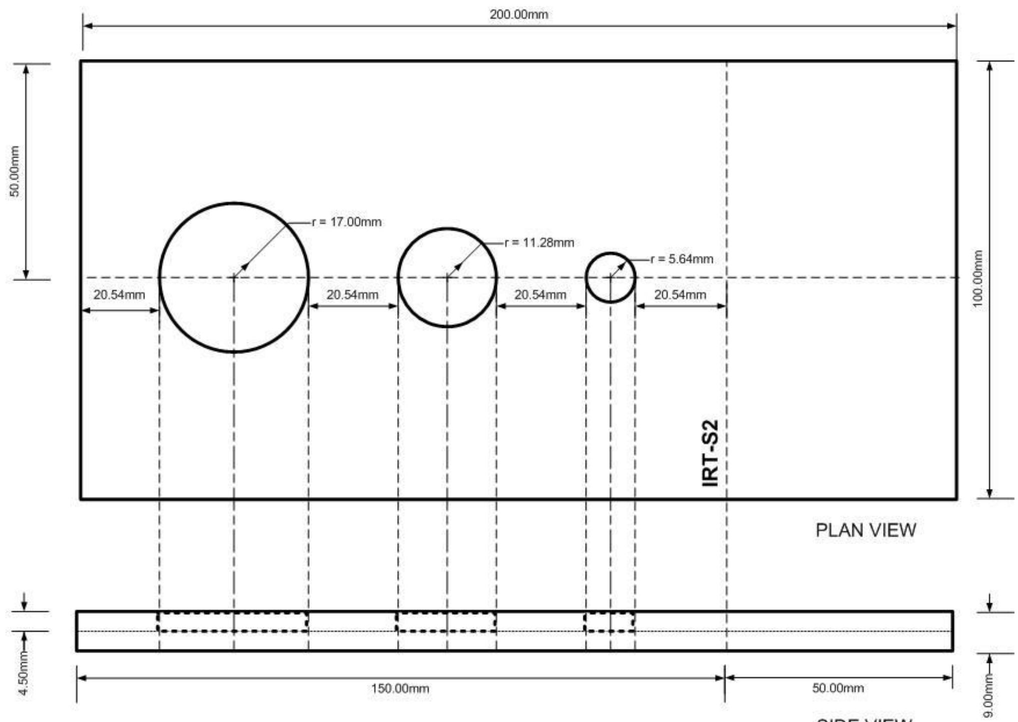

Figure 12: Dimension of the plate, Plan View and Side View of IRT-S2

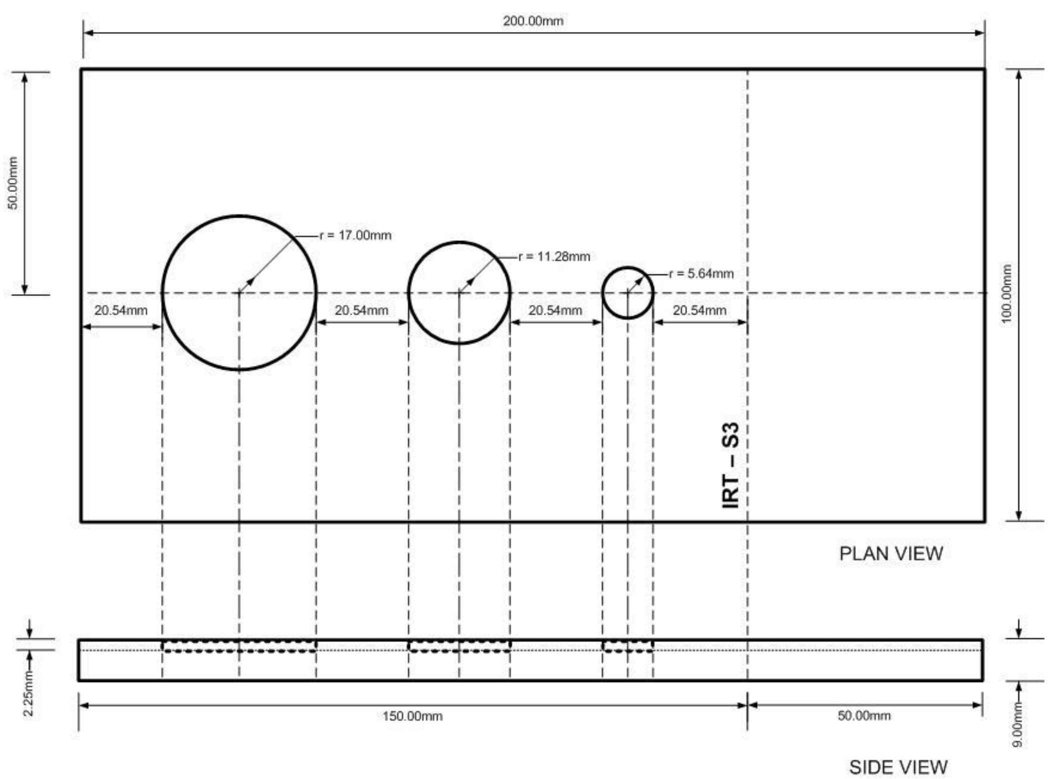

Figure 13: Dimension of the plate, Plan View and Side View of IRT-S3

Figure 14: The actual steel plates sample (from left) IRT-S1, IRT-S2 and IRT-S3

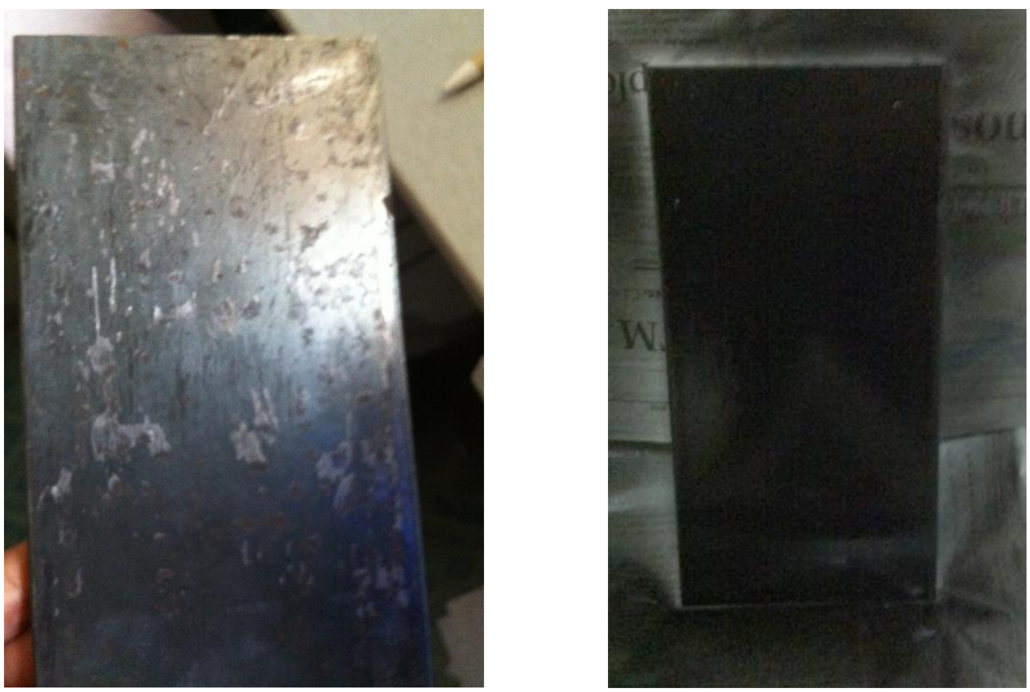

Figure 15: The front surface of steel plate before painting (left) and after painting (right)

3.2.2. Project Activity 2: Conducting the experiment – Infrared Thermography Experiment I

3.2.2.1. Recommendation from previous research and experiment

From previous infrared thermography experiment done by Mohd. Aliff Muniff on 2012, there are few notes need to take into account while conducting the experiment later on.

The experiment is recommended to be done on darker room or lab in order to reduce the effect of reflection which can affect the thermal image taken by the infrared camera. Other than that, heater mat is preferable to be use compared to halogen lamp. It is because heater mat can conduct heat more efficient and uniform compared to halogen lamp. Heater mat will convert electricity directly to heat, while halogen lamp will convert electricity to light energy and eventually to heat energy. Besides, halogen lamp will focus more heat at the centre of the plates which will cause un-uniform heat distribution across the surface of the plates.

3.2.2.2. List of equipment and materials

The Active Infrared Thermography NDT experiment setup is shown in **Figure 18** by using:

- FLIR® T640 Infrared Camera
- Heater Mats (3 units)
- Steel plates IRT-S1, IRT-S2, IRT-S3
- Controller
- Thermocouple Type K
- Computer and FLIR® software
- Binder clips
- Gloves
- G-clamp

While the material used are glass wool and aluminium foil

Figure 16: Among the equipment and material used in the experiment

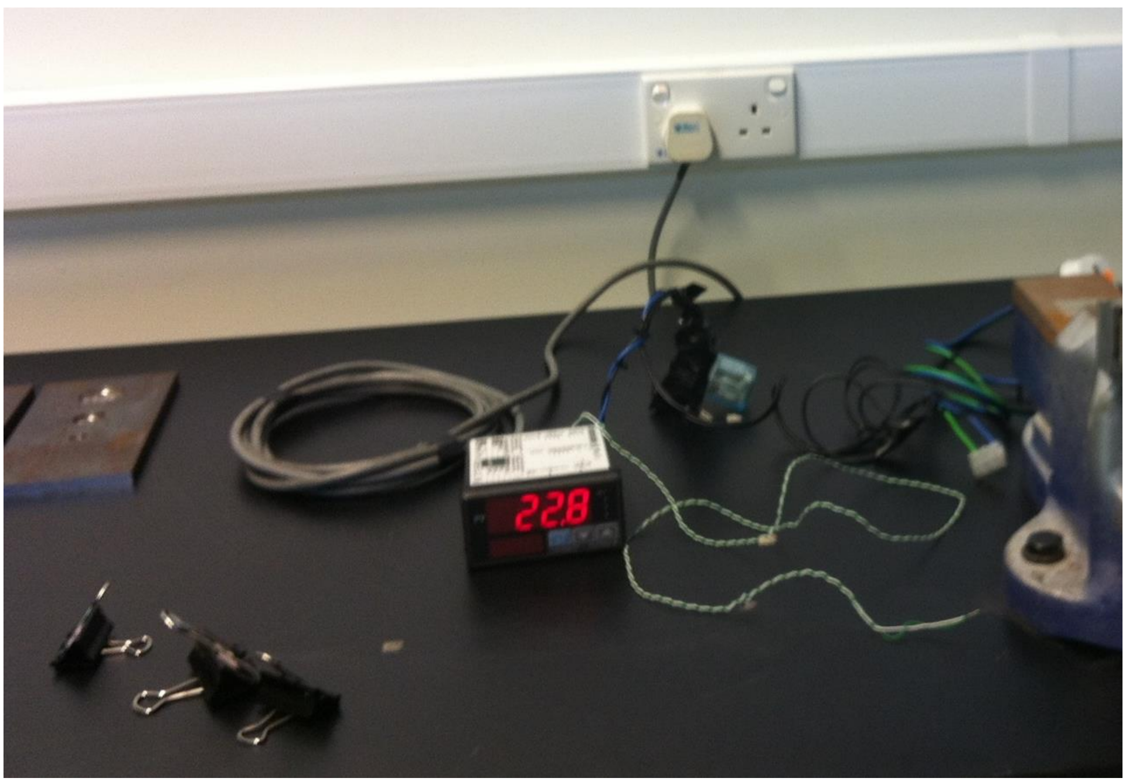

Figure 17: Among the equipment and material used in the experiment

3.2.2.3. Experiment setup

The setup of the experiment are as follows:

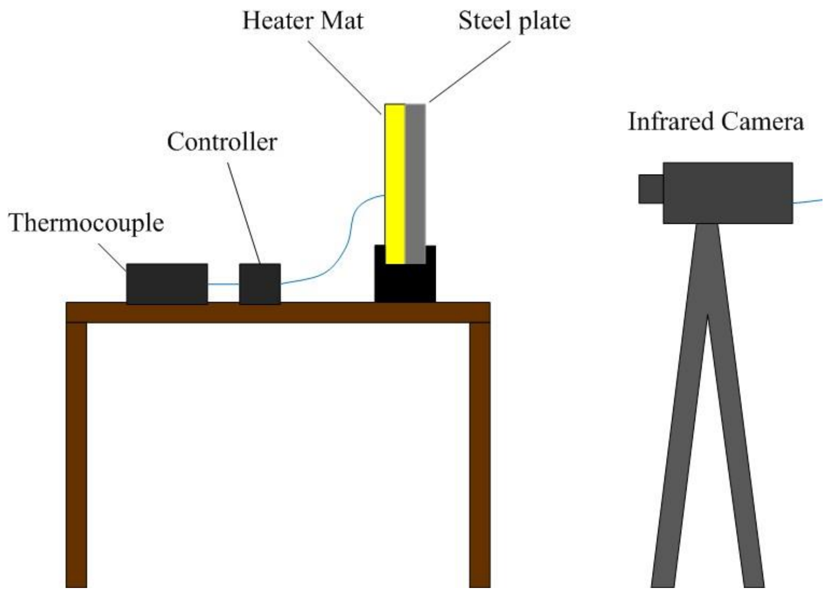

Figure 18: Equipment Setup for Active Infrared Thermography experiment

Figure 19: Real equipment Setup for Active Infrared Thermography experiment

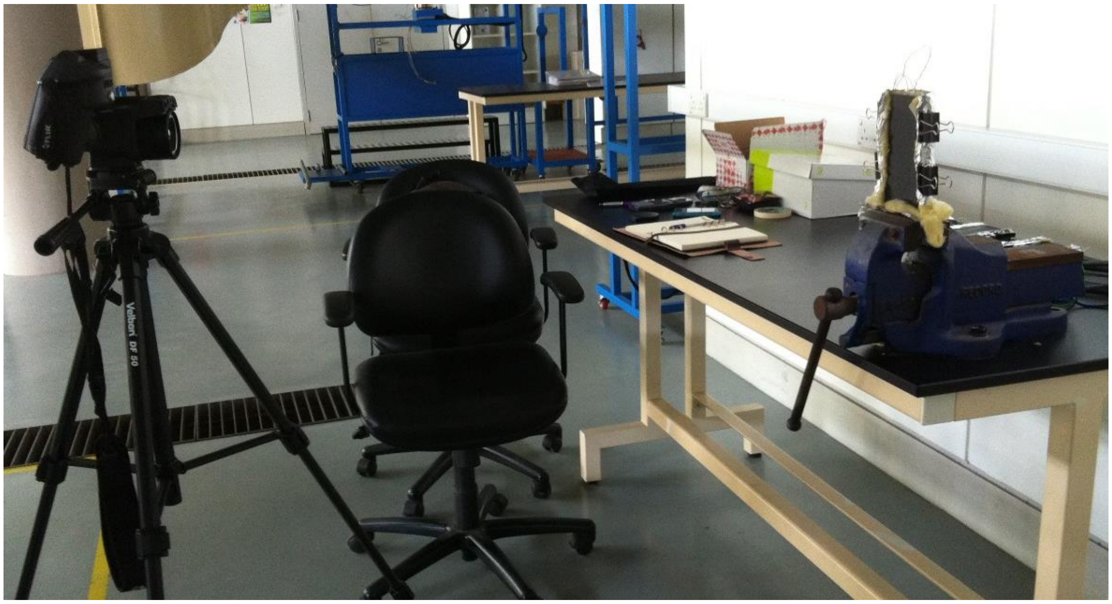

Figure 20: Real equipment Setup for Active Infrared Thermography experiment

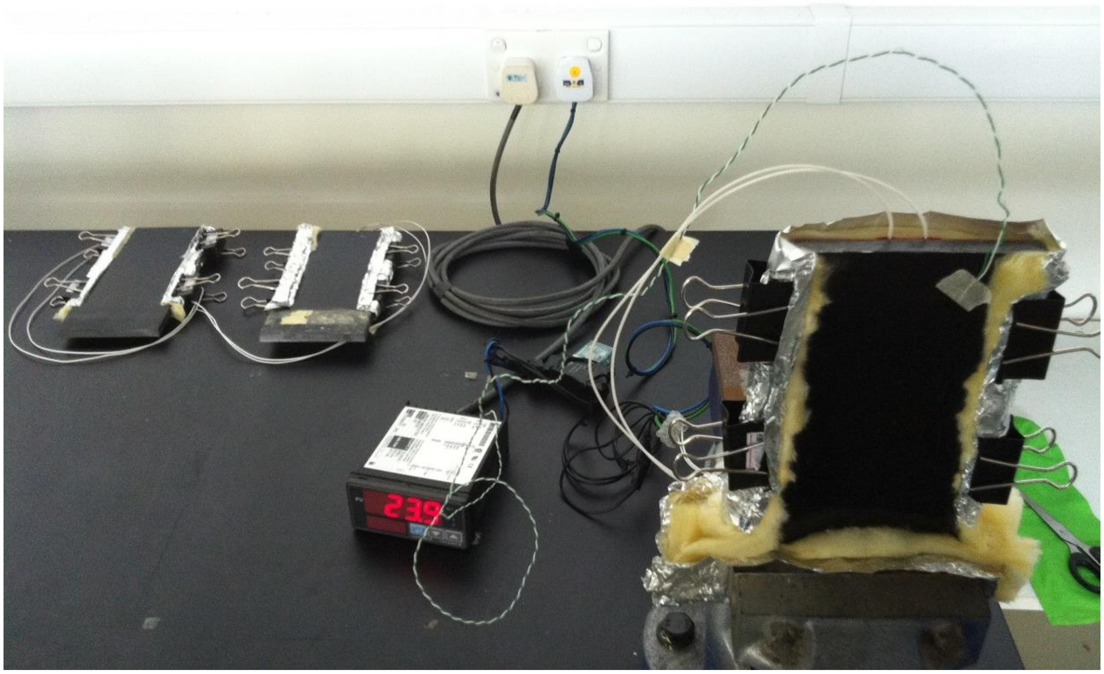

Figure 21: Real equipment Setup for Active Infrared Thermography experiment

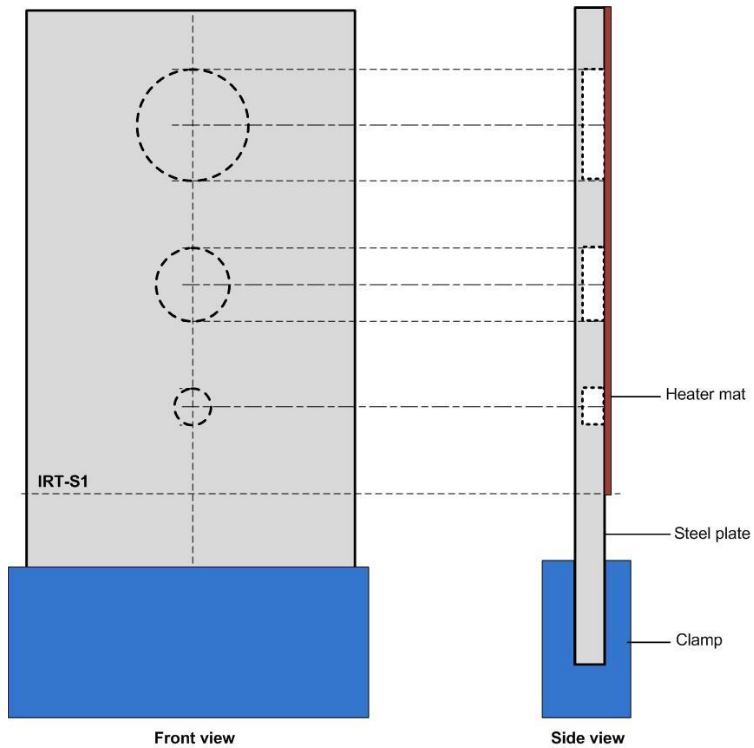

Figure 22: Heater mat configuration at the front of IRT-S1 (without insulation)

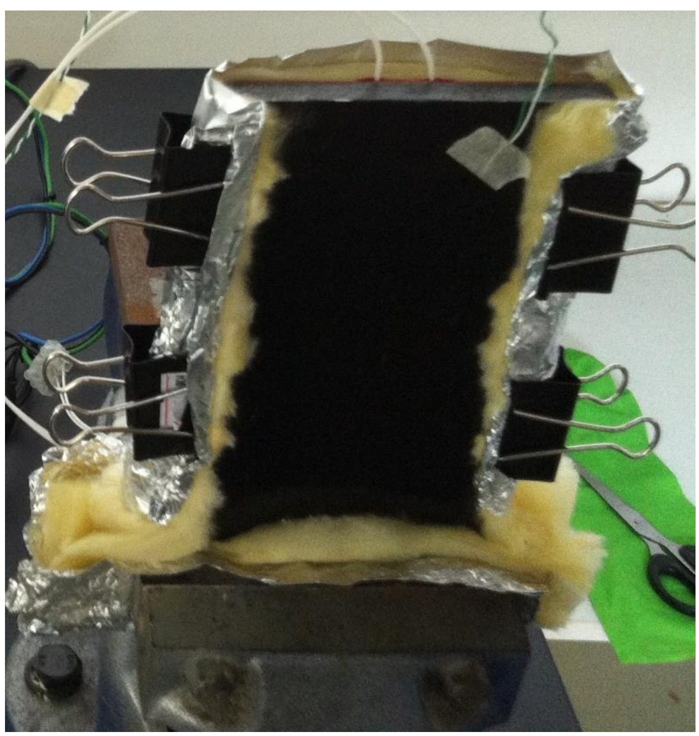

Figure 23: Heater mat configuration at the front of IRT-S1 (with insulation)

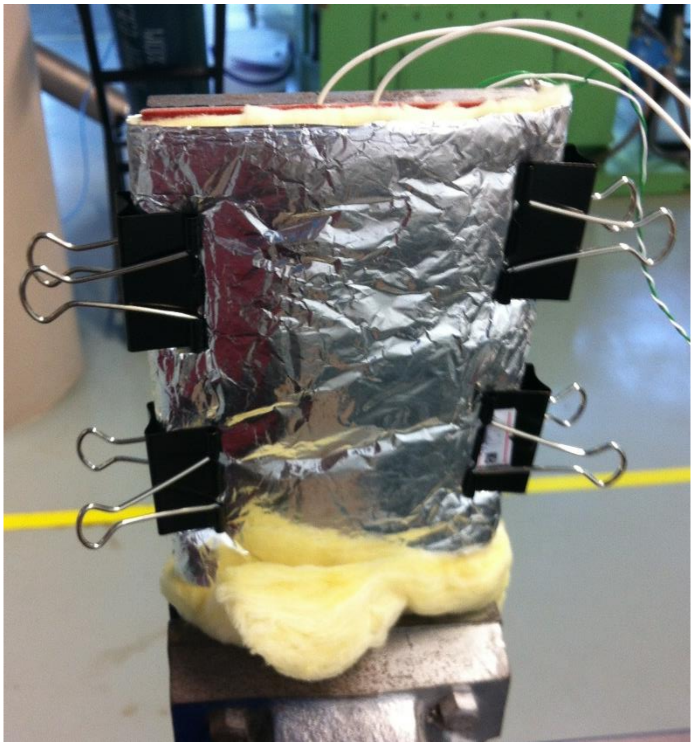

Figure 24: Heater mat configuration at the back of IRT-S1 (with insulation)

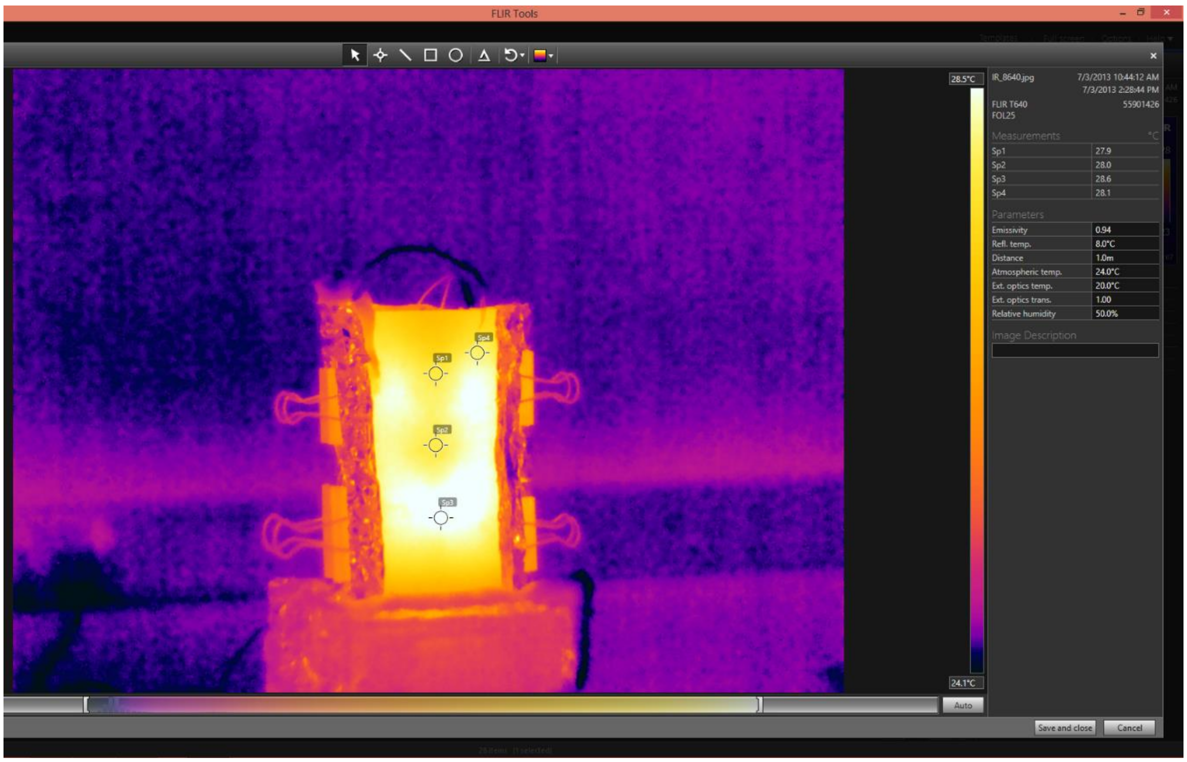

Figure 25: Image analysis using FLIR® software

3.2.2.4. Procedure of the experiment

The procedure of the experiment is as follows:

1. One (1) heater is attached at the front of the steel plate IRT-S1, with the defect surface facing the heater mat (Refer **Figure 22**).
2. Glass wool is placed at the side and back of the plates to insulate the heat and minimizing heat loss to the surrounding.
3. The infrared camera then is placed at 1m distance from the steel plate.
4. Thermocouple is placed at any part of the plates without "defects" in order to obtain temperature at original thickness (9mm).
5. Heater mat then is turned on and the steel plate will be heated. At the same time, infrared camera will record the front part of the steel plate for 3.40 minutes.
6. Infrared image is taken for every 20 seconds and data taken is tabulated in **Table 6.**
7. The thermal images are recorded for further analysis.
8. The experiment is repeated for sample IRT-S2 and IRT-S3, and observed data are recorded in **Table 7** and **Table 8** respectively.
9. Data obtained are analysed in FLIR® software and tabulated in **Chapter 4.1: Data tabulation - Infrared Thermography Experiment I**

Note:

1. Each heater mat is assigned to each steel plates to reduce the risk of damage to the heater mat due to frequent peel off from the plates.
2. The peak temperature of heater mat is 300ºC.
3. The reading for Temperature at normal thickness, T_n will be taken at any point in the plates with no defects.
4. In step 9 of the procedure, all images will need to be corrected due to reflection, by putting reflective temperature in each image taken. The reflective temperature is obtained by crumpling the aluminium foil and the infrared image will be taken,

by setting the emissivity value to 1.0. The temperature reading on the aluminium foil will be regarded as reflective temperature for the respective image (**ISO 18434-1:2008 E**)

5. The FLIR® software is unable to analyse infrared video. Therefore, author will take the image within 20 seconds interval, which is the shortest interval can be made by the infrared camera.

3.2.3. Project Activity 3: Steel plate modification

A steel plate was obtained from a welding shop and modified to fit the condition for the experiment. The steel plate, IRT-S4 is a readily-corroded plate Refer **Figure 26.** A 60-mm radius of round shape was left corroded while the other surface was polished to obtain a shine surface. Refer **Figure 27** for the dimension of IRT-S4 plate.

Figure 26: The surface condition of the steel plate before it was polished

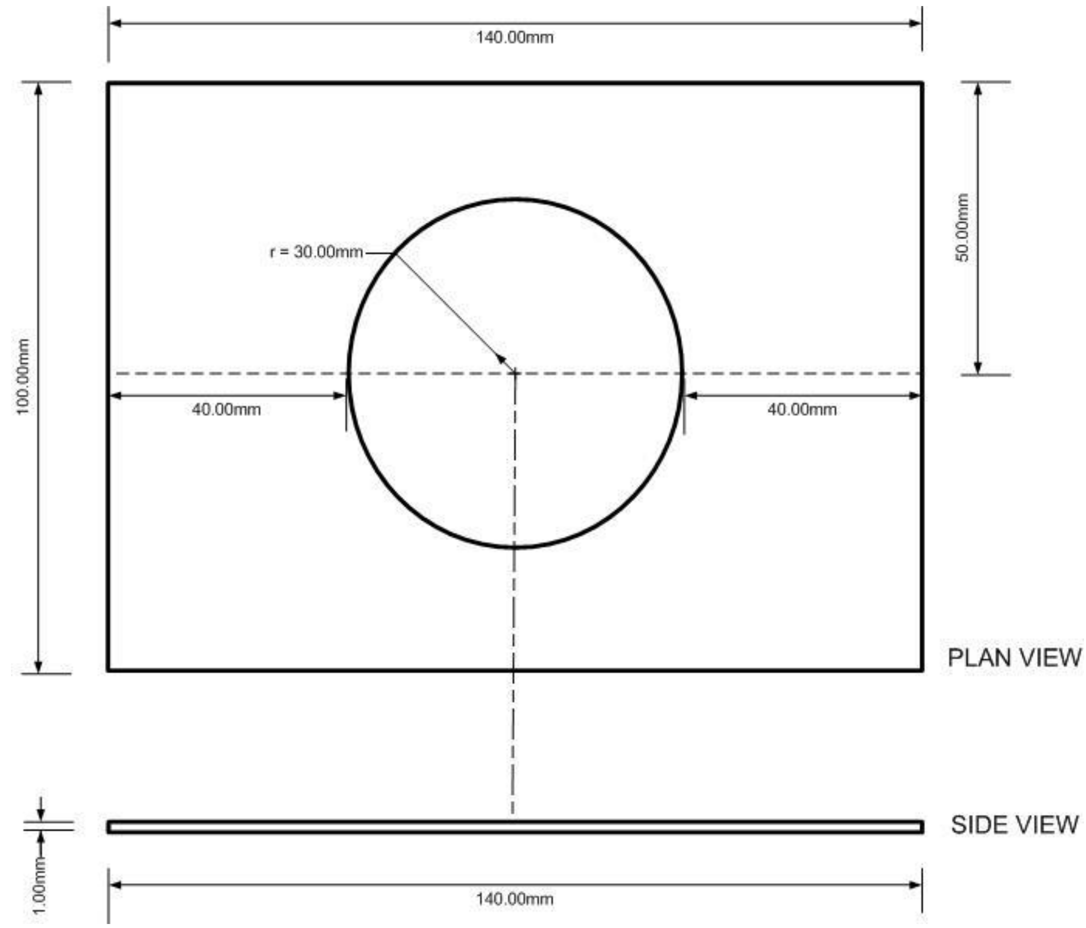

Figure 27: Dimension of the plate, Plan View and Side View of IRT-S4

3.2.3.1. Procedure

The procedure of the modification of IRT-S4 plate is as follows:

1. The marking on the plate is made by using permanent marker pen. Refer **Figure 28.**
2. The outside part of the circular marking is then polished by using sand paper. Refer **Figure 29.** The inner part of the circular marking was left corroded as per illustrated in **Figure 30**
3. The whole area of the plate is painted by using black-paint sprayer (including the corroded-circular part).
4. The surface of plate should show a uniform colour, as per stated in **Figure 31.**

Figure 28: The surface of IRT-S4 was marked with 60-mm radius of circular-shape

Figure 29: Polishing the outer part of circular shape in progress

Figure 30: The outside part of the circular shape was completely polished

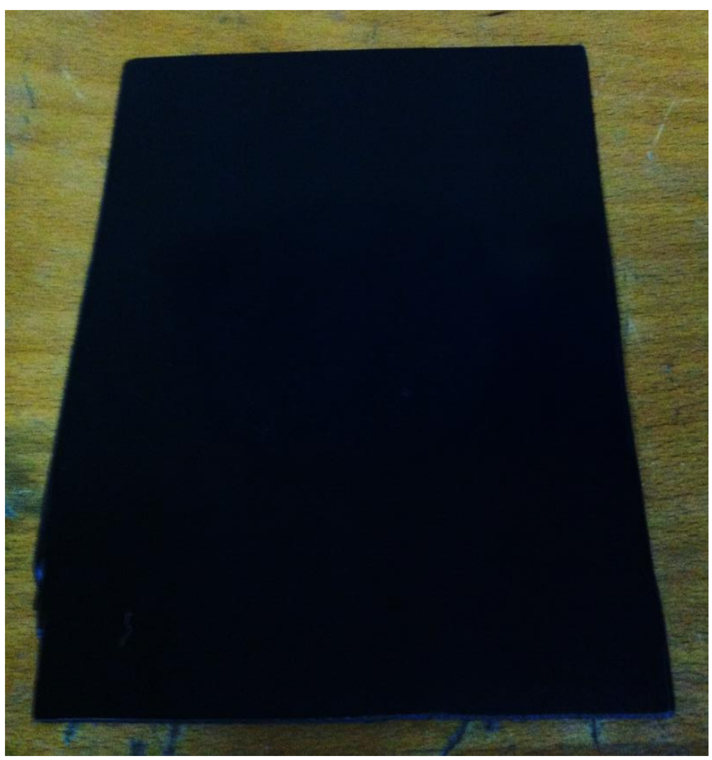

Figure 31: The surface of the plate after painting

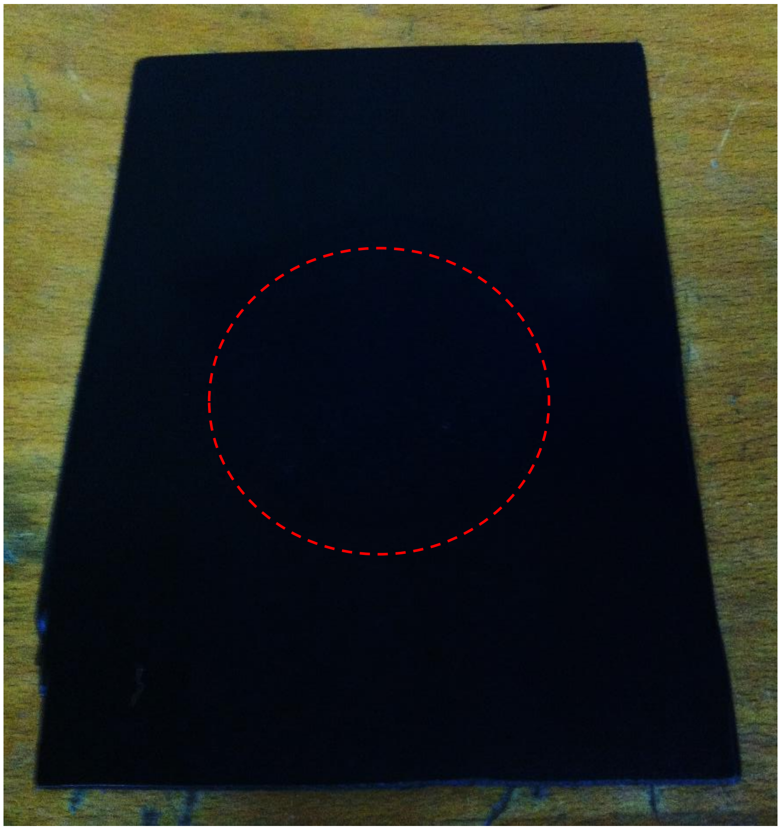

Figure 32: The location of corrosion (in red circular) hidden under the paint

3.2.4. Project Activity 4: Conducting the experiment – Infrared Thermography Experiment II

The objective of the experiment is to detect corrosion under paint by using infrared camera. The expected result is that the corroded part hidden under the paint will have a different colour (due to different temperature) than the polished part in the infrared images.

3.2.4.1. List of equipment and materials

The list of equipment (refer **Figure 33**) used in the experiment are as follows:

- FLIR® T640 Infrared Camera
- 200W spotlight
- Steel plate IRT-S4

Figure 33: The equipment used in the experiment

3.2.4.1. Experiment Setup

The setup of the experiment are as follows:

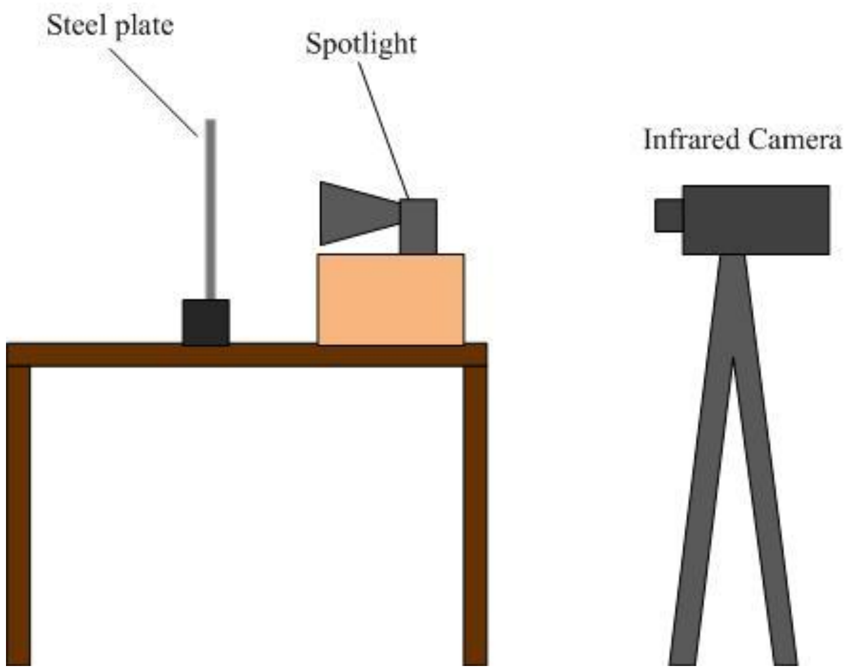

Figure 34: Equipment Setup for IRT-S4 Active Infrared Thermography experiment

Figure 35: Real equipment Setup for IRT-S4 Active Infrared Thermography experiment

3.2.4.2. Procedure of the experiment

The procedure of the experiment is as follows:

1. IRT-S4 plate is setup according to **Figure 34.**
2. Spotlight is then located in front of the plates, with distance between them is **10 cm.**
3. The spotlight is turned on for **15 seconds** to heat the front surface of IRT-S4 plate.
4. The then spotlight was put aside immediately and the images of the plate are taken by using infrared camera.
5. Infrared images is taken for every 20 seconds for 2 minutes and 20 seconds.
6. Thermal images were taken and recorded for further analysis.
7. Data obtained are analysed in FLIR® software and tabulated in **Table 9** in **Chapter 4.2: Data tabulation - Infrared Thermography Experiment II**

Note:

1. The spotlight was turned on for 15 seconds due to thin steel plate which can absorb high amount of heat in a short period of time.

3.3. Gantt chart

Table 4: Gantt chart for the project

Activities	**Final Year Project I (FYPI)**														**Final Year Project II (FYPII)**													
	1	2	3	4	5	6	7	8	9	10	11	12	13	14	1	2	3	4	5	6	7	8	9	10	11	12	13	14
Early data gathering			■	■	■																							
Detailed studies						■	■																					
Material acquisition and experiment preparation								■	■	■	■	■																
Project Activity 1: Steel Plates Fabrication												■	■															
Project Activity 2: Infrared Thermography Experiment I														■	■	■	■	■	■	■	■	■						
Project Activity 3: Steel plate modification																							■					
Project Activity 4: Infrared Thermography Experiment II																								■	■	■		
Final Data Analysis																											■	■

3.4. Key Milestones

Table 5: Key Milestones for the project

Activities	**Final Year Project I (FYPI)**														**Final Year Project II (FYPII)**													
	1	2	3	4	5	6	7	8	9	10	11	12	13	14	1	2	3	4	5	6	7	8	9	10	11	12	13	14
Completion of **Project Activity 1**: Steel Plates Fabrication													●															
Completion of **Project Activity 2**: Infrared Thermography Experiment I																						●						
Completion of **Project Activity 3**: Steel plate modification																							●					
Completion of **Project Activity 4**: Infrared Thermography Experiment II																										●		
Completion of Final Data Analysis																											●	

CHAPTER 4

4. RESULTS AND DISCUSSION

4.1. Data tabulation - Infrared Thermography Experiment I

(The remainder of this page is intentionally left blank)

4.1.1. Steel plate: IRT-S1

- Defect Depth: 75% of 9mm (6.75mm mass loss)
- Distance: 1.0m
- Reflective Temperature: 24.5 ºC
- Emissivity: 0.94

Table 6: Temperature reading at thinned area, T (ºC) recorded for sample IRT-S1

Time (min.)	Temp (ºC)				Temp Difference (ºC)		
	normal thickness T_n (ºC)	Radius			Radius		
		17.00mm	11.28mm	5.64mm	17.00mm	11.28mm	5.64mm
0.00	26.3	25.7	25.7	26.1	0.6	0.6	0.2
0.20	27.5	27.0	27.0	27.5	0.5	0.5	0
0.40	29.1	28.5	28.5	29.0	0.6	0.6	0.1
1.00	30.5	29.9	29.9	30.2	0.6	0.6	0.3
1.20	31.9	31.5	31.4	31.4	0.4	0.5	0.5
1.40	33.3	32.7	32.6	32.3	0.6	0.7	1
2.00	34.6	34.1	33.7	33.1	0.5	0.9	1.5
2.20	35.8	35.4	34.8	34.2	0.4	1	1.6
2.40	36.8	36.5	36.1	35.1	0.3	0.7	1.7
3.00	38.1	37.7	37.4	36.4	0.4	0.7	1.7
3.20	39.4	39.0	38.5	37.1	0.4	0.9	2.3
3.40	40.6	40.0	39.7	37.7	0.6	0.9	2.9

4.1.2. Plate: IRT-S2

- Defect Depth: 50% of 9mm (4.50mm mass loss)
- Distance: 1.0m
- Reflective Temperature: 25.3 ºC
- Emissivity: 0.94

Table 7: Temperature reading at thinned area, T (ºC) recorded for sample IRT-S2

Time (min.)	Temp (ºC)				Temp Difference (ºC)		
	normal thickness T_n (ºC)	Radius			Radius		
		17.00mm	11.28mm	5.64mm	17.00mm	11.28mm	5.64mm
0.00	24.6	24.6	24.6	24.5	0	0	0.1
0.20	26.3	25.5	25.7	26.2	0.8	0.6	0.1
0.40	28.1	27.1	27.5	28.1	1	0.6	0
1.00	30.0	29.0	29.5	29.9	1	0.5	0.1
1.20	31.8	30.8	31.4	31.5	1	0.4	0.3
1.40	33.3	32.4	33.1	33.1	0.9	0.2	0.2
2.00	35.3	34.3	34.9	34.7	1	0.4	0.6
2.20	37.1	36.1	36.5	35.7	1	0.6	1.4
2.40	38.7	37.9	38.0	36.9	0.8	0.7	1.8
3.00	40.4	39.4	39.8	38.3	1	0.6	2.1
3.20	41.9	40.7	41.3	39.6	1.2	0.6	2.3
3.40	43.5	42.8	42.6	40.8	0.7	0.9	2.1

4.1.3. Steel plate: IRT-S3

- Defect Depth: 25% of 9mm (2.25mm mass loss)
- Distance: 1.0m
- Reflective Temperature: 24.2 ºC
- Emissivity: 0.94

Table 8: Temperature reading at thinned area, T (ºC) recorded for sample IRT-S3

Time (min.)	Temp (ºC)				Temp Difference (ºC)		
	normal thickness T_n (ºC)	Radius			Radius		
		17.00mm	11.28mm	5.64mm	17.00mm	11.28mm	5.64mm
0.00	24.7	24.6	24.6	24.6	0.1	0.1	0.1
0.20	26.6	26.0	26.1	26.6	0.6	0.5	0
0.40	28.4	27.6	27.9	28.5	0.8	0.5	0.1
1.00	30.0	29.2	29.6	30.0	0.8	0.4	0
1.20	31.5	31.0	31.4	31.5	0.5	0.1	0
1.40	33.4	32.8	33.2	33.1	0.6	0.2	0.3
2.00	34.8	34.1	34.6	34.8	0.7	0.2	0
2.20	36.4	35.9	36.2	35.8	0.5	0.2	0.6
2.40	37.9	37.5	37.8	37.3	0.4	0.1	0.6
3.00	39.5	39.1	39.3	38.6	0.4	0.2	0.9
3.20	41.1	40.6	40.8	40.2	0.5	0.3	0.9
3.40	42.5	42.2	42.2	41.5	0.3	0.3	1.0

The images taken during experiment for sample IRT-S1, IRT-S2, and IRT-S3 are provided in the **Appendix I**, **Appendix II**, and **Appendix III** respectively.

4.2. Data tabulation - Infrared Thermography Experiment II

4.2.1. Steel Plate IRT-S4

- Distance: 1.0m
- Reflective Temperature: 24.9 ºC
- Emissivity: 0.94

Table 9: Temperature reading at corroded area, Tc (ºC) recorded for sample IRT-S4

Time (min.)	**Temp (ºC)**		**Temp Difference (ºC)**
	normal thickness T_n (ºC)	**Corroded Area, T_c**	
0.00	39.3	40.5	1.20
0.20	34.6	35.4	0.80
0.40	31.6	32.4	0.80
1.00	30.2	30.6	0.40
1.20	29.7	30.0	0.30
1.40	28.9	29.1	0.20
2.00	28.2	28.3	0.10
2.20	27.6	27.7	0.10

The images taken during experiment for sample IRT-S4 are provided in the **Appendix IV**.

4.3. Data analysis - Infrared Thermography Experiment I

The value of Temperature Difference, ΔT can be obtained by using the formula in **Equation 1.**

$$\mathbf{\Delta T = |\ Tn\ - T\ |} \qquad \text{-----------------------------------} \textbf{ Equation 1}$$

Where,

ΔT = Temperature Difference (ºC)

T_n = Temperature at normal thickness (ºC)

T = Temperature at thinned area (ºC)

Figure 36, **Figure 38**, and **Figure 40** show a Temperature at normal thickness, T_n VS Temperature at thinned area, T for steel plate sample IRT-S1, IRT-S2, and IRT-S3 respectively.

While **Figure 37**, **Figure 39**, and **Figure 41** show Temperature Difference, ΔT between Temperature at normal thickness, T_n and Temperature at thinned area, T for steel plate sample IRT-S1, IRT-S2, and IRT-S3 respectively.

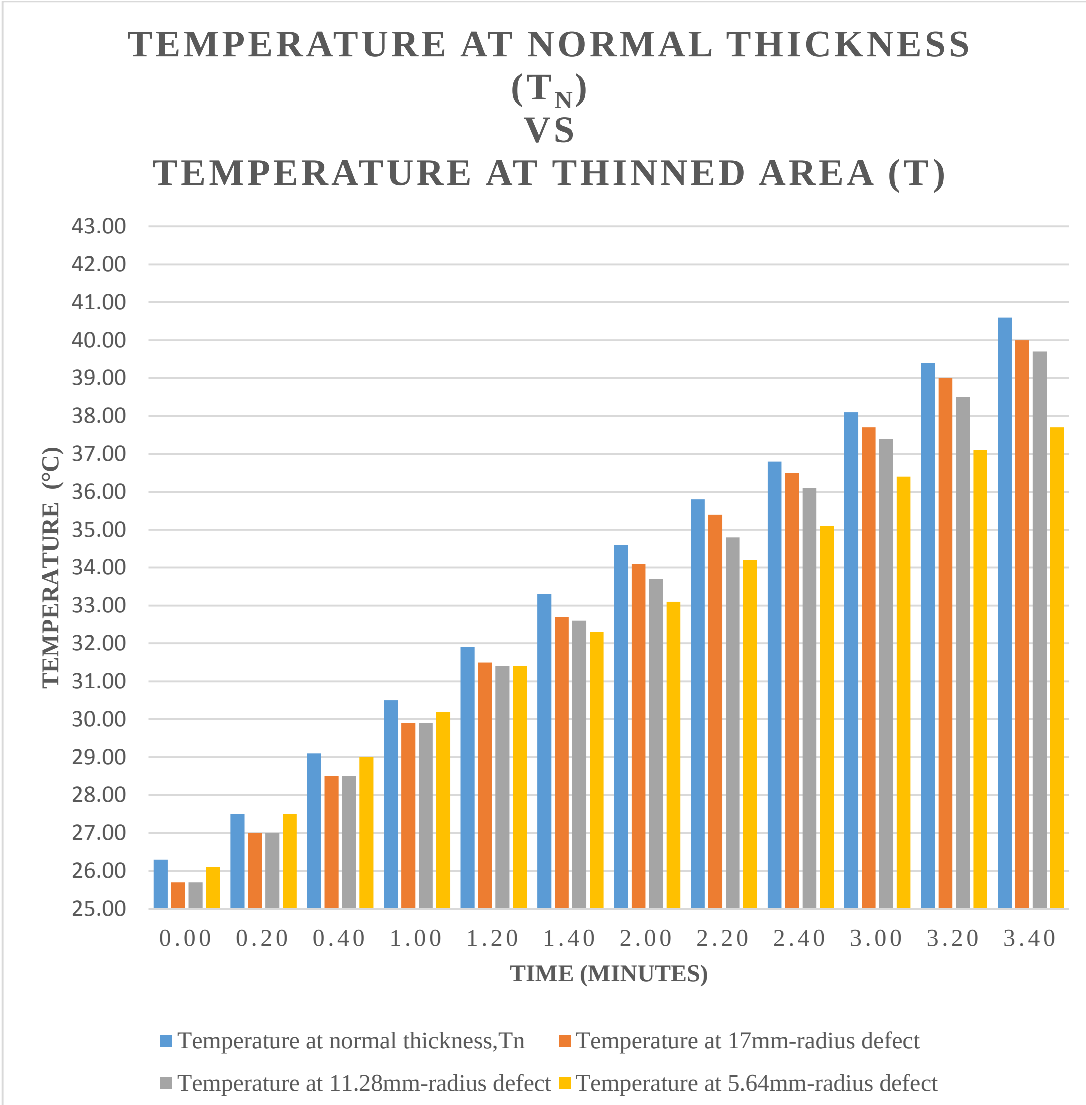

Figure 36: Temperature at normal thickness, (Tn) VS Temperature at thinned area (T) for IRT-S1 (75% mass loss)

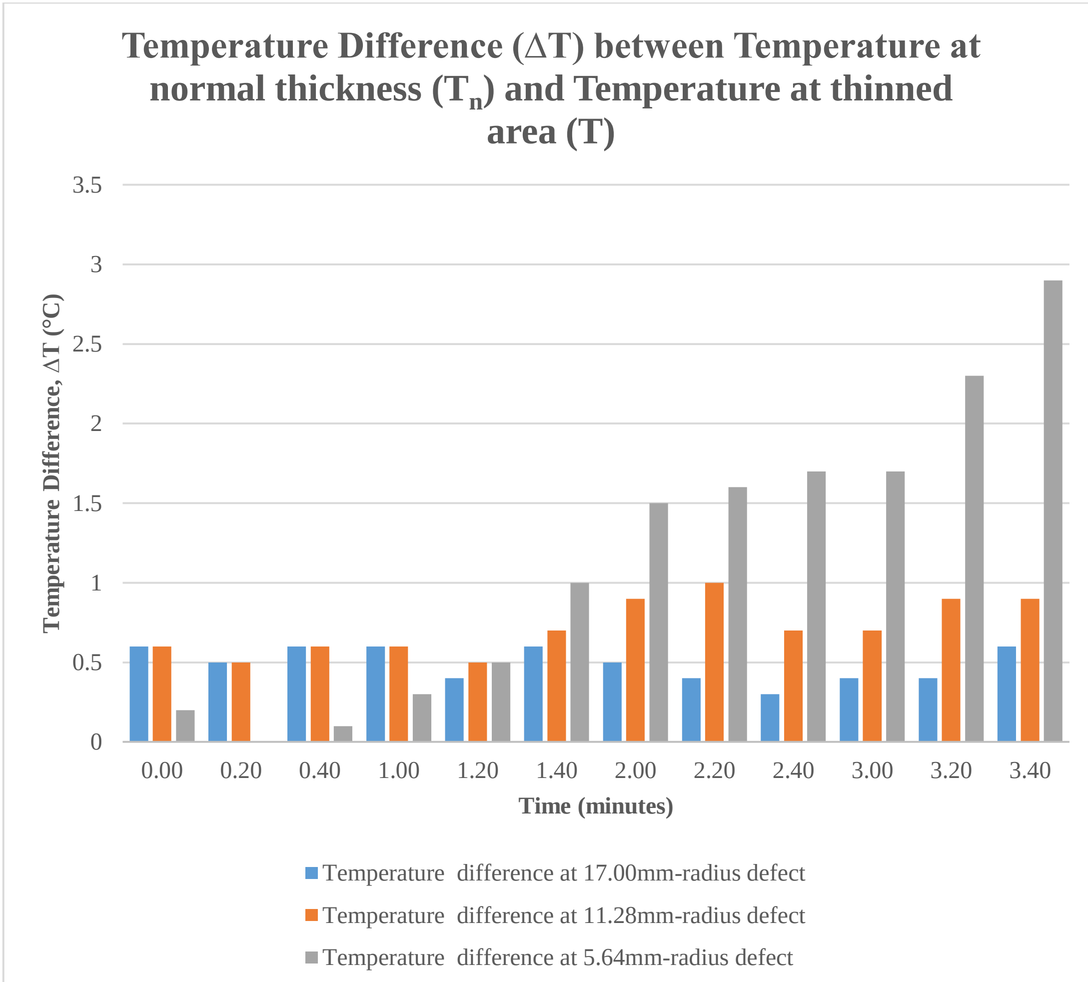

Figure 37: Temperature Difference (ΔT) between Temperature at normal thickness, (Tn) and Temperature at thinned area (T) for IRT-S1 (75% mass loss)

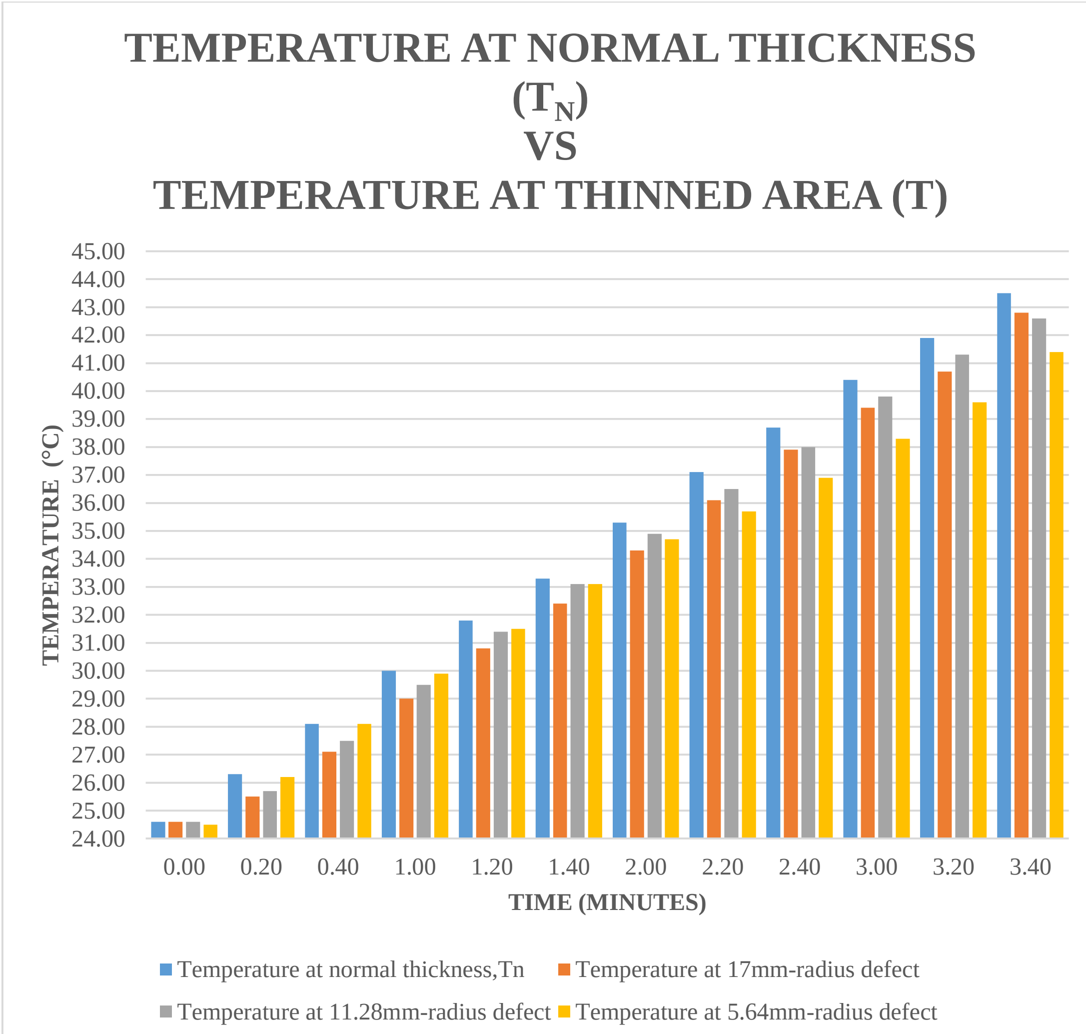

Figure 38: Temperature at normal thickness, (Tn) VS Temperature at thinned area (T) for IRT-S2 (50% mass loss)

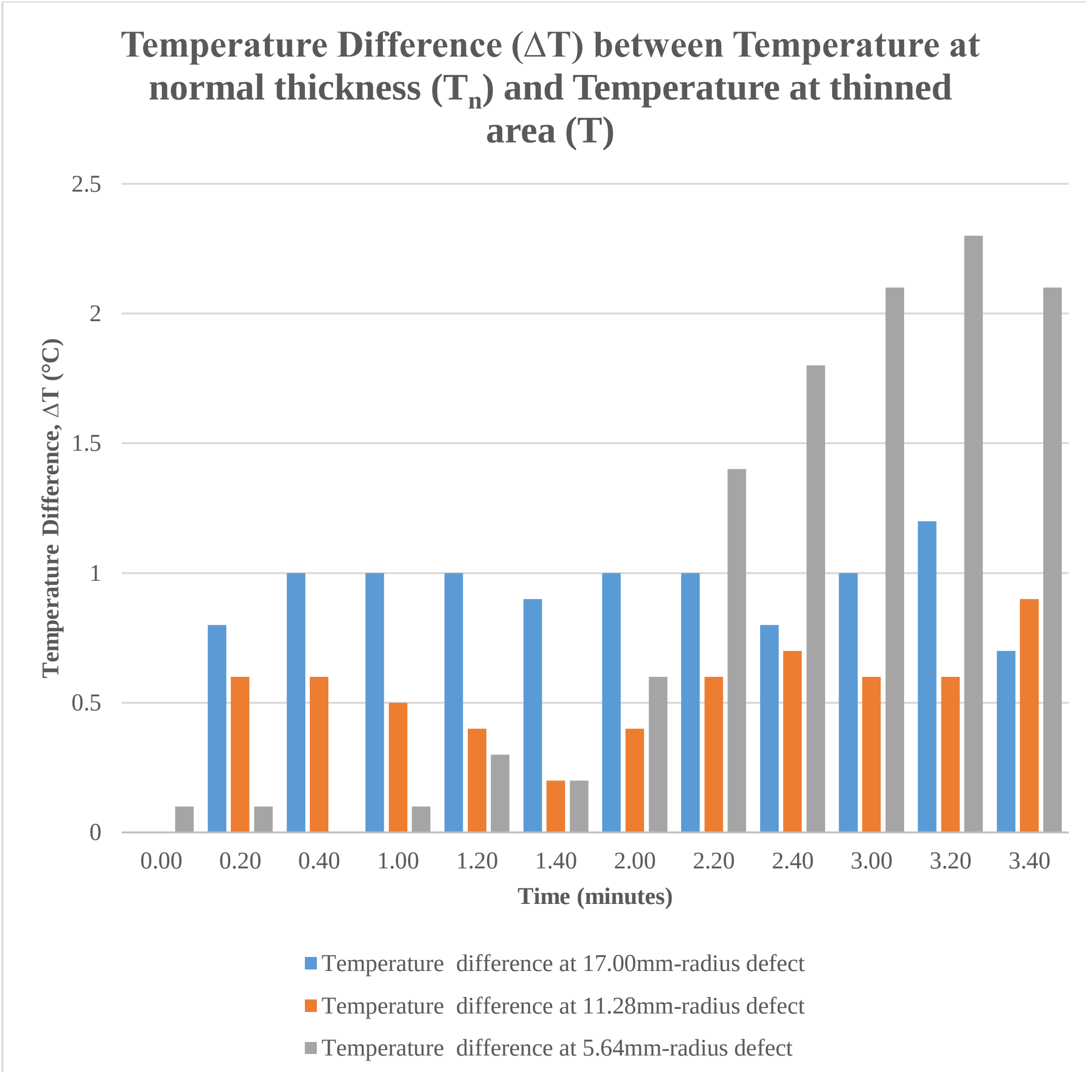

Figure 39: Temperature Difference (ΔT) between Temperature at normal thickness, (Tn) and Temperature at thinned area (T) for IRT-S2 (50% mass loss)

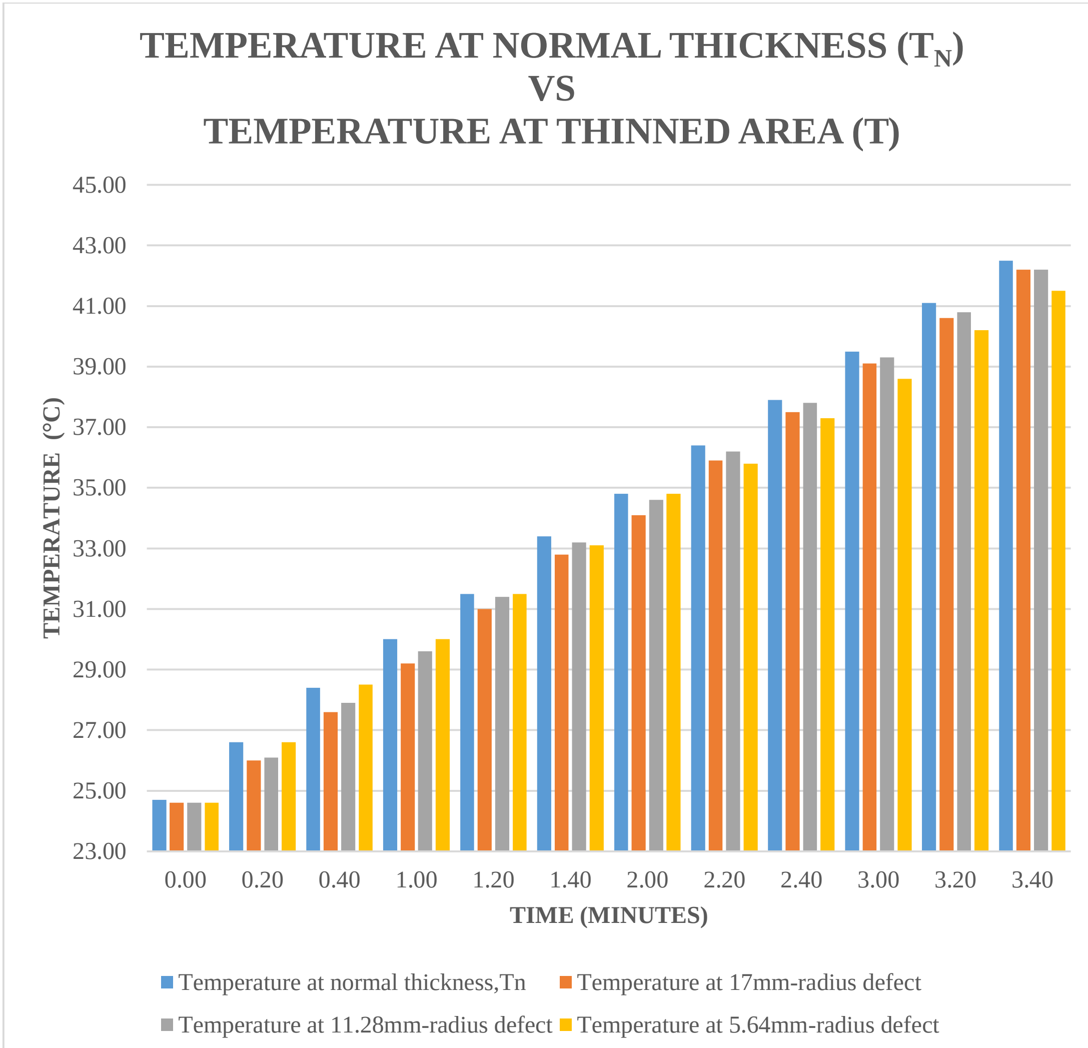

Figure 40: Temperature at normal thickness, (Tn) VS Temperature at thinned area (T) for IRT-S3 (25% mass loss)

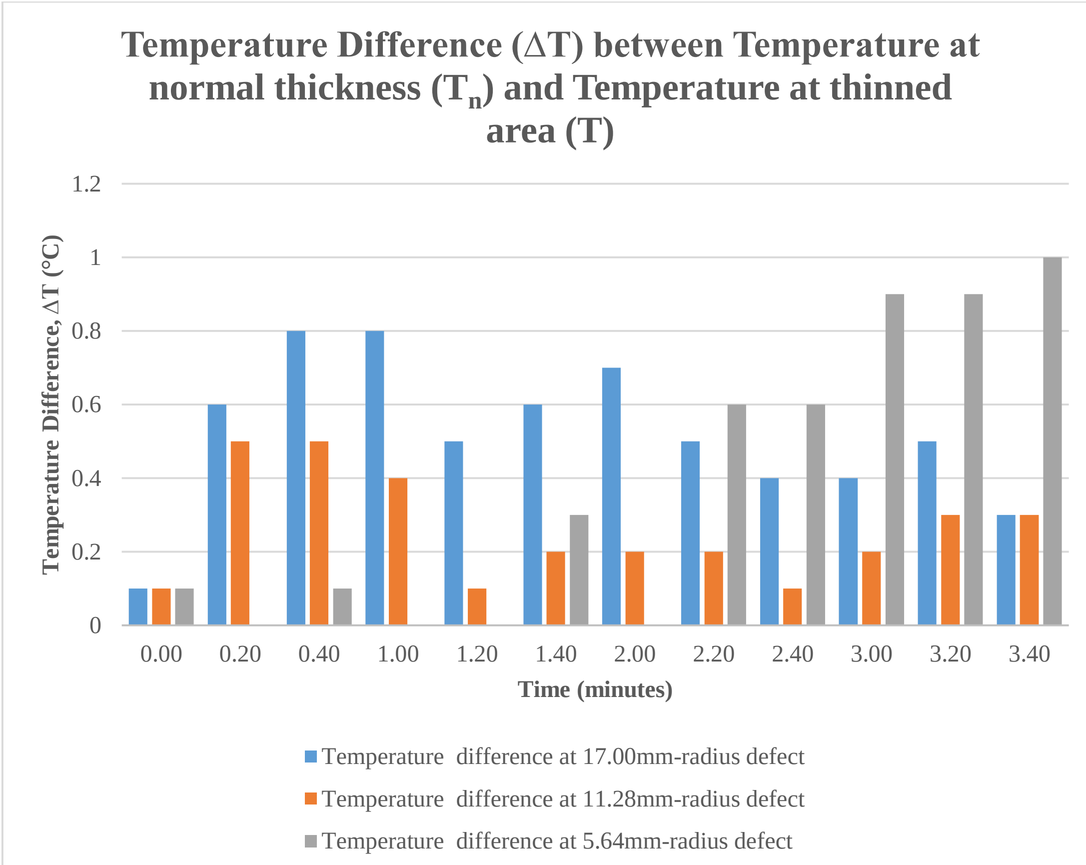

Figure 41: Temperature Difference (ΔT) between Temperature at normal thickness, (Tn) and Temperature at thinned area (T) for IRT-S3 (25% mass loss)

4.4. Data analysis - Infrared Thermography Experiment II

The value of Temperature Difference, ΔT can be obtained by using the formula in **Equation 2.**

$$\Delta T = |\ Tc\ - Tn\ | \qquad \text{------------------------------------} \textbf{ Equation 2}$$

Where,

ΔT = Temperature Difference (ºC)

T_n = Temperature at normal thickness (ºC)

T_c = Temperature at corroded area (ºC)

Figure 42 shows a Temperature at normal thickness, T_n VS Temperature at corroded area, T_c for steel plate sample IRT-S4.

While **Figure 43** shows Temperature Difference, ΔT between Temperature at corroded area (T_c) and Temperature at normal thickness (T_n).

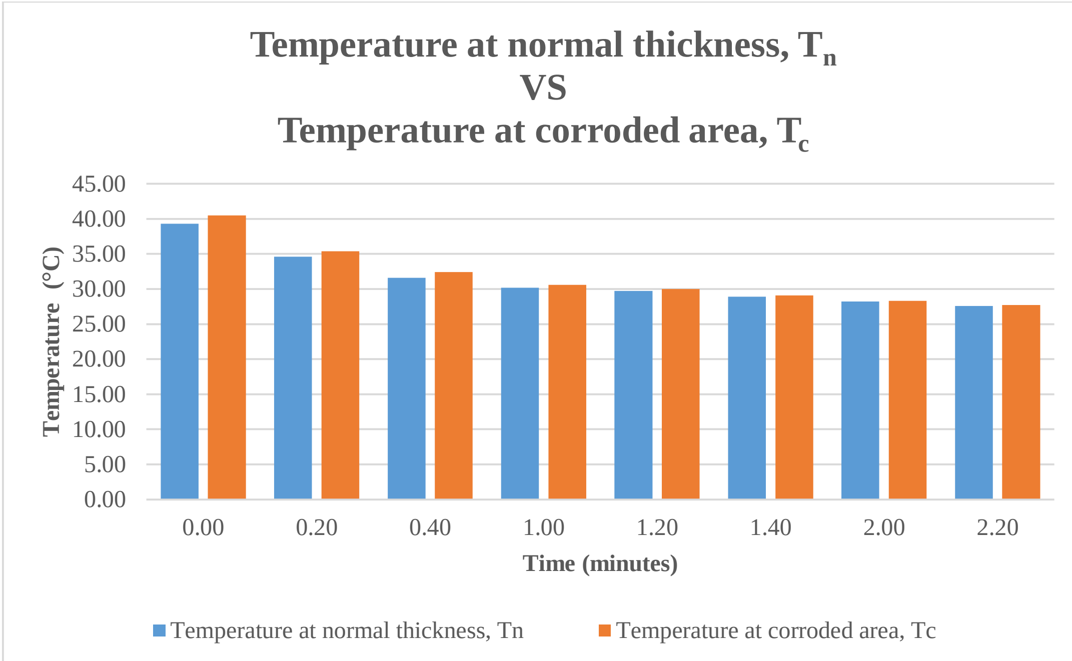

Figure 42: Temperature at normal thickness, (Tn) VS Temperature at corroded area (Tc) for steel plate sample IRT-S4

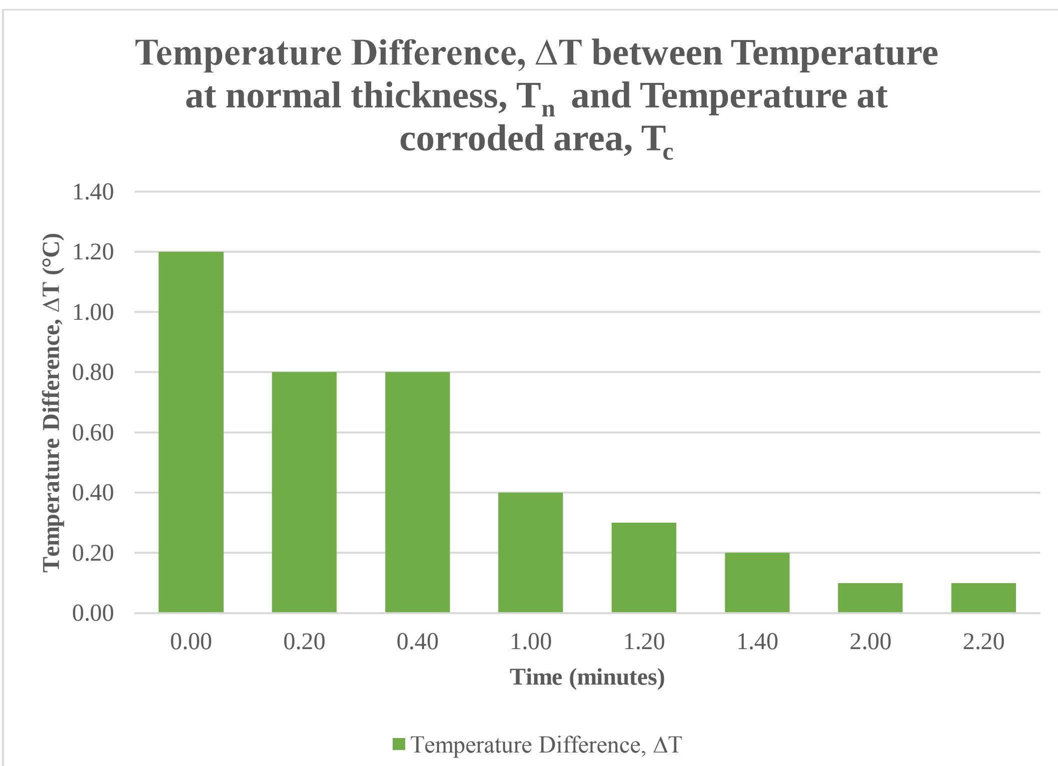

Figure 43: Temperature Difference (ΔT) between Temperature at normal thickness, (Tn) and Temperature at corroded area (Tc)

4.5. Discussion

4.5.1. Infrared Thermography Experiment I

Through qualitative interpretation on the images obtained, it is proven that active infrared thermography can detect metal thinning by using active infrared thermography method. Using normal visual inspection, it is impossible to detect the defects hidden at the back of the steel plates. However, by using active infrared thermography method, the detection of the defects is possible. Refer **Figure 4.1**.

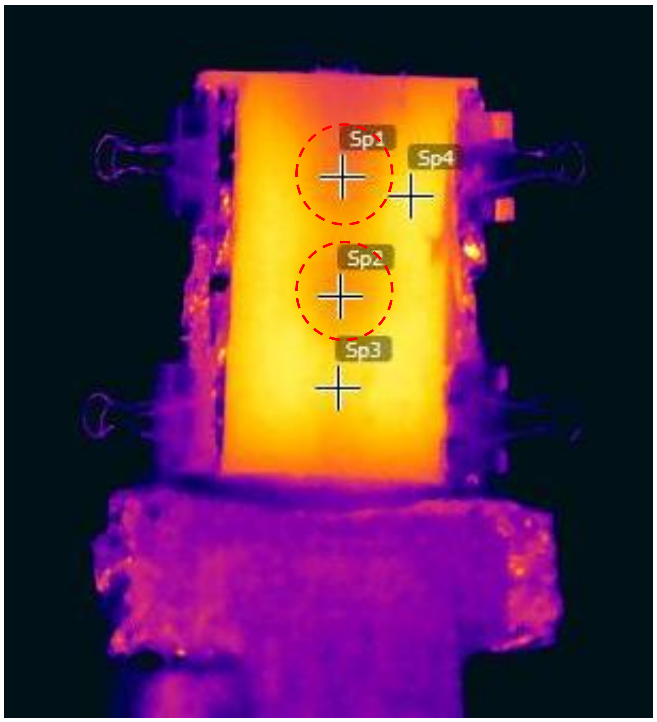

Figure 44: Infrared image during 0.20 minutes for IRT-S1 steel plate. Note that the thinning behind the plate is detectable and spotted (in circular markings)

The detection is possible due to the discontinuity of the steel volume is disturbing the heat flux. This disturbance is detected through thermal maps emitted through the surface of heat and eventually captured by the infrared camera. The temperature difference between the normal surface (no thinning) and thinned surface is high enough to be detected, thus leading to a positive confirmation on the hypothesis that mass loss can be identified by using this method.

Transient heat transfer

The experiment is focusing on the heat transfer in transient state, where change in temperature occur. Based on the images taken during the experiment, the defects can be detected starting from time at 0 minute until 1 minute (image at 0 minute, 0.20 minute, 0.40minute, and 1 minute). Images taken after 1 minute are showing a steady state condition of heat transfer thus making the defect detectability is difficult (and causing the data analysis after 1 minutes are not accurate). Refer **Figure 45** and **Figure 463** for comparison.

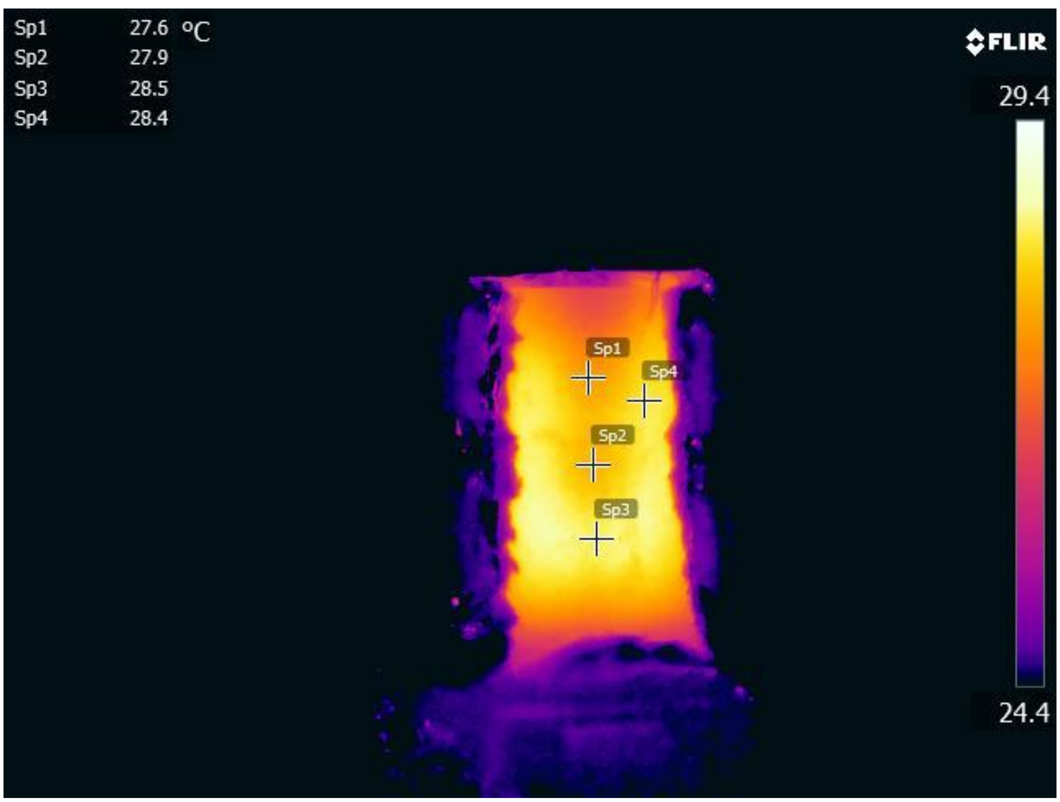

Figure 45: The Infrared image for IRT-S3 at 0.20 minute

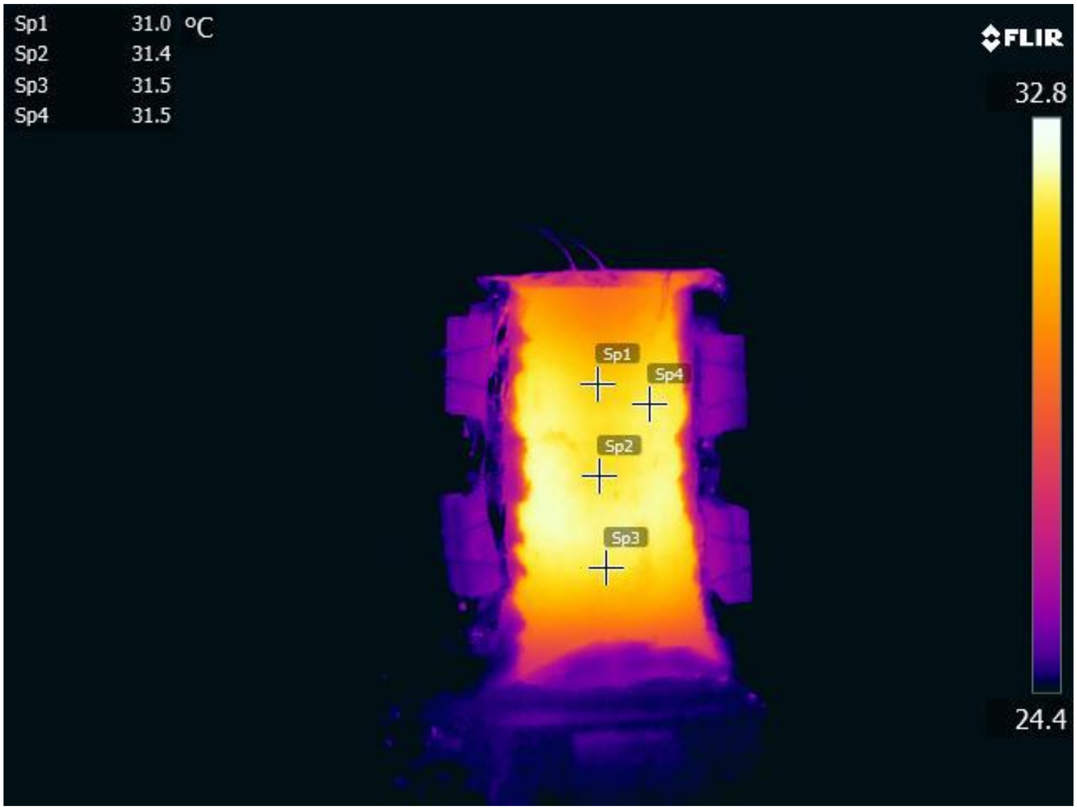

Figure 46: The Infrared image for IRT-S3 at 1.20 minute

Based on **Figure 36**, **Figure 38**, and **Figure 40**, it is shown that the temperatures are different across time due to different in mass loss size and volume. For IRT-S1, IRT-S2 and IRT-S3, defects with 17-mm radius shows the highest temperature difference, followed by the 11.28mm-radius and 5.65-mm radius.

It is also discovered that <u>during within 0 to 1 minute, the 5.64mm defect size image is almost negligible or not visible</u>. This also conform the early hypothesis that as the defect size become smaller, the detectability of the mass loss will be harder due to small volume of mass loss.

According to **Figure 37**, **Figure 39**, and **Figure 41**, it is observed that as the defect size is increasing, the temperature difference with Temperature at normal thickness, T_n is increasing. The 17-mm radius defects yield the highest temperature difference, followed by the 11.28-mm radius defects and lastly by 5.64-mm radius defects.

Also based on the experiment, the difference in depth of mass loss between IRT-S1 (75% mass loss), IRT-S2 (50% mass loss) and IRT-S3 (25% mass loss) does not give much temperature difference value. However, since the project is focusing on qualitative interpretation, thus the results obtained can be used to conclude that Infrared Thermography method can be used to detect mass loss from 25% depth until 75% depth, or more.

In overall, it is safe to conclude that the first objective of this project, which is to qualitatively detect pipe wall thinning or pitting in steel pipe using Active Infrared Thermography method is achieved. The results obtained also contribute to the confidence of the third objective, which is to identify the potential of Active Infrared Thermography as early NDT identification method to detect mass loss.

4.5.2. Infrared Thermography Experiment II

Based on the infrared images taken during Infrared Thermography Experiment II, the qualitative interpretation able to prove that active infrared thermography can detect corrosion under paint by using active infrared thermography method. It is difficult to detect corrosion under paint at the surface of the steel plates through normal visual inspection. However, by using active infrared thermography method, the detection of the defects is possible. Refer **Figure 47**.

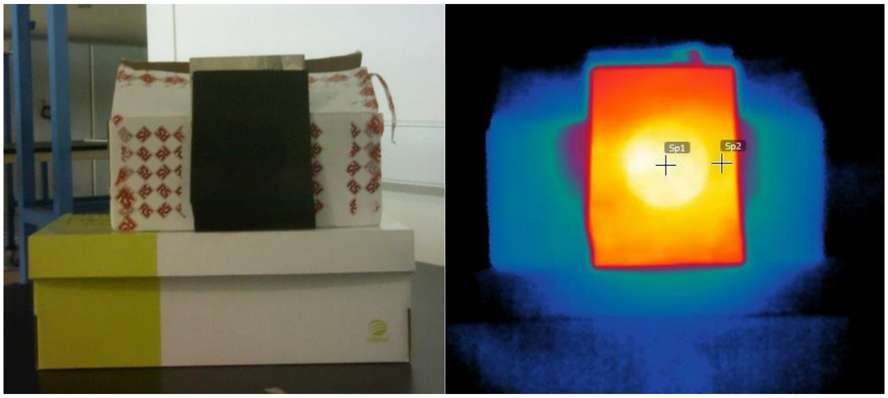

Figure 47: Normal Image (left) compared to Infrared image (right). Note that the corroded area is detected in Infrared Image (in circular marking)

Through analysis using FLIR® software, the temperature difference between Temperature at corroded area (T_c) and Temperature at normal thickness (T_n) was obtained.

Through the image processing analysis, corroded area shows a higher temperature compared to non-corroded area. The reason is that corrosion builds up resistance and resistance causes heat (Peterson, C., 2012). The extra heat causes by the corrosion will results to un-uniform heat flow. The un-uniform heat flow then are portrayed in thermal maps of the steel surface and eventually detected by infrared camera.

Based on **Graph 8**, the temperature difference is high enough and detectable to observe the temperature change between the two surface conditions. Therefore, the second objective of the experiment which is to qualitatively detect corrosion under paint at the surface of steel pipe using Active Infrared Thermography method is a success. The results also contribute to the confidence of potential of Active Infrared Thermography as early NDT identification method to detect corrosion under paint in steel surface.

Cooling effect

For Infrared Thermography Experiment II, the method of cooling is used to detect the corrosion under paint. It is because the heat simulation used in the experiment is a spotlight. The spotlight heat the surface of the steel plate and removed after 15 seconds, (refer **Figure 4.5**) and the infrared images will be taken. This verify on why the trend in **Graph 7** and **Graph 8** is showing a decreasing regression, compared to **Graph 1** through **Graph 6**.

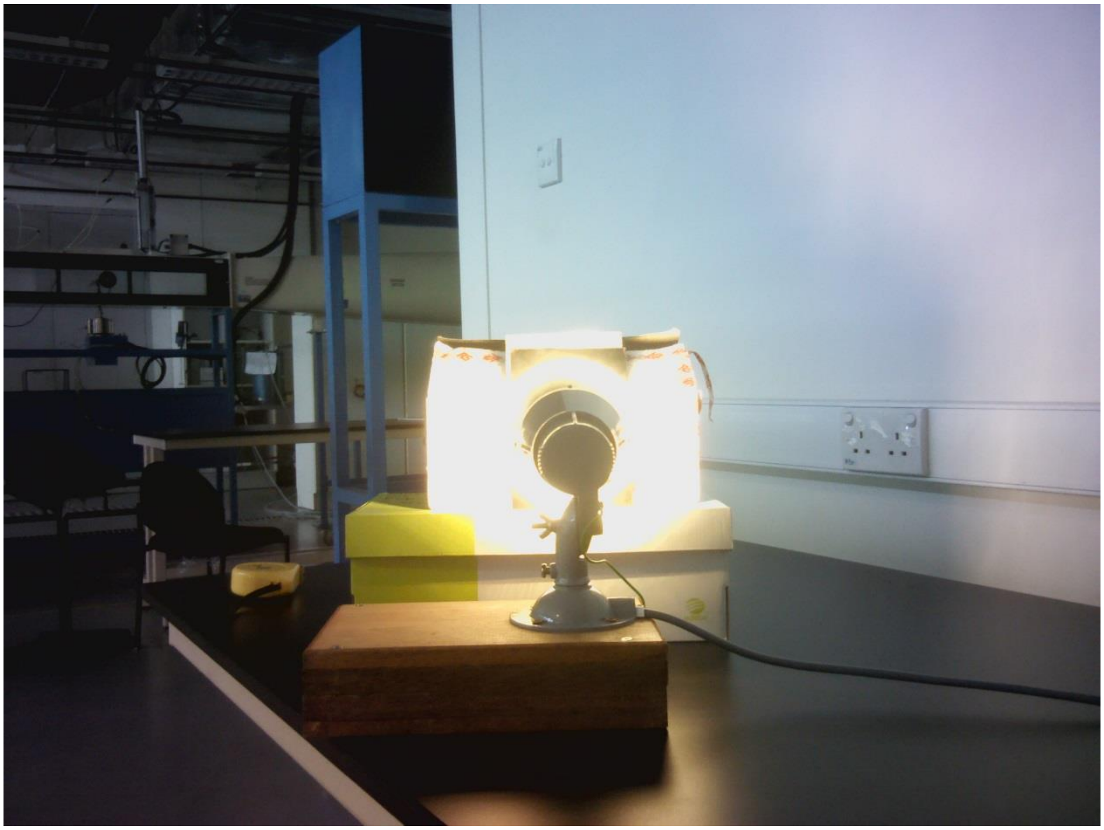

Figure 48: Using spotlight as heat stimulation equipment in Infrared Thermography Experiment II

CHAPTER 5

5. CONCLUSION AND RECOMMENDATION

Based on the results obtained in **Project Activity 2** and **Project Activity 4** respectively, the first and second objective of the project are successfully achieved. Both pipe wall thinning and corrosion under paint can be detected through infrared thermography method.

In addition, from the success of **Project Activity 1** until **Project Activity 4**, the research successfully fulfil the third objective, which is to identify the potential of Active Infrared Thermography. There is a high potential for the method to be implemented in the industry as early identification method and complementary to NDT process to detect mass loss and corrosion under paint in steel surface

5.1. Recommendation

Based on discussion with FYP Supervisor, it is proposed that a new heater mat configuration can be applied to the experiment setup for **Project Activity 2**. The objective of the new configuration is to enhance and improve heat transfer from the mat to the steel, thus contributing towards better experiment results. The proposed new configuration also will be used to confirm the uniformity of the heat transfer of the current configuration. Refer **Figure 5.1** for the current configuration setup VS. proposed configuration setup.

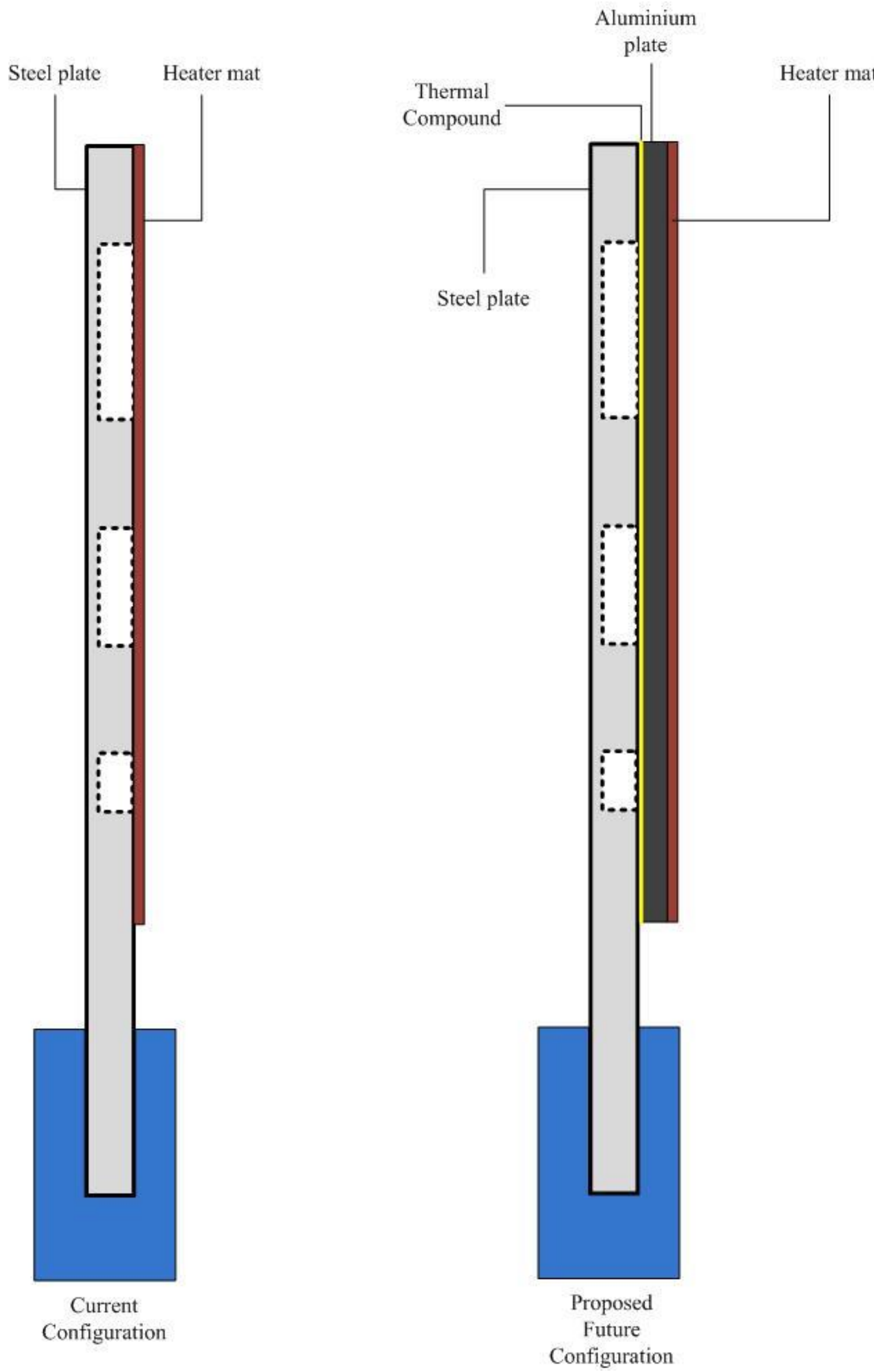

Figure 49: Current heater mat configuration VS. Proposed Future Configuration

5.2. Lesson learnt, problem faced and solutions.

There are few recommendations for future project work, which are listed as follows:

1. Book CNC Machine earlier to avoid last-minute long queue because the machine also is shared with lab unit and Research Office.
2. When buying steel plates, consider ±3mm of thickness for CNC machining flattening process, in order for the machine to obtain relatively flat surface.
3. When buying heater mat, make sure that the area of the mat is fit with the area of the steel plates.
4. Buy heater mat from a reputable company such as RS Malaysia to avoid any problem with the specification of the material.
5. Use foam type of insulator for better heat insulation.
6. To obtain a better thermal image, the experiment can be done in Dark Room available in Block 16.
7. Find a better method to heat the pipe in real-life application, such as flash-light heater or heater gun to obtain efficient heating.

REFERENCES

Ahn, S. N. (2001). *Fracture Behavior of Straight Pipe and Elbow with Local Wall Thinning*. Busan, South Korea; Hitachi, Japan.: Pukyong National University; Yokohama National University.

Alexander Steel, AMCOM CPO.NDT. (2013). *Fabrication of Corrosion Under Paint (CUP) Test Standards and Evaluation of Select Nondestructive Original Equipment Manufacturers' (OEM) Methodology, Process, and Performance to Detect Corrosion Under Paint (Task N.0808).* USA: Executive Agent Office of the Assistant Secretary of the Army for Installations, Energy and Environment, Department of Defense.

Basile, G., Clienti, C., Fargione, G., Geraci, A., & Risitano, A. (2011). *Detection of Defects in Pipelines Using Transient Analysis of Thermal-Induced Flux.* Dipartimento di Ingeneria Industriale e Meccanica, Facoltà, Università di Catania, Italy: FLIR Technical Series, Application Note for Research & Science.

Basrawi, M., & Keck, D. (2003). *Nondestructive Testing Technologies for the Oil Industry.* SPE 13th Middle East Oil Show & Conference.

Bond, L. (26 June, 2012). *NDT Method Summary*. Retrieved from www.ndt-ed.org: http://www.ndt-ed.org/GeneralResources/MethodSummary/MethodSummary.htm

Cool Cosmos & NASA. (23 June, 2013). *Teachers Guide to the Infrared*. Retrieved from coolcosmos.ipac: http://coolcosmos.ipac.caltech.edu/image_galleries/ir_zoo/lessons/background.html

Firdaus, M. (2012). *The Enhancement of NDT Techniques Through Active Thermal Infrared Thermography to Identify Corrosion under Insulation (CUI) in Downstream Piping.* Malaysia: Universiti Teknologi PETRONAS.

Gergenova, Z., Nesteruk, D., & Shiryaev, V. (2005). *Infrared Thermographic Nondestructive Testing System.* XI Modern Technique and Technologies.

Ghali, V., & Mulaveesala, R. (2010). *Comparative Data Processing Approaches for Thermal Wave Imaging Techniques for Non-Destructive Testing.* DOI:10.1007/s1120-011-0059-0.

Grainger QuickTips Technical Resources. (15 July, 2013). *Grainger QuickTips Technical Resources*. Retrieved from Grainger QuickTips Technical Resources: http://www.grainger.com/Grainger/static/thermal-imaging-applications-uses-features-345.html

Hung, Y., Chen, Y., Ng., S., Huang, Y., & et.al. (2009). *Review and Comparison of Shearography and Active Thermography for Non-destructive Evaluation.* China: City University of Hong Kong.

Infrared Training Center. (2011). *Thermography Level 2 Handouts.* Danderyd, Sweden: Infrared Training Center.

Kim, J., & Park, C. (2003). *Effect of Length of Thinning Area on the Failure Behavior of Carbon Steel Pipe Containing a Defect of Wall Thinning.* Daejoen, South Korea: Chosun University; Korea Electric Power Research Institute (KEPRI).

Kim, J., Park, C., & Lee, S. (2009). *ocal Failure Criteria for Wall-Thinning Defect in Piping Components based on Simulated Specimen and Real-Scale Pipe Tests.* Daejon, Republic of Korea: Gwangju University & Korea Electric Power Research Institute.

Madaras, E., & Anastasi, R. (2005). *Terahertz NDE for Under Paint Corrosion Detection and Evaluation.* NASA Langley Research Center, Hampton: Nondestructive Evaluation Sciences Branch.

Malcolm, A. (24 July, 2013). *Some of the Worst Cases of Corrosion*. Retrieved from alanmalmcom.hubpages.com: http://alanmalmcom.hubpages.com/hub/Some-of-the-Worst-Cases-of-Corrosion

McConnel, M. (2010). *Applications of Thermography in Diagnosing Corrosion and Material Issues In Today's Refinery.* NACE Internation Conference & Expo 2010.

Miyazaki, K., Kanno, S., Ishiwata, M., Hasegawa, K., & et.al. (2001). *Fracture and General Yield for Carbon Steel Pipes with Local Wall Thinning.* Japan: Hitachi Ltd., Yokohama National University.

Muniff, M. (2012). *The Enhancement of Non-Destructive Testing through Active Thermal Infrared Thermography to Identify Piping Failure*. Malaysia: Universiti Teknologi PETRONAS.

Peterson, C. (12 July, 2013). *Peterson Predictive Maintenance: Infrared Thermal Imaging*. Retrieved from Peterson Predictive Maintenance: http://www.petersonpredict.com/tech_infraredimaging.php

Raj, B., Jayakumar, T., & Thavasimuthu, M. (2007). *Practical Non-Destructive Testing.* Kalpakkam, India: Alpha Science International Ltd.

Ron Newport Academy of Infrared Thermography. (19 February, 2013). *Detecting Thinning in Pipe Walls Using Infrared Thermography*. Retrieved from Maintenance Resources: http://www.maintenanceresources.com/referencelibrary/ezine/pipethinig.html

Shen, G., & Li, T. (2007). Infrared Thermography for High-Temperature Pressure Pipe. *Insight Vol 49*.

Swiderski, W. (2012). *Detecting Corrosion in Metal Elements of Ammunition by IR Thermography Methods*. Zielonka, Poland: Military Institute of Armament Technology.

Takahashi, K., Kato, A., Ando, K., Hisatsune, M., & et.al. (2006). *Fracture and Deformation Behaviors of Tee Pipe with Local Wall Thinning*. Japan: Yokohama National University, Hitachi Ltd.

Vageswar, A., Balasubraniam, K., Krishnamurthy, C., Jayakumar, T., & Raj, B. (2008). Periscope Infrared Thermography for Local Wall Thinning in Tubes. *NDT&E Int.*, 275-282.

Xu, Z., Wu., X., Li, J., & Kang, Y. (2012). Assessment of Wall Thinning in Insulated Ferromagnetic Pipes Using the Time-to-Peak of Differential Pulsed Eddy-Current Testing Signal. *NDT&E Int*, 51; 24-29.

Yolken, H. T., & Matzanin, G. A. (12 July, 2008). *Detecting Hidden Corrosion*. Retrieved from machinerylubrication.com: www.machinerylubrication.com/Read/1363/detect-corrossion-oil

APPENDICES

APPENDIX I: IRT-S1 Active Infrared Thermography Images

APPENDIX II: IRT-S2 Active Infrared Thermography Images

APPENDIX III: IRT-S3 Active Infrared Thermography Images

APPENDIX IV: IRT-S4 Active Infrared Thermography Images

APPENDIX I

IRT-S1 Active Infrared Thermography Experiment Images

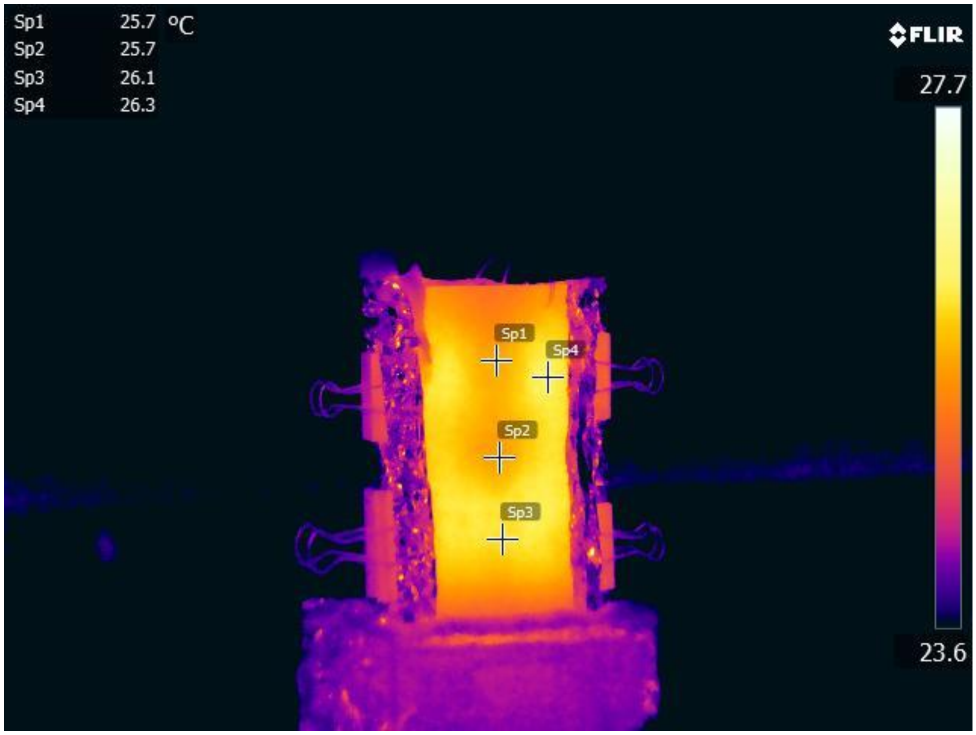

Figure 50: Infrared image at 0.00 min.

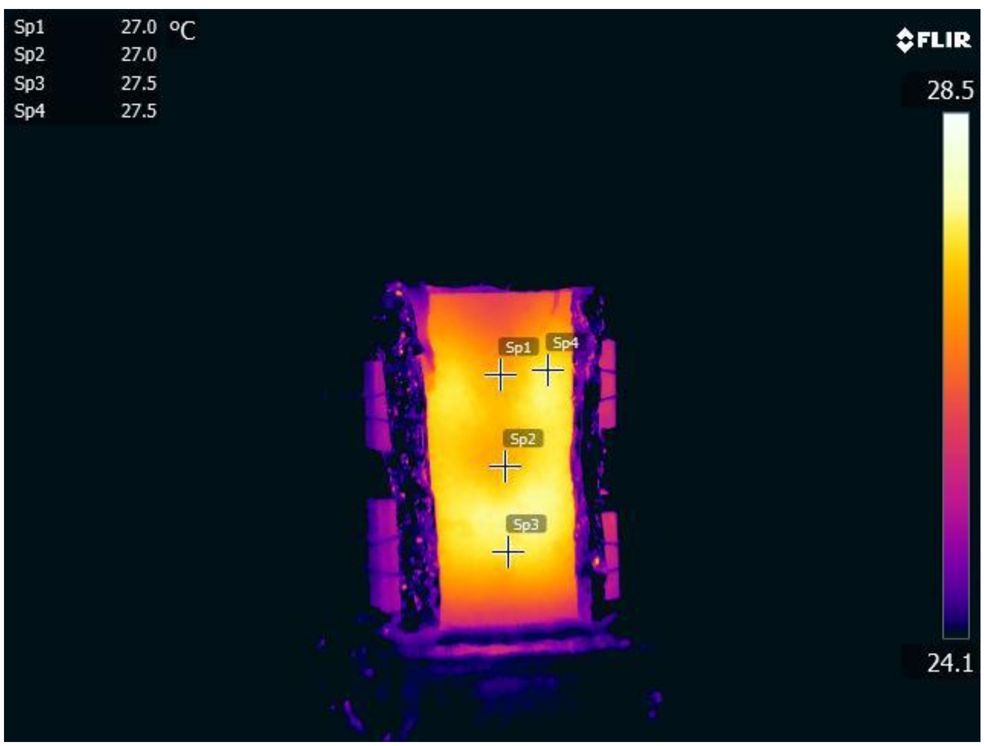

Figure 51: Infrared image at 0.20 min

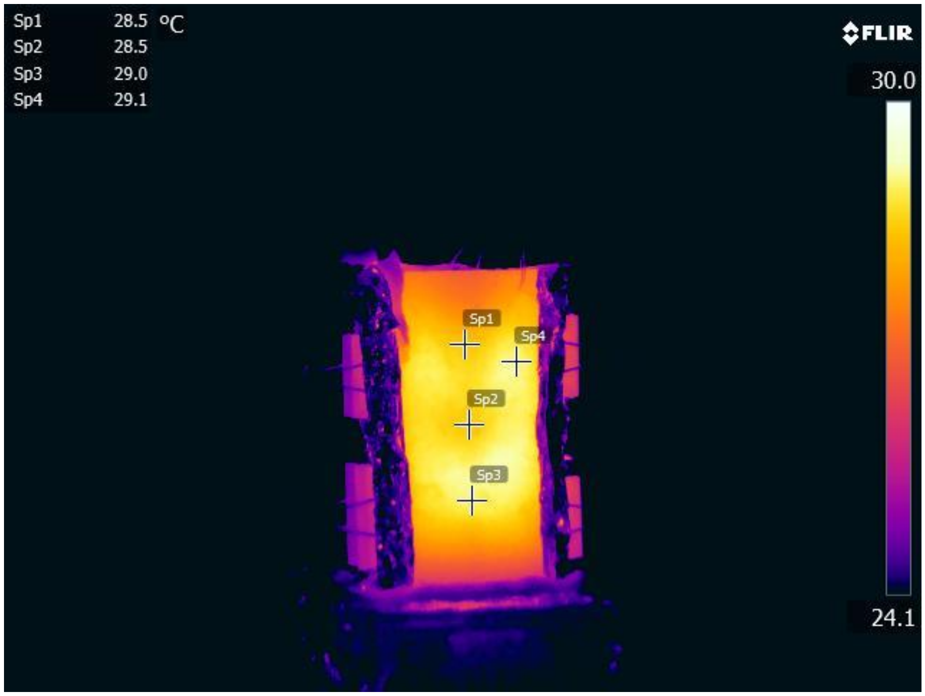

Figure 52: Infrared image at 0.40 min.

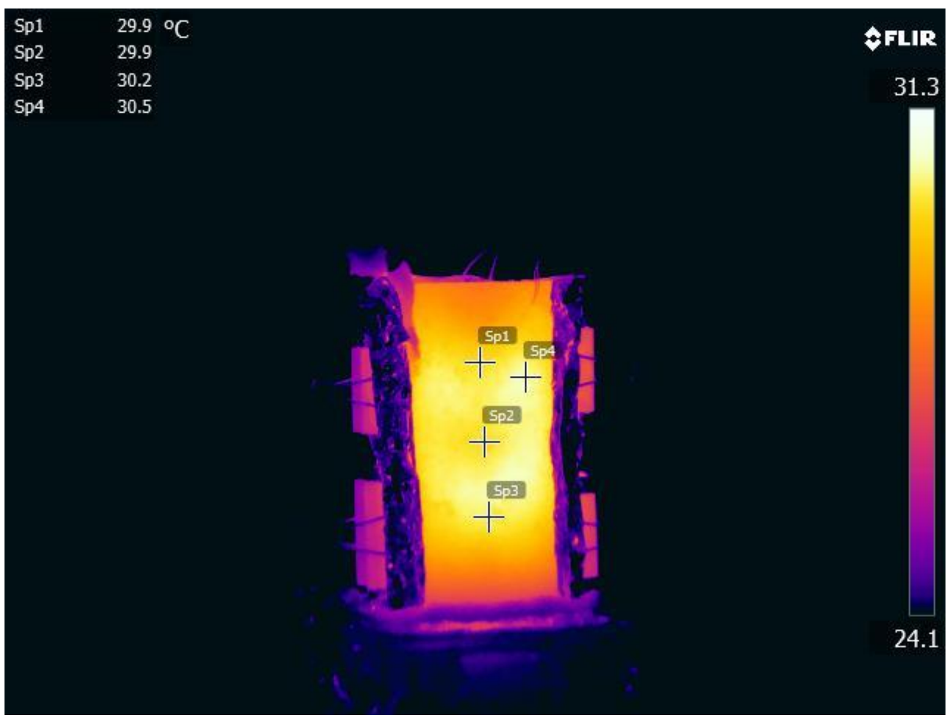

Figure 53: Infrared image at 1.00 min.

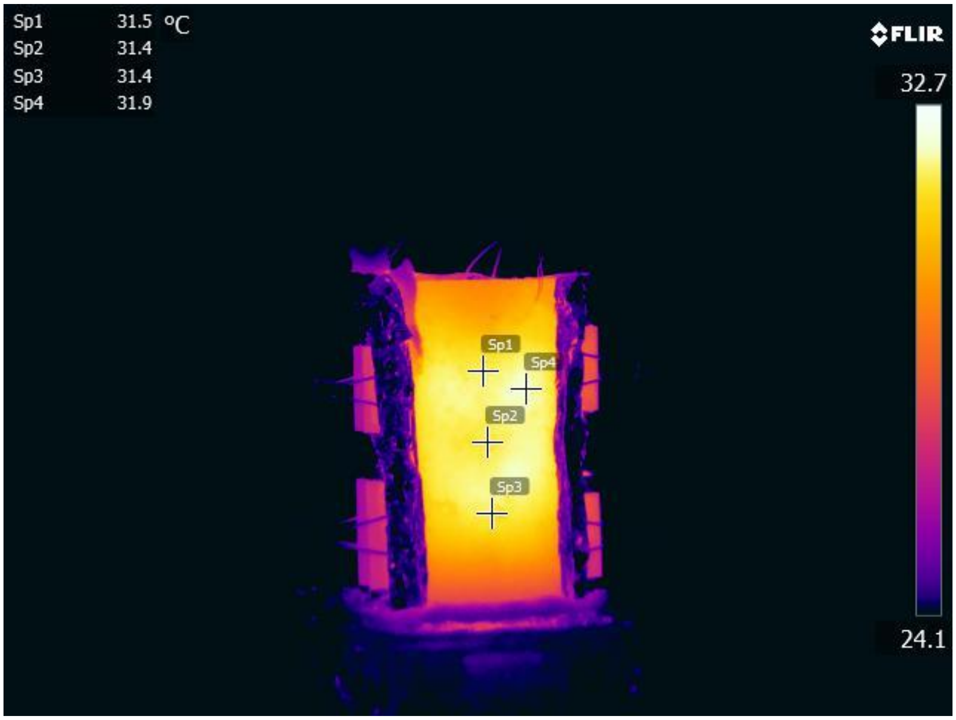

Figure 54: Infrared image at 1.20 min.

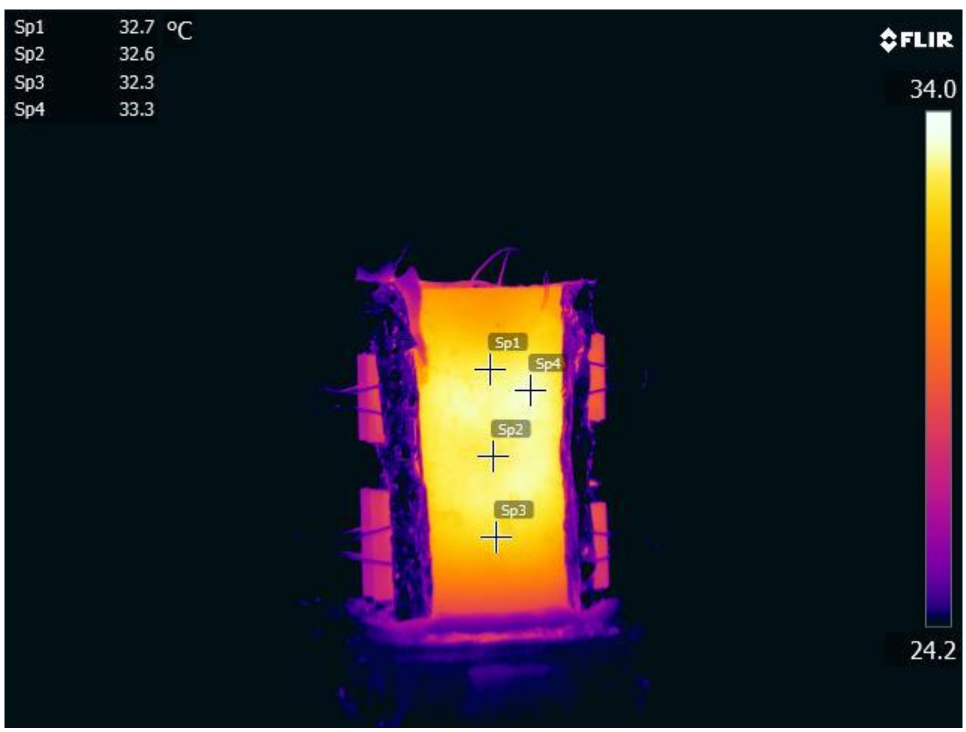

Figure 55: Infrared image at 1.40 min.

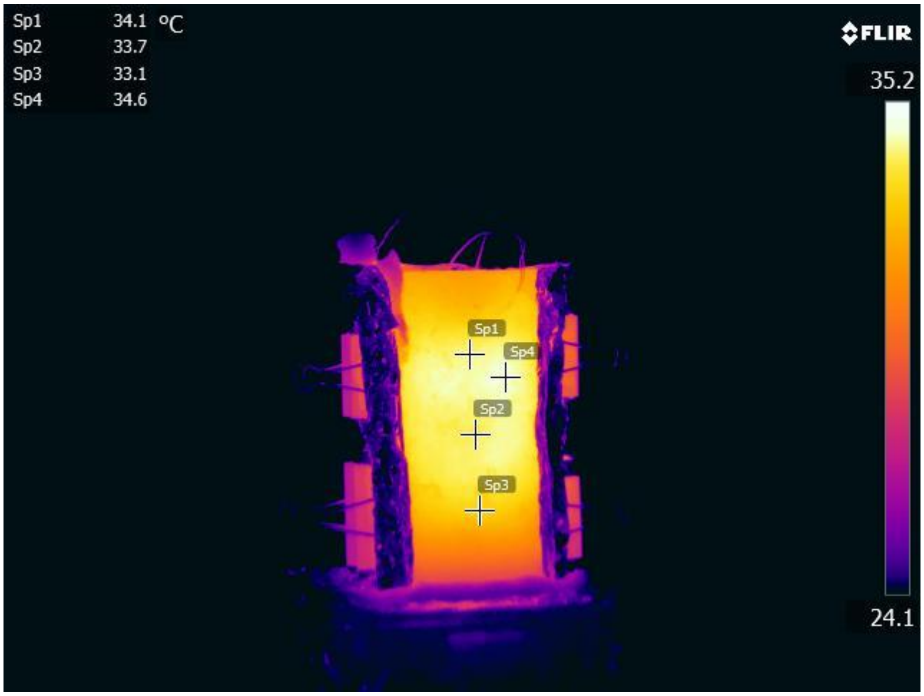

Figure 56: Infrared image at 2.00 min.

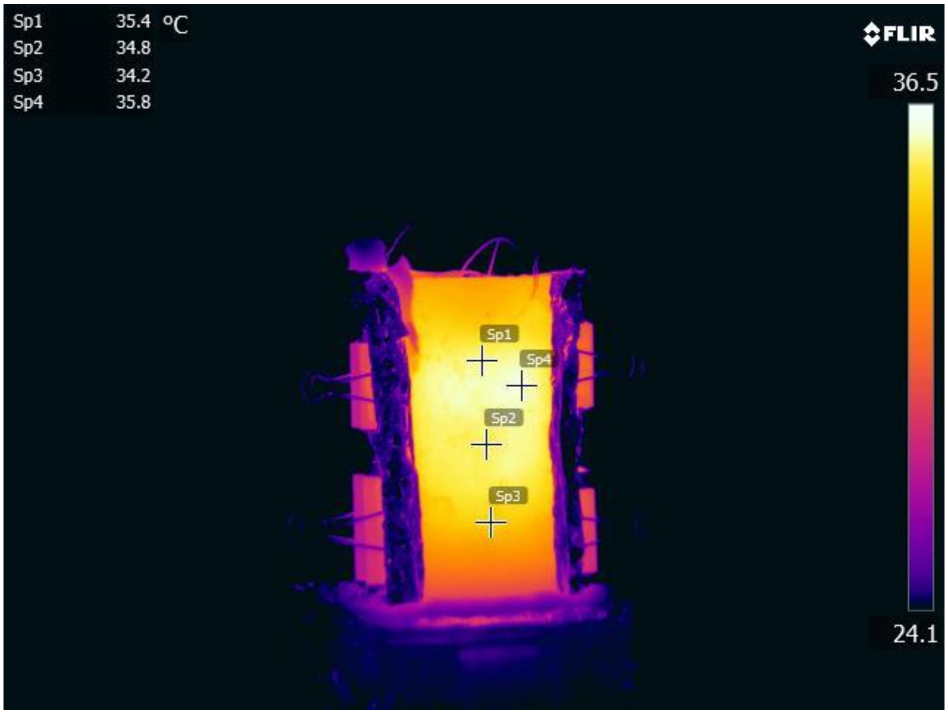

Figure 57: Infrared image at 2.20 min.

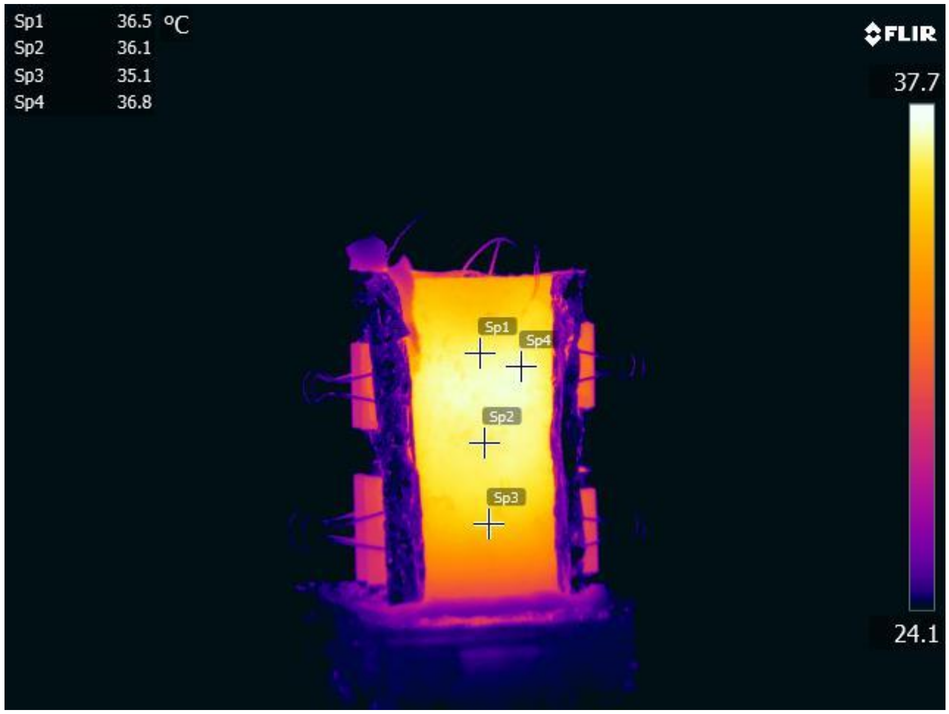

Figure 58: Infrared image at 2.40 min.

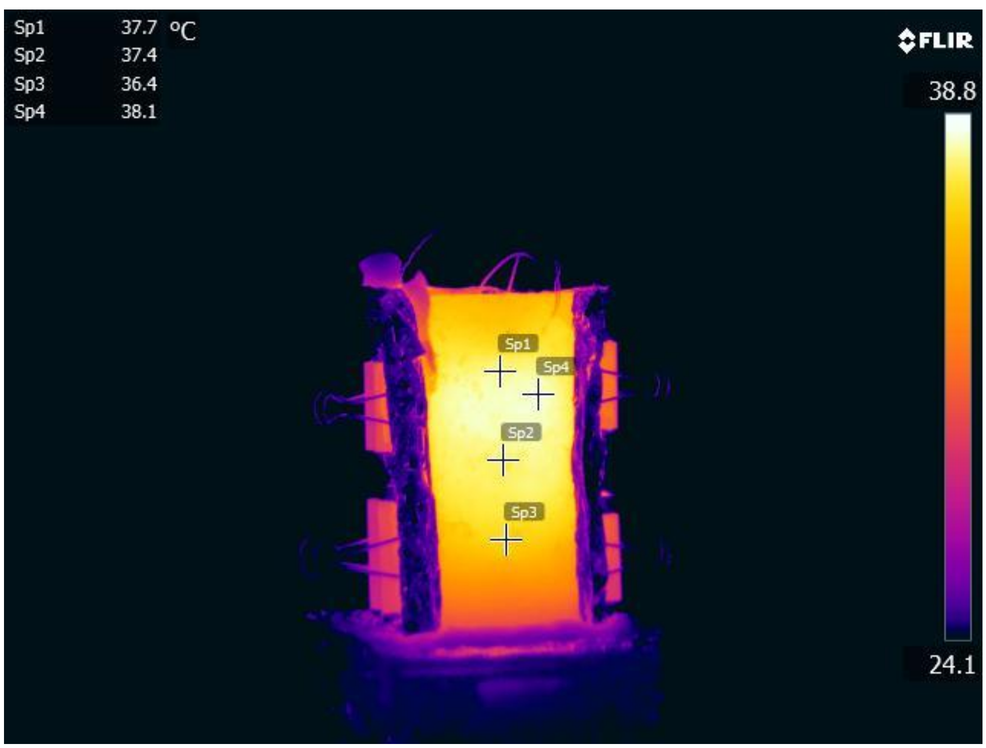

Figure 59: Infrared image at 3.40 min.

APPENDIX II

IRT-S2 Active Infrared Thermography Experiment Images

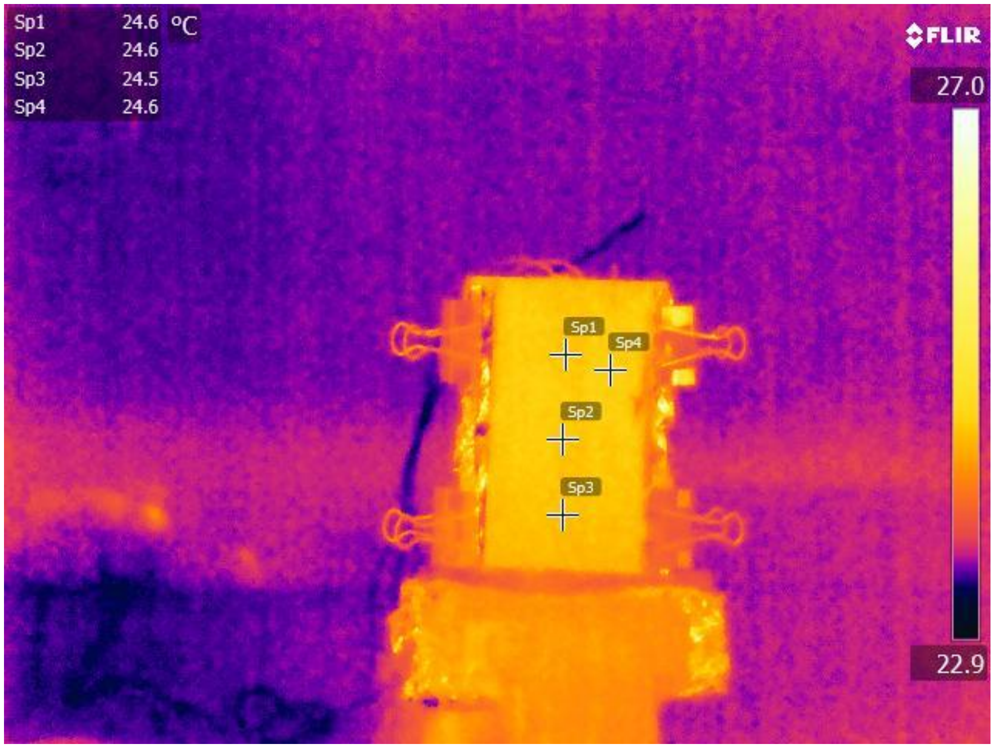

Figure 60: Infrared image at 0.00 min.

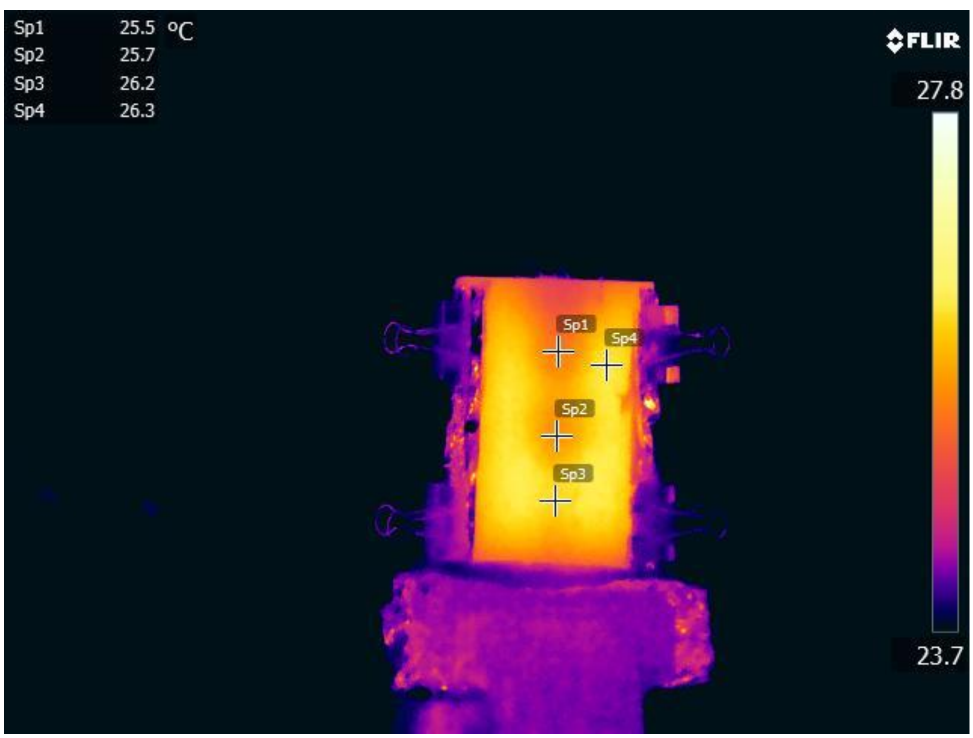

Figure 61: Infrared image at 0.20 min.

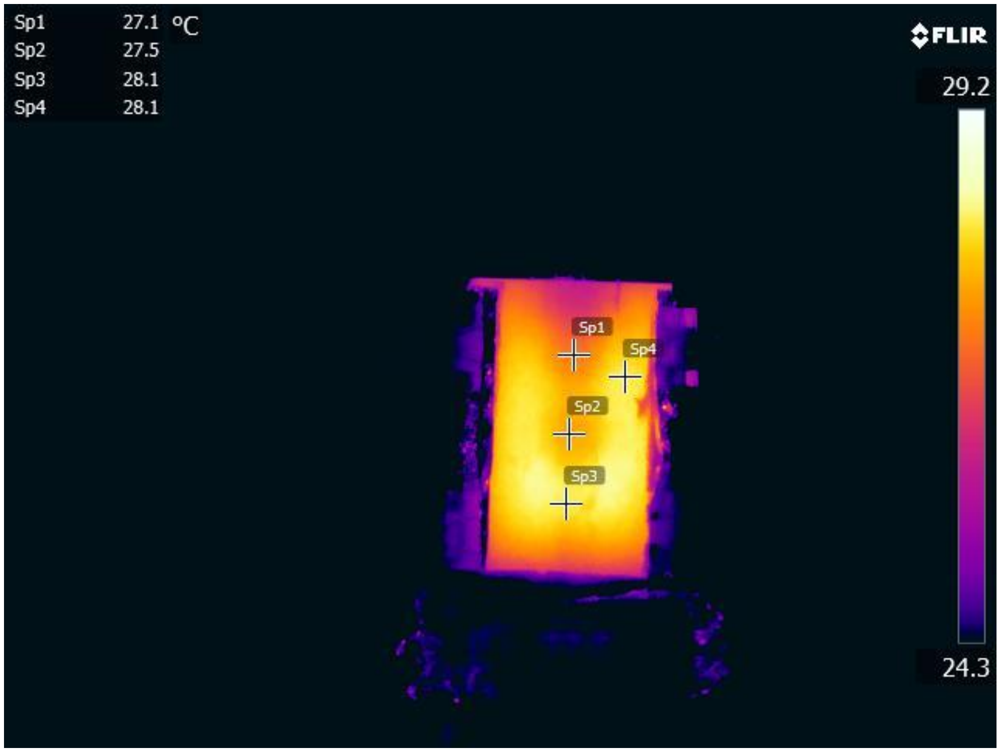

Figure 62: Infrared image at 0.40 min.

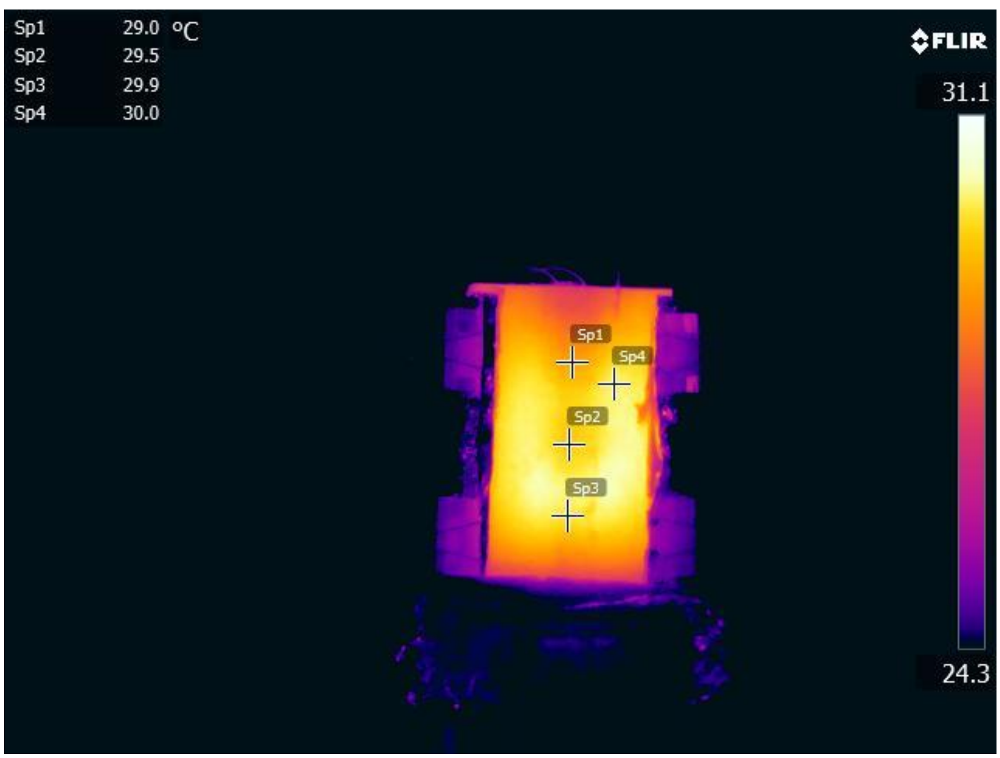

Figure 63: Infrared image at 1.00 min.

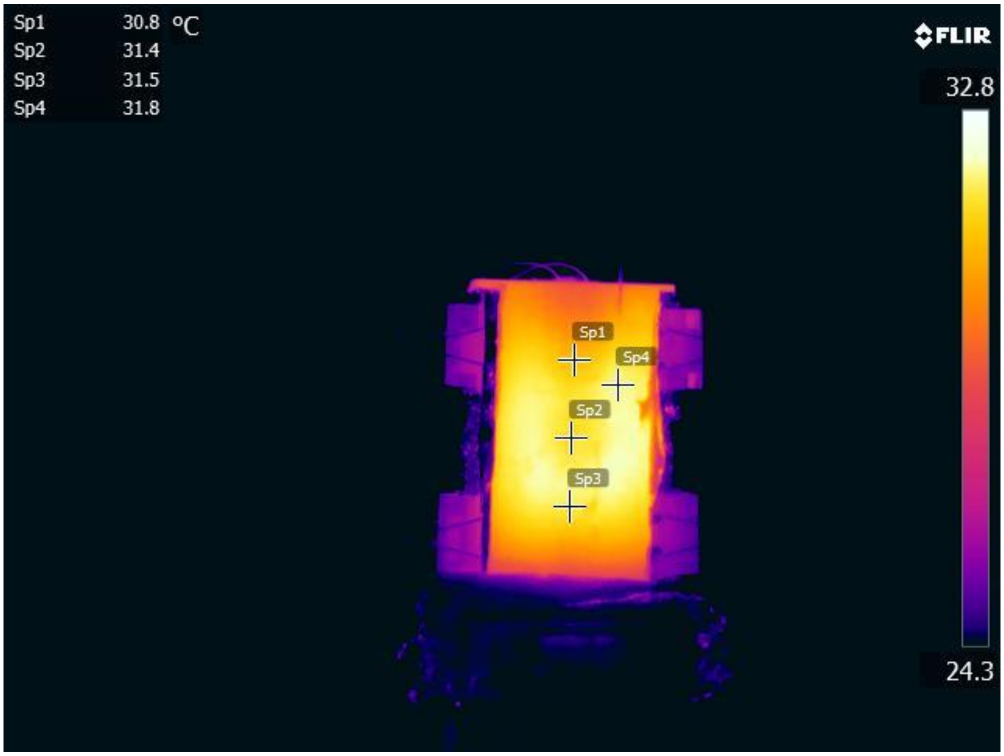

Figure 64: Infrared image at 1.20 min.

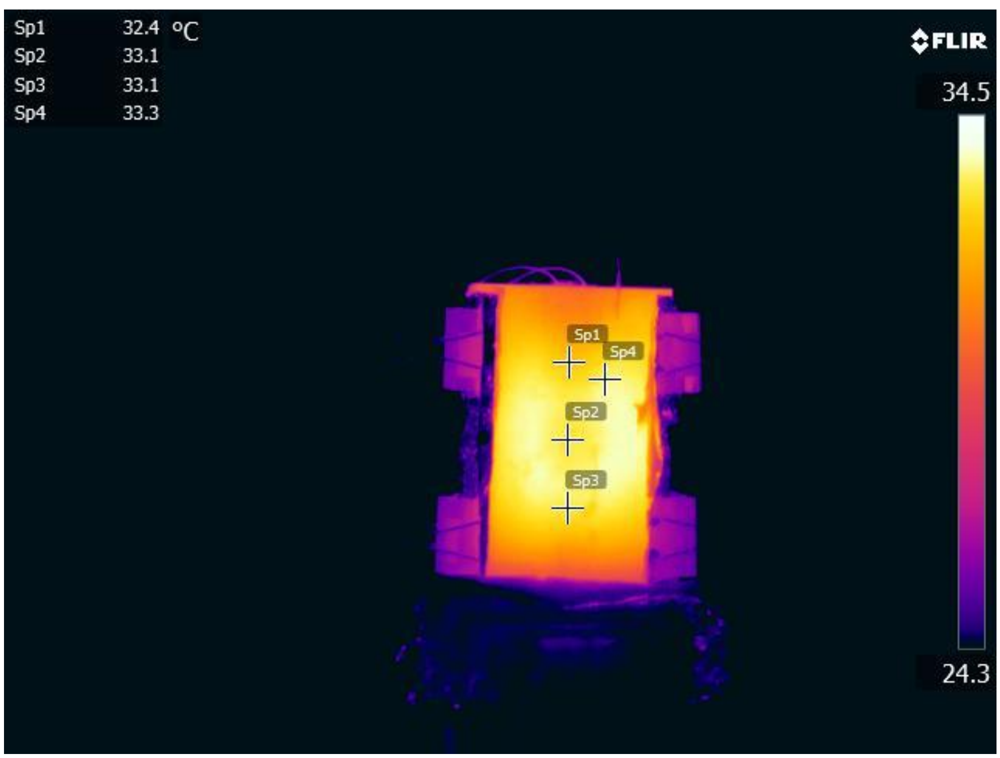

Figure 65: Infrared image at 1.40 min.

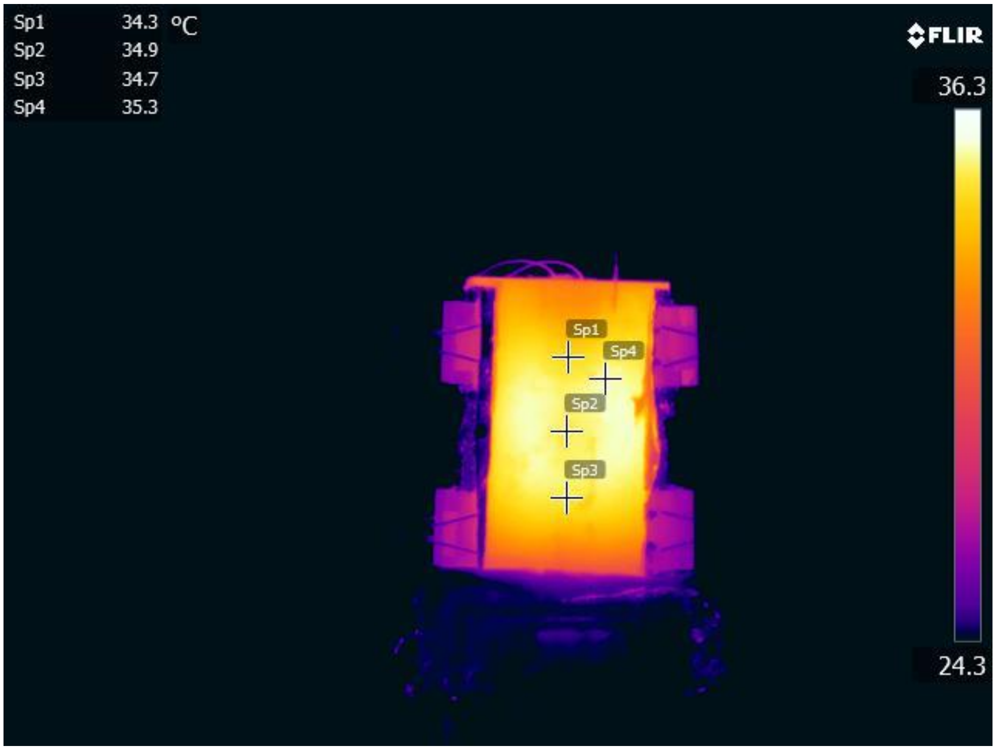

Figure 66: Infrared image at 2.00 min.

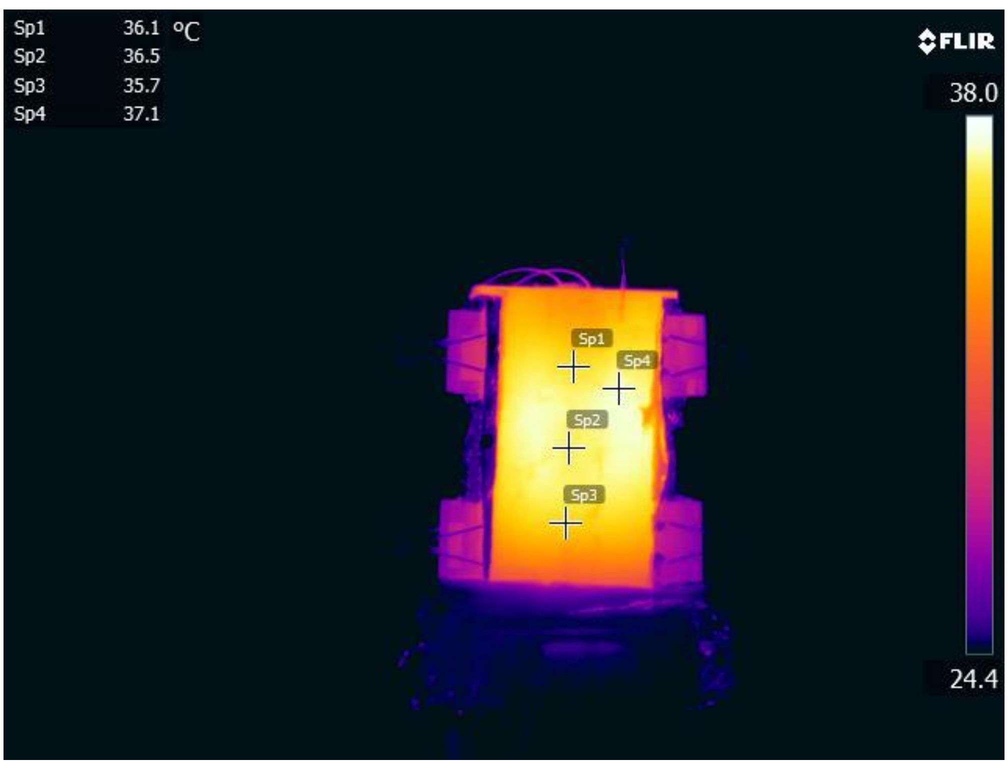

Figure 67: Infrared image at 2.20 min.

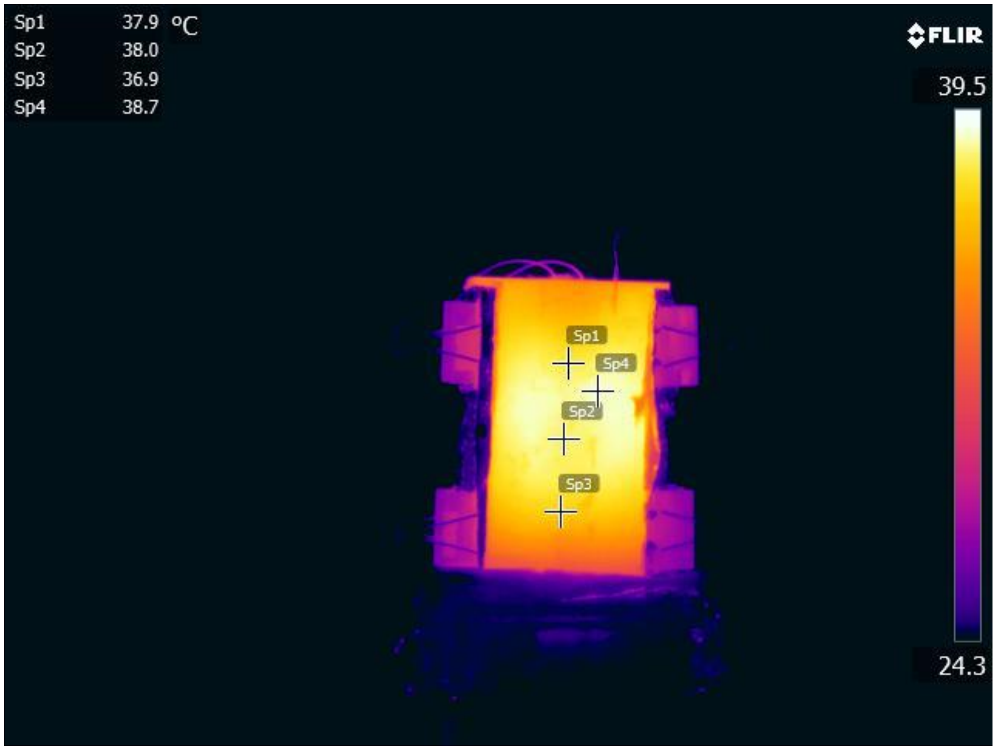

Figure 68: Infrared image at 2.40 min.

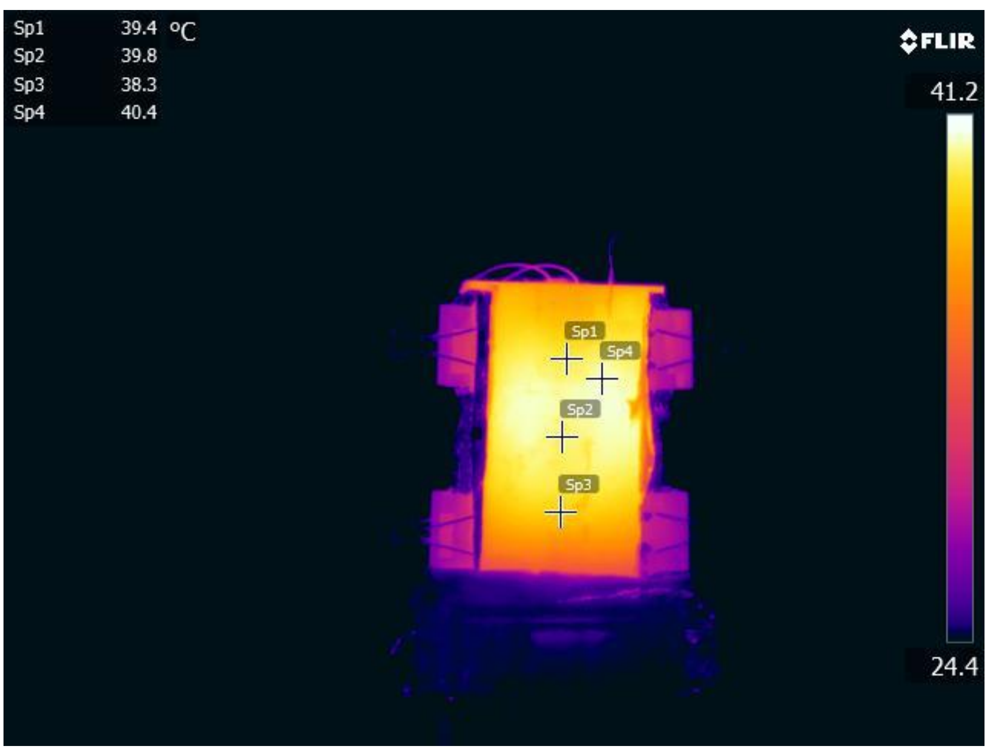

Figure 69: Infrared image at 3.00 min.

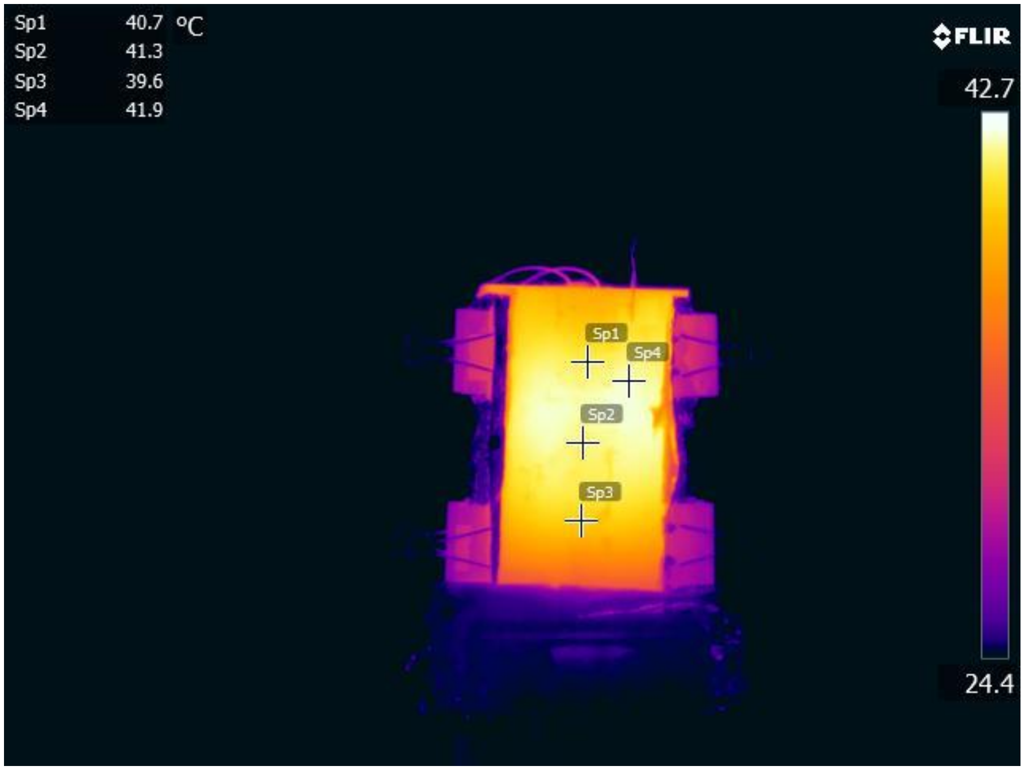

Figure 70: Infrared image at 3.20 min.

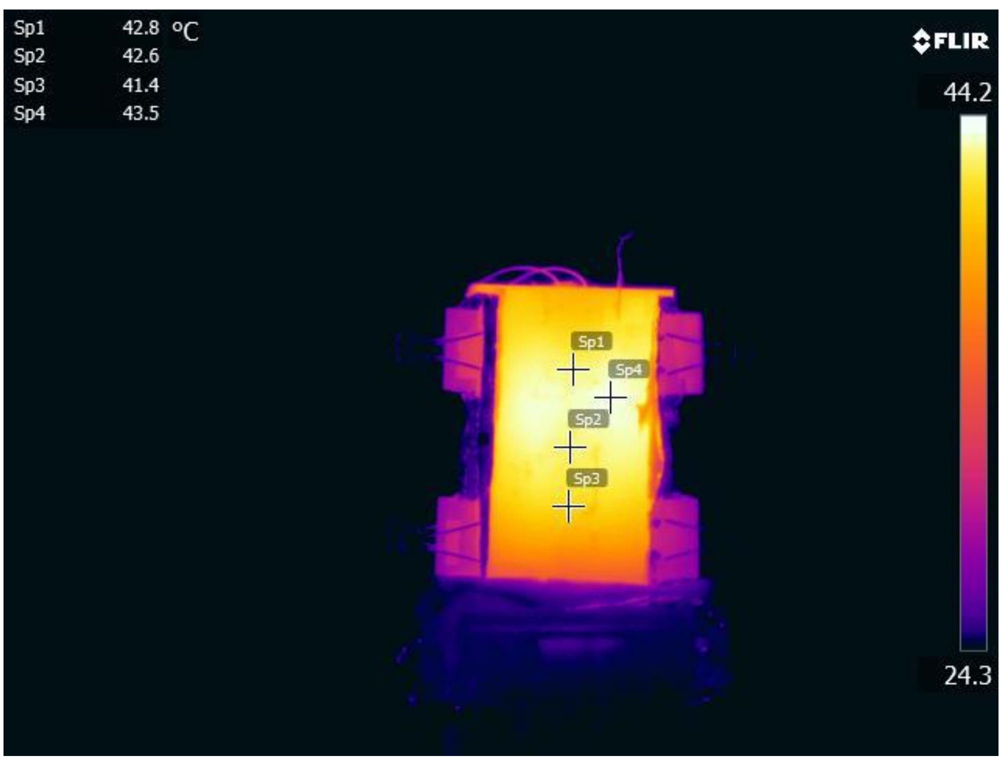

Figure 71: Infrared image at 3.40 min.

APPENDIX III

IRT-S3 Active Infrared Thermography Experiment Images

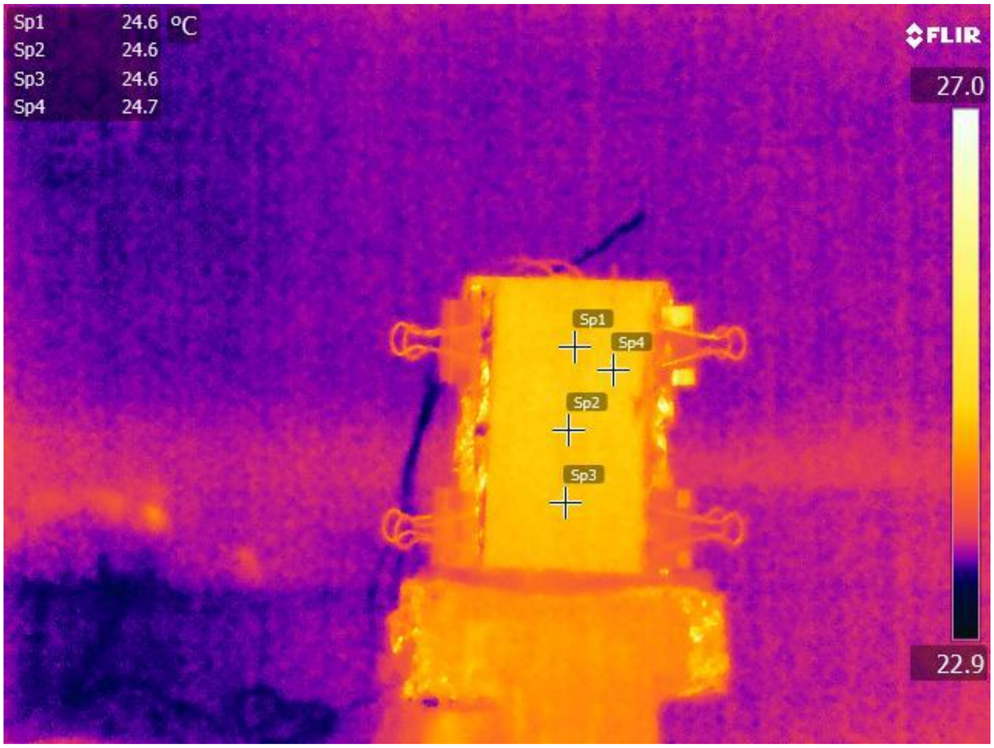

Figure 72: Infrared image at 0.00 min.

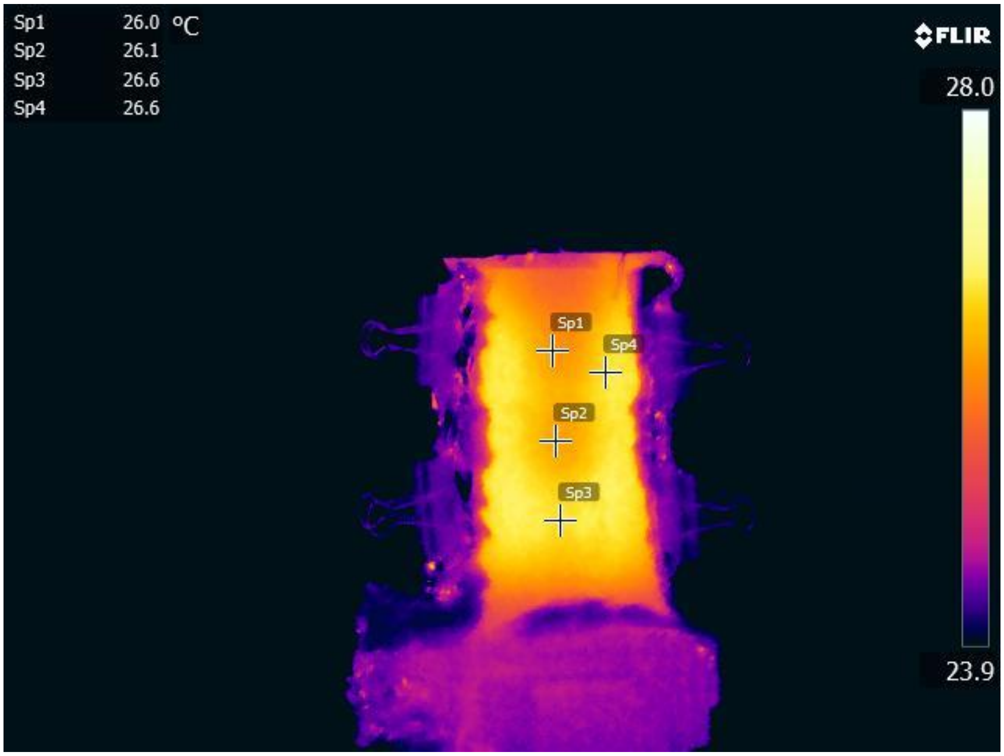

Figure 73: Infrared image at 0.20 min.

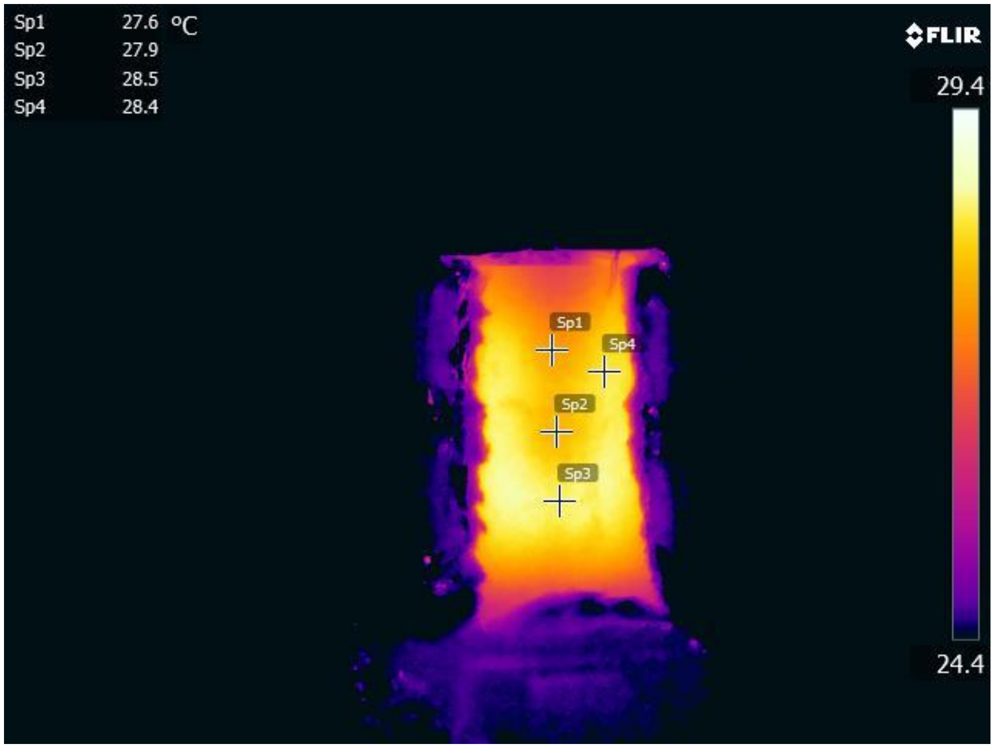

Figure 74: Infrared image at 0.40 min.

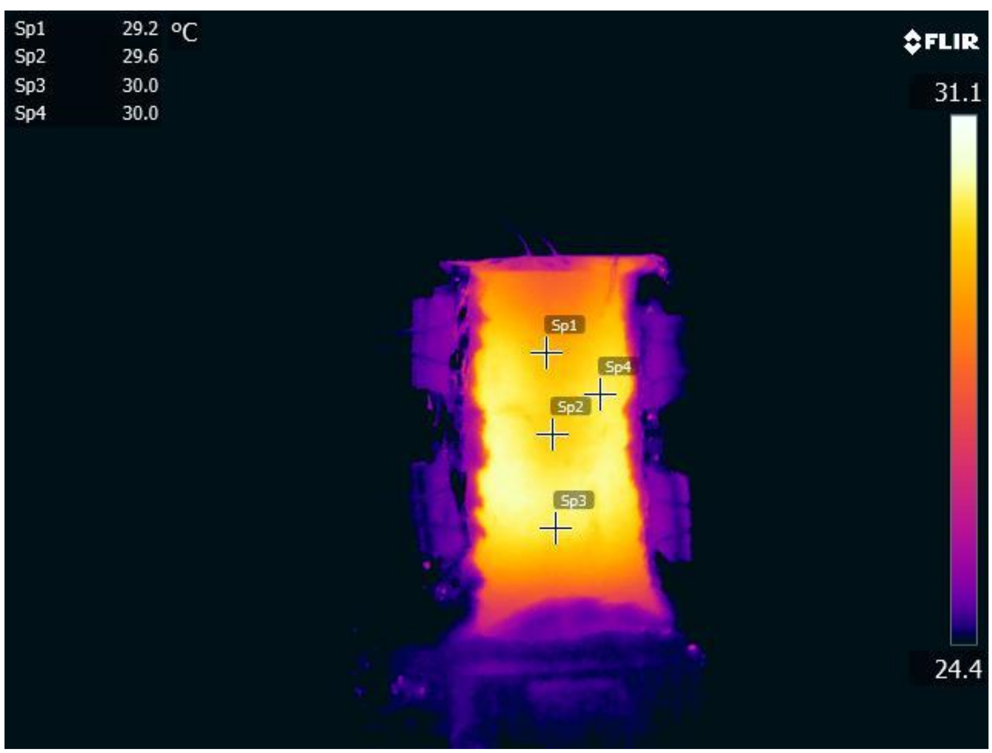

Figure 75: Infrared image at 1.00 min.

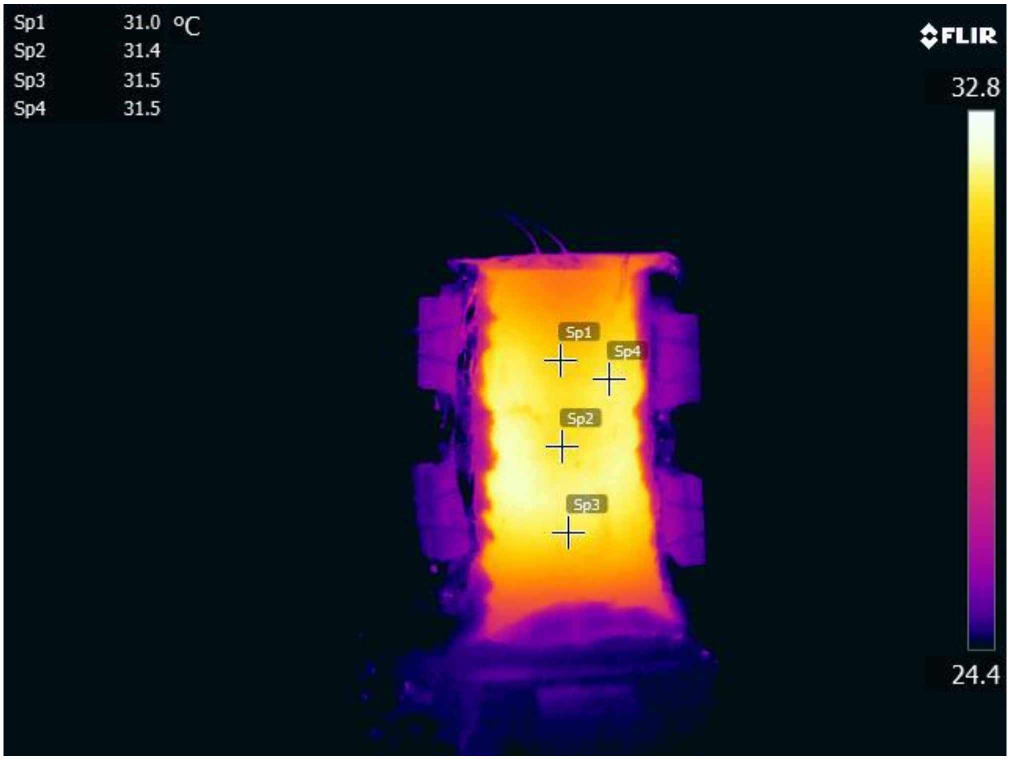

Figure 76: Infrared image at 1.20 min

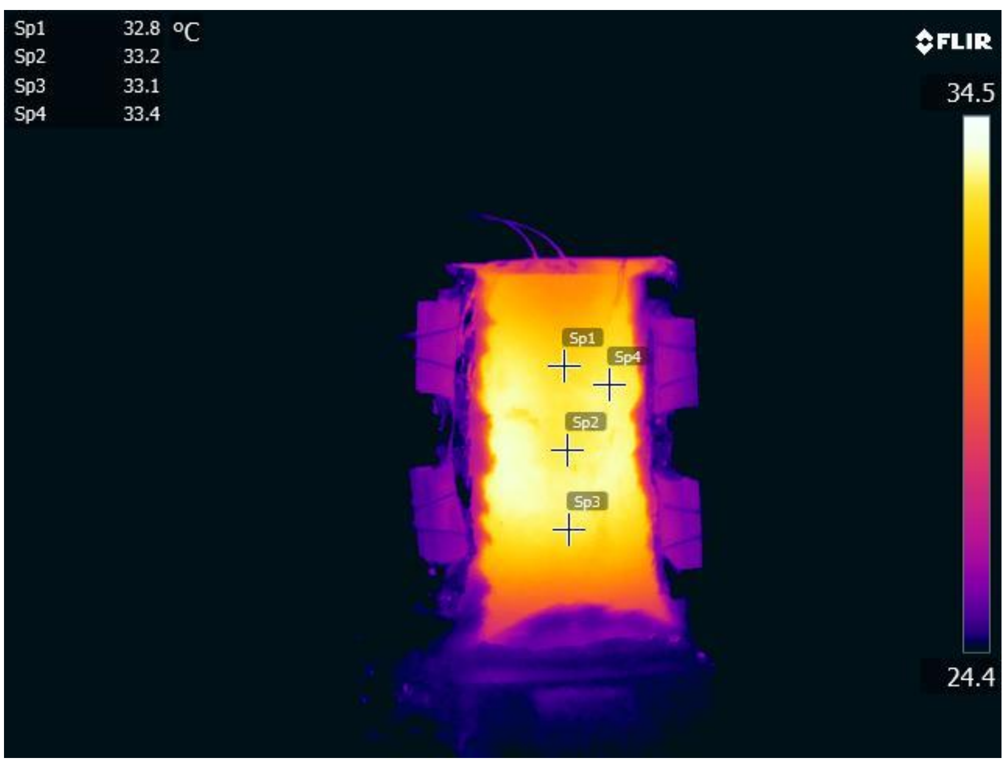

Figure 77: Infrared image at 1.40 min.

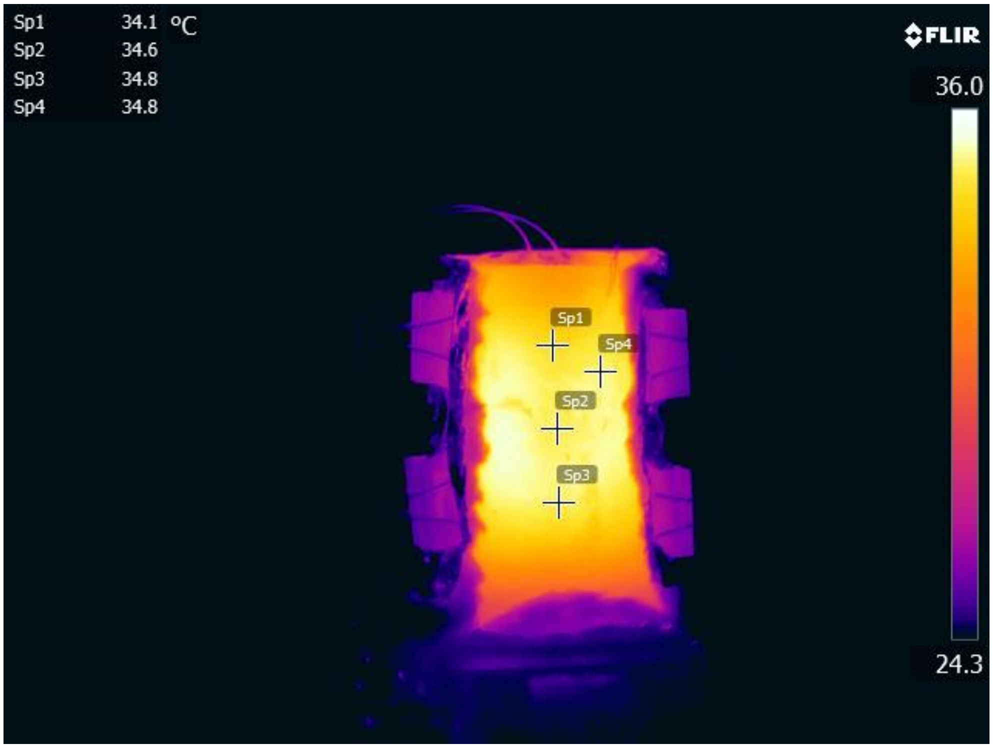

Figure 78: Infrared image at 2.00 min.

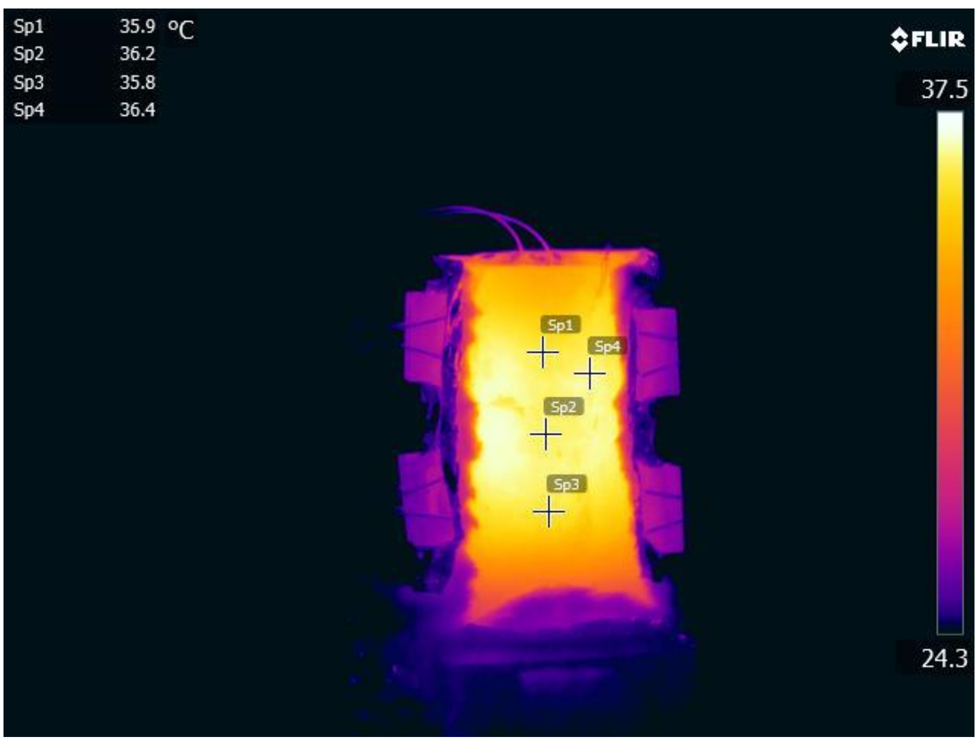

Figure 79: Infrared image at 2.20 min.

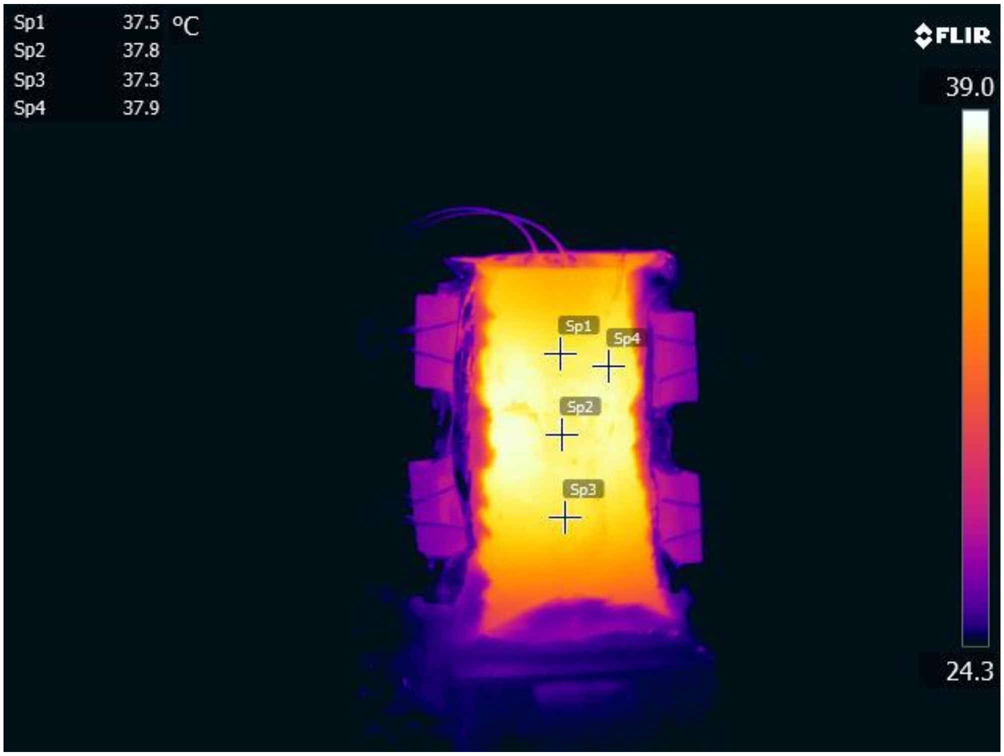

Figure 80: Infrared image at 2.40 min.

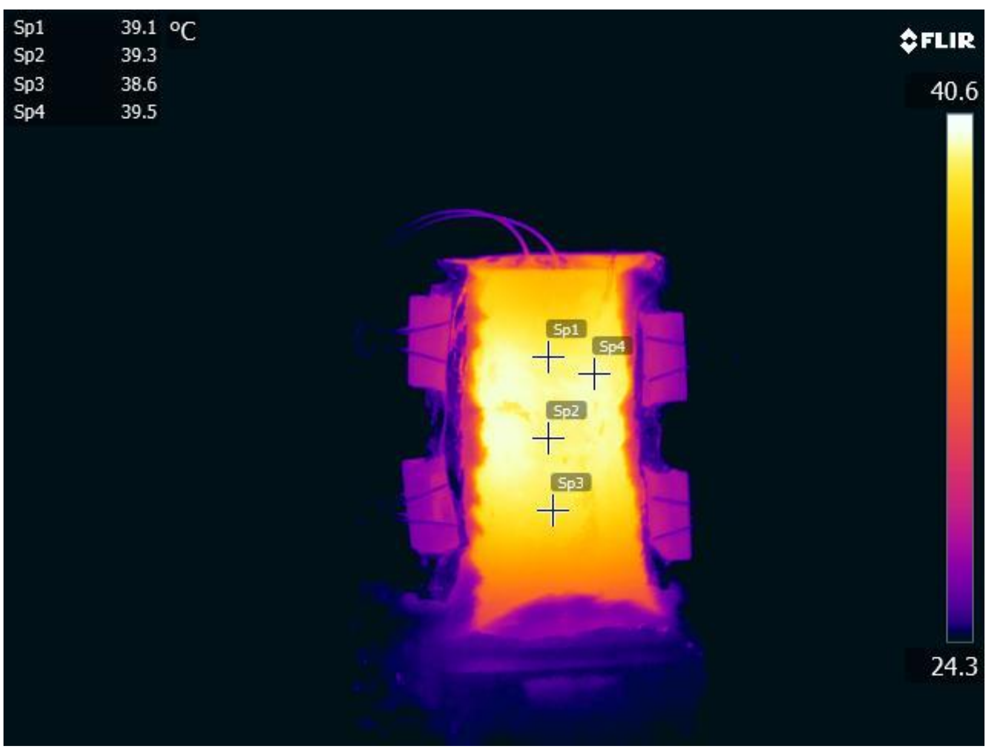

Figure 81: Infrared image at 3.00 min.

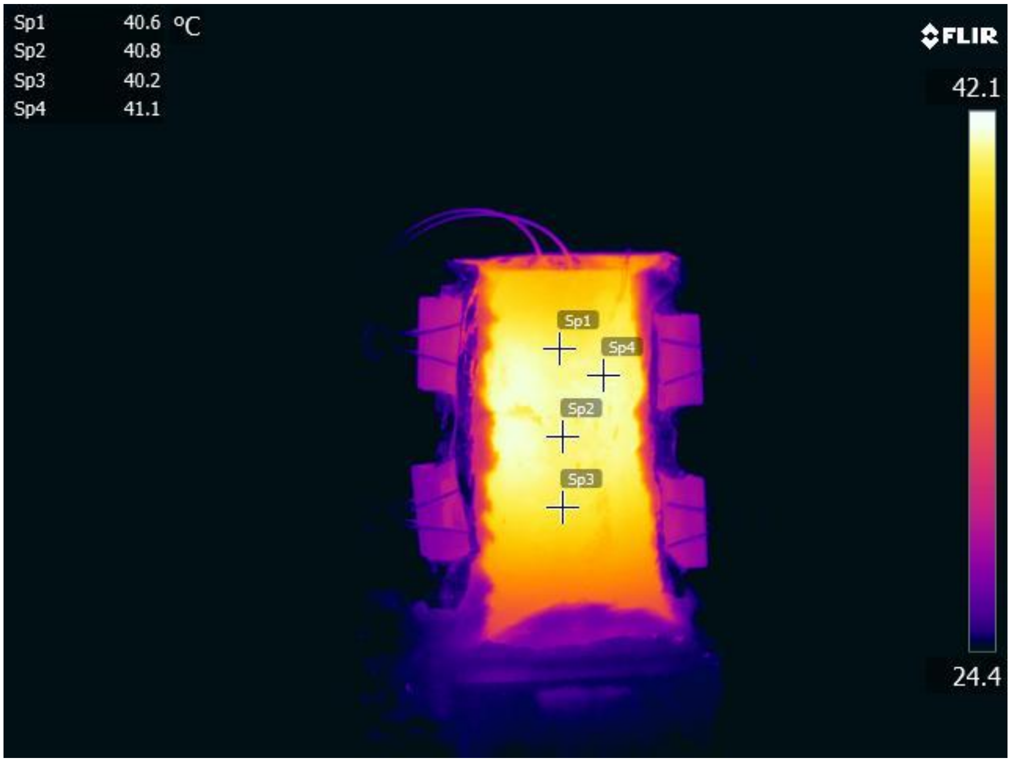

Figure 82: Infrared image at 3.20 min.

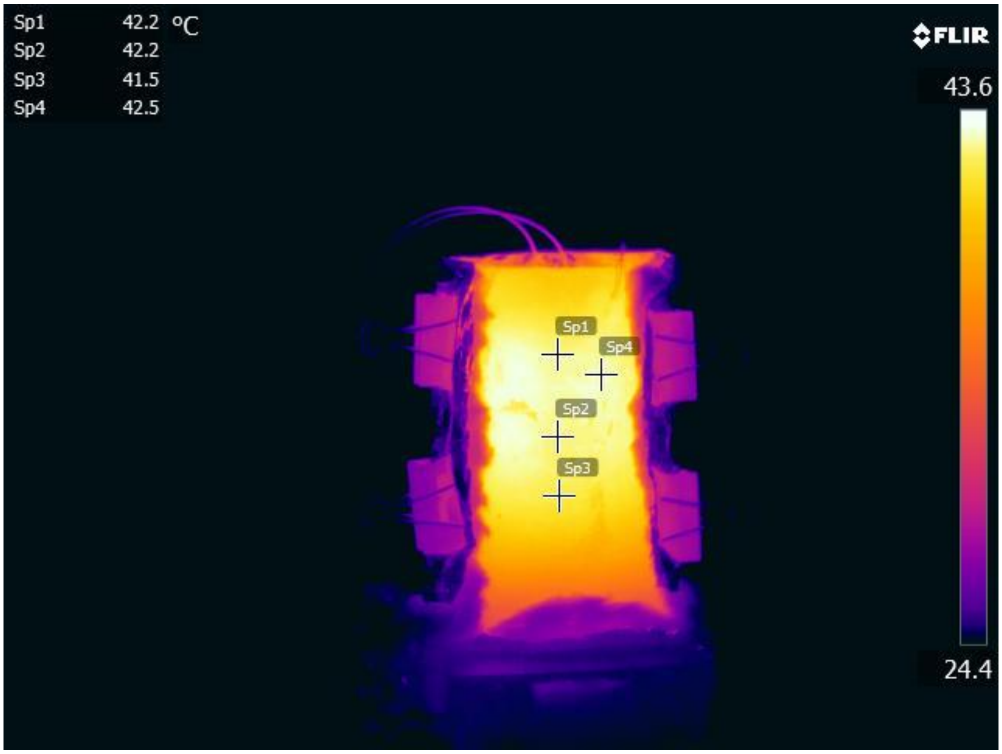

Figure 83: Infrared image at 3.40 min.